FINAL REPORT

Dune and Beach Dynamics in Galveston County, Texas, 1994 to 1998: Critical Information for Coastal Management

James C. Gibeaut and Roberto Gutiérrez

A Report of the Texas Coastal Coordination Council pursuant to National Oceanic and Atmospheric Administration Award No. NA770Z0202

Bureau of Economic Geology
Noel Tyler, Director
The University of Texas at Austin
Austin, Texas 78713-8924

June 1999

CONTENTS

FIGURES

TABLES

EXECUTIVE SUMMARY

Introduction

Changes in beach and dune topography along the Gulf of Mexico shoreline in Galveston County, Texas were documented by comparing topographic transects oriented perpendicular to the shoreline (beach profiles) at 32 locations. All profiles were measured in September 1994 and again in November 1997. Subsets of the profiles were measured in 1995, 1996, and within weeks before and after Tropical Storm (TS) Frances in September 1998. Data on ocean level, waves, wind, and surface currents were compiled for the period to examine the response of the shoreline to certain conditions. In conjunction with this study, airborne laser terrain mapping (ALTM) surveys were conducted in November 1997, August 1998, and September 1998. The ALTM surveys were sponsored by the National Aeronautics and Space Administration (NASA) and have been evaluated for their usefulness in beach and dune studies.

Beach and Dune Dynamics

From 1994 to 1998, eight tropical storms and hurricanes affected the northwestern Gulf of Mexico. Of these eight storms only TS's Josephine in October 1996 and Frances in September 1998 caused significant changes in the dunes and beaches of the upper Texas coast. Conditions generated by TS Josephine appear to have just exceeded the threshold above which significant episodic erosion occurs along the upper Texas coast, particularly in areas with high long-term shoreline erosion rates. Based on the Josephine conditions and other storms that did not cause significant erosion, it is estimated that the threshold conditions are ocean levels that exceed 0.9 m above sea level, as recorded by the Pleasure Pier tide gauge, and coincident wave heights that exceed 3 m for at least 12 hours, as recorded by the National Data Buoy Center buoy #42035 offshore of Galveston Bay. Lower threshold conditions will apply if the beaches and dunes have not fully recovered from a previous storm.

TS Frances caused significantly more erosion than TS Josephine did. Vegetation line retreat caused by Josephine was 5 to 15 m along West Beach on Galveston Island, and for Frances it was 15 to 25 m. Frances also completely eroded foredunes that rose 2.5-m above the

beach berm tops and caused overwash whereas Josephine only removed or cut back 1.5- to 2-m high incipient dunes and sand piles. Preliminary data show that TS Frances did not erode and washover dunes that were more than 3-m above the beach berm tops or where the dune system was more than about 40-m wide. These areas are on the west end of Bolivar Peninsula, and an area on West Beach 11 to 14 km northeast of San Luis Pass where long-term shoreline retreat rates are relatively low. Additional data will be collected in 1999 to define better the effects of TS Frances.

TS Josephine was 500 km south of Galveston Bay when peak water levels and wave heights occurred along the Galveston County shoreline. Maximum wind speed at this time was only 30 kts. Coastal residents and managers should note that such a weak and distally tracking storm can cause significant beach and dune changes and concomitant property damage and management issues. Real-time data on water level and wave heights are available for the Galveston area, and emergency responders could monitor these data during a storm and get an indication of the damage to expect. Officials should also be aware of the present conditions of the beach and dune system along the coast in order to anticipate the effects of the next storm.

Airborne Laser Terrain Mapping

Airborne laser terrain mapping (ALTM) is a new technique to obtain highly accurate and detailed topographic measurements of the earth's surface. ALTM involves combining a scanning laser, a device that records aircraft motion, and high-accuracy Global Positioning System receivers. During three separate missions in November 1997, August 1998, and September 1998, we mapped topography along 160 km of Gulf of Mexico shoreline. The swath of data along the shoreline is 200 m wide and covers the active beach and seaward-most dunes from Sabine Pass to the Brazos River. In addition to the shoreline swath, we mapped all of Bolivar Peninsula.

The ALTM mission was a joint effort between the Bureau of Economic Geology, The Center for Space Research (CSR) of the University of Texas at Austin, the Texas State Aircraft Pooling Board, STARLINK Inc. of Austin, Texas, and Optech Inc. of Ontario Canada, the maker of the laser altimeter system. Optech installed their Airborne Laser

Terrain Mapper on a specially modified Cessna 206 single-engine aircraft owned and operated by the Texas State Aircraft Pooling Board. Technicians at the Aircraft Pooling Board installed geodetic and navigation GPS antennas and a differential GPS navigation system provided by STARLINK.

Our results show that we can efficiently and accurately acquire beach and dune surveys along hundreds of kilometers of coast using ALTM. Vertical precision is 8 to 15 cm (Root Mean Square Error). Absolute accuracy is also 8 to 15 cm after subtracting a bias error determined by comparing ALTM data with road surveys. Data point spacing for these surveys is 2 m, and the mapping swath width is about 200 m, which can cover the beach, foredune, secondary dunes, and structures. It is apparent that ALTM can measure beaches and dunes with enough accuracy and detail to make significant advances in mapping shoreline position, in measuring the shapes and sand volumes of foredunes and beaches, in assessing the coast for susceptibility to storm damage, and in measuring the effects of storms.

INTRODUCTION

During the passage of Tropical Storm Josephine in October 1996, the dunes and beaches along Galveston County, Texas significantly eroded and put many structures at risk of failure. In September 1998 Tropical Storm Frances caused even greater erosion and destruction. The objectives of this project were to (1) monitor changes in the beach and dune system, (2) describe and explain the patterns of beach and dune change since 1994, and (3) conduct and evaluate an airborne laser altimeter survey, also known as airborne laser terrain mapping (ALTM). The project was funded by the Texas Coastal Management Program (TCMP) and the National Aeronautics and Space Administration (NASA). This report compares 32 beach profiles (topographic transects oriented perpendicular to the shoreline) measured in 1994 and again in 1997 along the Galveston County Gulf of Mexico shoreline. Additionally, a subset of these profiles were measured in 1995, 1996, and before and after Tropical Storm Frances in 1998. These additional measurements are also presented in this report. Also included is a description and evaluation of the ALTM surveys. Although the TCMP portion of this project has ended, NASA-sponsored research will continue to provide data and analysis through 2001.

PATTERNS OF BEACH AND DUNE CHANGE

Methods

In November 1997, we resurveyed 32 dune and beach topographic transects established in 1994 as part of the Texas Natural Resources Inventory (Fig. 1). Subsets of these transects were surveyed in 1995, 1996, and before and after Tropical Storm Frances in 1998 (Table 1). These transects, from here on referred to as beach profiles, begin from a temporary datum marker behind the foredune or scarp and continue along a path oriented perpendicular to the shoreline to wading depth. An electronic total station was used to measure heights relative to the datum marker, and the horizontal and vertical positions of the markers were determined using geodetic Global Positioning System techniques. Beach profiles presented in this report, however, are plotted with distances and heights relative to the datum points. Points along the profile were measured where there were changes in slope and at important features such as the vegetation line and the boundary between dry and wet sand.

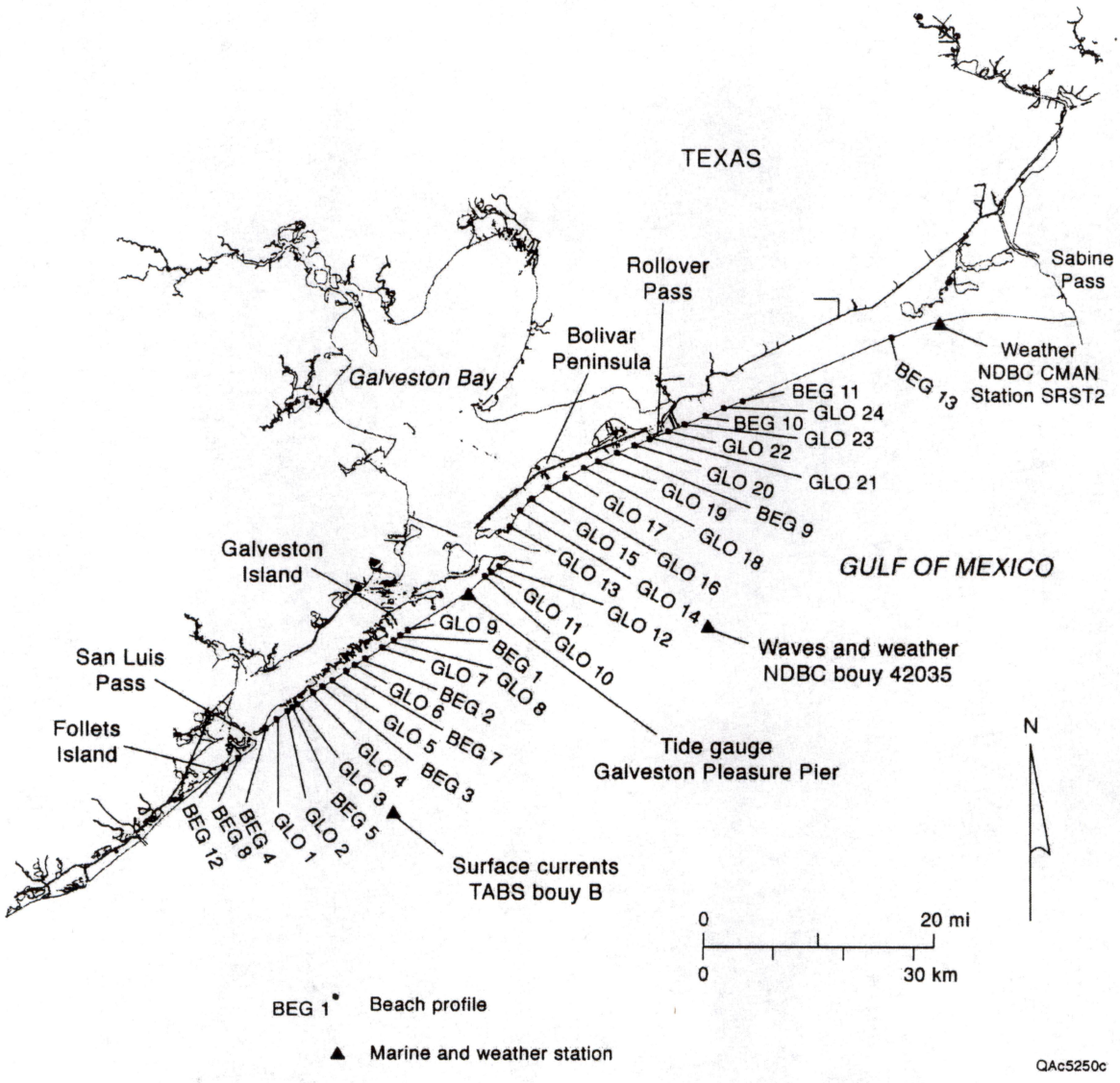

Figure 1. Map of the upper (southeast) Texas coast showing beach profile and oceanographic and meteorological stations. The NDBC CMAN station is a coastal weather station located at Sea Rim State Park and operated by the National Data Buoy Center. The station provides hourly wind direction and speed as well as other standard weather measurements. The NDBC buoy records weather observations and non-directional wave data. The tide gauge at the Galveston Pleasure Pier is operated by the Blucher Institute of Texas A&M University at Corpus Christi for the National Oceanic and Atmospheric Administration. This station records water levels and standard deviations of the water levels. The station also records weather observations. The TABS (Texas Automated Buoy System) buoy is operated by Texas A&M University for the Texas General Land Office. This buoy records surface current direction and speed.

Table 1. Beach profiles measured along the upper Texas coast from September 1994 to March 1999. See figure 1 for profile locations.

Profile	Date (year, month, day)
BEG01	940913,960624, 971111
BEG02	940913, 950427, 960624, 971001, 971111, 971209, 980428, 980808, 980916, 981007, 981022, 981203, 990302
BEG03	940910, 950427, 971112
BEG04	940911, 950426, 971112, 980915
BEG05	940914, 971113, 980916
BEG07	940914, 960624, 971112
BEG08	940914, 950430, 960616, 961026, 970906, 970920, 971112, 971209, 980428, 980809, 980915, 981022, 981203, 990302,
BEG09	940925, 950428, 971109,
BEG10	940926, 971110,
BEG11	971110
BEG12	971113, 980916
BEG13	980415
GLO01	940911, 971112, 980916
GLO02	940911, 950428, 971112
GLO03	940911, 971112
GLO04	940911, 971112, 980808, 980916
GLO05	940910, 971112
GLO06	940910, 971111
GLO07	940913, 960624, 971111
GLO08	940913, 971113
GLO09	940913, 971111, 980916
GLO10	940912, 971111
GLO11	940912, 971111
GLO12	940912, 971111,
GLO13	940925, 950429, 971109, 980417
GLO14	940925, 971109
GLO15	940925, 950430, 971109
GLO16	940925, 971109
GLO17	940927, 950429, 971109
GLO18	940927, 971109
GLO19	940925, 971109
GLO20	940926, 950430, 971110, 980918
GLO21	940926, 971110
GLO22	940926, 971110, 980918
GLO23	940926, 971110
GLO24	940926, 971110, 980918

Plots of the beach profiles are presented in Appendix A. Beach and dune volume was determined by calculating the area of the profile above an elevation that is approximately mean low tide. An assumption was made that the profile was uniform 0.5 m to each side, hence the

profile area is multiplied by 1 m to yield the volume of a slice of the beach. Volume is expressed as cubic meters per meter of shoreline. The computer program "Beach Morphology Analysis Package" (BMAP) developed by the U. S. Army Corps of Engineers was used for the volume calculations. The position of the shoreline along each profile was generally picked as the upper berm crest, but some profiles had no discernable crest. To aid the interpretation of the shoreline position for profiles without a distinct berm crest, all profiles in the time series were graphed on the same plot, and profiles with berm crests guided where the shoreline should be picked for profiles without berm crests. The elevation of the shoreline picked on the profiles may vary by as much as 0.5 m between the surveys of a given profile. The vegetation line was recorded in the field as the seaward most point from which vegetation spreads continuously landward.

Data on waves, water level, wind, and surface currents were acquired for the entire period from 1994 to 1998 or just for particular storm events depending on the type of data. Locations of the various meteorological and oceanographic stations from which data were acquired are shown in figure 1. Tropical storm and hurricane tracks and wind velocities were obtained from the National Hurricane Center (Figs. 2 and 3). Data were analyzed and compared to changes in the beach profiles.

Results

Beach profiles, 1994 to 1997

A comparison of the 1994 and 1997 transects shows that from the Galveston seawall to 4-km northeast of San Luis Pass the vegetation line moved landward 5 to 15 m (Fig. 4a). Within 4 km of San Luis Pass, large shifts in the position of the vegetation line occurred. Within a kilometer of the pass, the vegetation line advanced seaward 35 m, but just 1 to 3 km northeast of the pass it retreated 22 m. The amount of vegetation line retreat was relatively small for a portion of West Beach in an area 11 to 15 km to the northeast of San Luis Pass (GLO-04 and BEG-03 area). Here retreat was only about 5 m. Vegetation line retreat was greater nearer the Galveston Seawall. One profile about 6-km southwest of San Luis Pass on Follets Island (BEG-08) experienced 11 m of vegetation line retreat. Along East Beach on the east end of Galveston

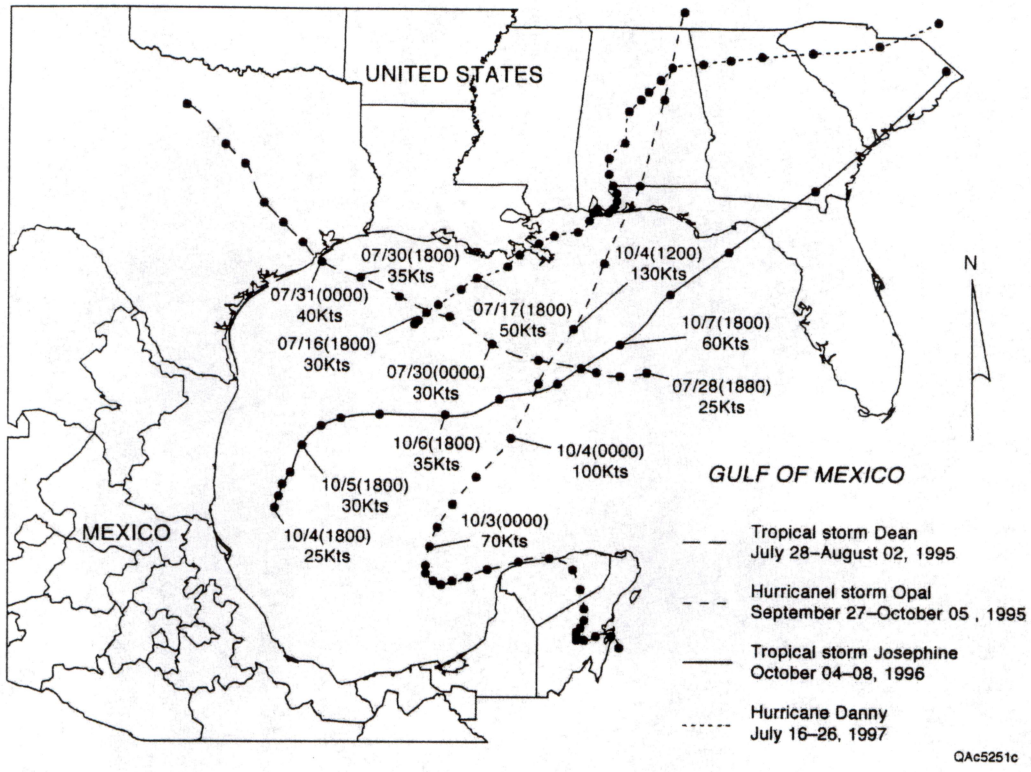

Figure 2. Wind speeds and tracks of tropical storms and hurricanes that affected the northwestern Gulf of Mexico from 1994 to 1997. No storms occurred in 1994.

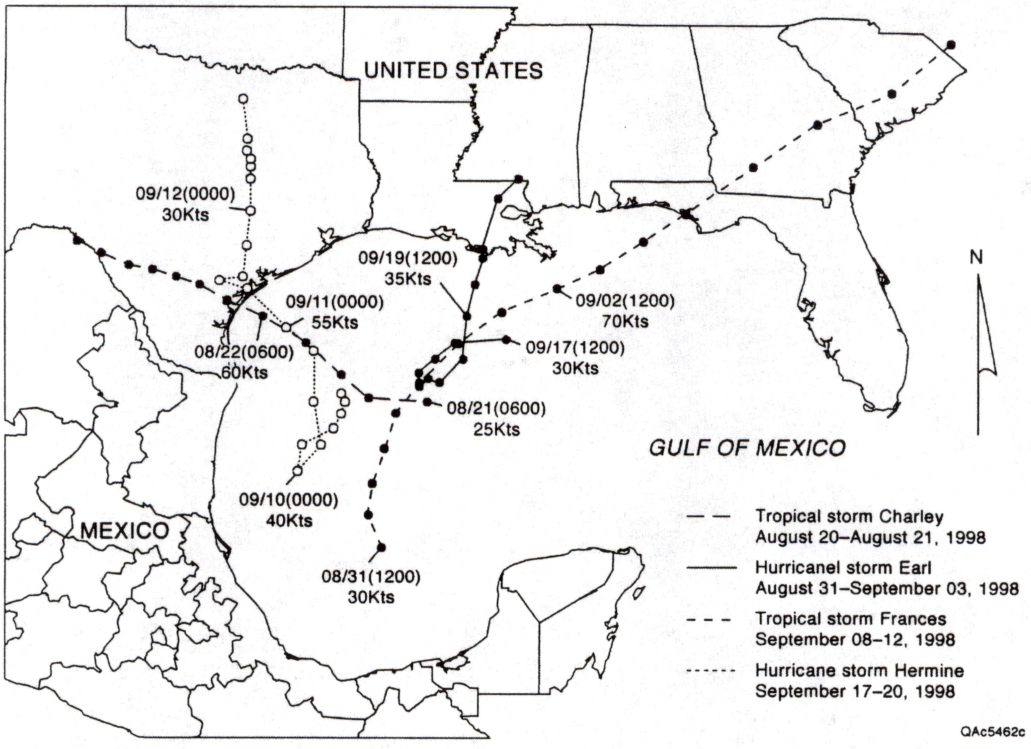

Figure 3. Wind speeds and tracks of tropical storms and hurricanes that affected the northwestern Gulf of Mexico in 1998.

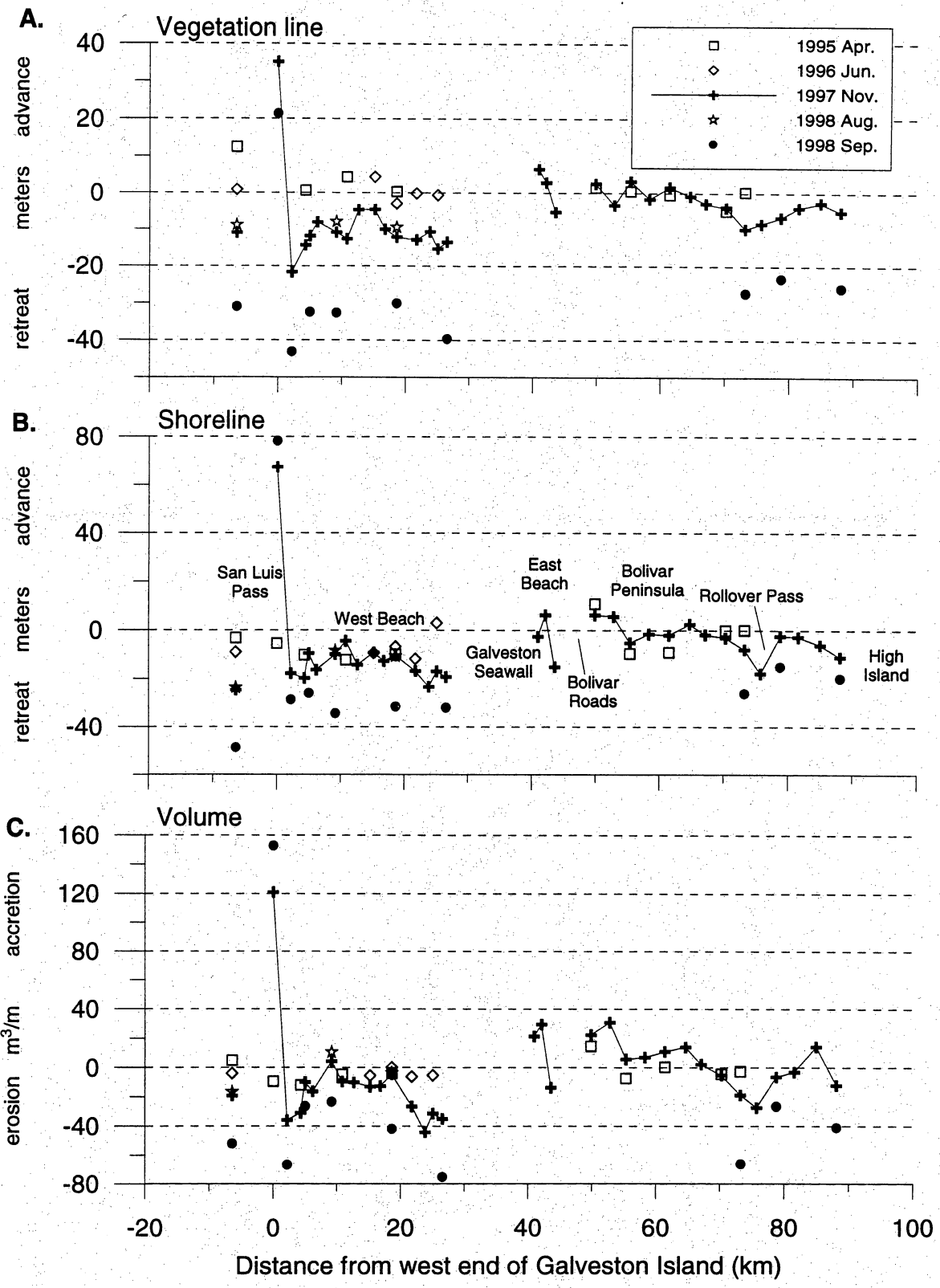

Figure 4. Cumulative change in beach profiles since September 1994: (A) vegetation line movement; (B) shoreline movement; and (C) profile volume change.

Island, the vegetation line advanced 3 to 6 m but retreated 5 m at a location closer to the jetties. On Bolivar Peninsula, 7 to 10 m of retreat occurred within several kilometers of Rollover Pass. The vegetation line remained relatively stable along the rest of Bolivar Peninsula.

Shoreline change from 1994 to 1997 (Fig. 4b) generally followed the same pattern as vegetation line change. Along West Beach and northern Follets Island except just northeast of San Luis Pass, the shoreline moved 4 to 23 m landward. Within a kilometer northeast of San Luis Pass, the shoreline advanced 67 m. On East Beach, the shoreline retreated 15 m at the eastern most location. The shoreline remained stable along western Bolivar Peninsula but retreated 18 m within 2 to 3 km southwest of Rollover Pass. The Shoreline was stable northeast of Rollover Pass but retreat increased to 11 m at High Island.

Sand volume also had generally the same pattern of change from 1994 to 1997 as the vegetation line and shoreline (Fig. 4c). The alongshore trends, however, were more pronounced. Loss of sand within 10-km southwest of the Galveston seawall exceeded 40 m^3/m. Along the relatively stable portion of West Beach away from the seawall, sand loss was less than 15 m^3/m, and at one location there was a small gain of sand (GLO-04). The same swings occurred in sand volume in the vicinity of San Luis Pass as occurred in the shoreline and vegetation line positions. The Follets Island profile, southwest of San Luis Pass, decreased in volume by 19 m^3/m. Two of the East beach profiles increased in volume, but the eastern most one decreased by 14 m^3/m. The beaches along the western Bolivar peninsula gained sand as did a location about 7 km northeast of Rollover Pass. For about 5-km southwest of Rollover Pass, the amount of sand loss reached 27 m^3/m.

Along Follets and Galveston Islands, the beaches in 1994 had a prominent berm and generally a convex profile shape. In November 1997, this berm had eroded, and the beach profiles seaward of the dune were generally linear or concave in shape. Erosion also either cut back or eroded completely incipient foredune deposits (low, discontinuous, vegetated mounds) mostly made up of sand that had been scraped from the beach and pushed up in front of the primary foredune or against a back-beach scarp. An exception to this change in beach shape along West Beach is the area adjacent to San Luis Pass (BEG-04) where a large amount of accretion occurred in the form of berm widening and new natural foredune growth.

Furthermore, in the relatively stable area in the vicinity of GLO-04 and BEG-03, the 1994 berm was eroded and the shoreline moved landward, but this erosion was offset by foredune growth landward of the 1994 vegetation line. Sand eroded from the berm may have been incorporated into the expanded foredune. Scarp retreat occurred northeast of San Luis Pass at GLO-01 and southwest of the Galveston seawall at GLO-09 and BEG-01.

Along the western portion of Bolivar Peninsula from GLO-13 to BEG-09, sand volume increased during the period from 1994 to 1997. The increase involved foredune growth (both natural and unnatural from beach scraping) and back-beach aggradation but not significant berm widening. From BEG-09 to Rollover Pass and just east of Rollover Pass at GLO-22, the beaches lost sand in the form of scarp retreat. In 1997, back-beach scarps 1- to 1.5-m high were present. At BEG-10, 8.5 km east of Rollover Pass, a large amount of sand in the form of artificial foredune growth (piles of sand scraped from the beach and pushed into piles) and vertical berm aggradation was added from 1994 to 1997. This location is within the influence of a pier 200 m to the northeast. The pier has caused a bulge in the shoreline extending about 200 m to each side. Farther to the northeast at GLO-24, the prominent 1994 berm and half of the foredune had been eroded by 1997.

Subsets of the profiles were measured in April 1995 and June 1996 (Table 1,Appendix A). These profiles show that particularly with respect to vegetation line movement and profile volume not much happened from September 1994 to the summer of 1996 before Tropical Storm (TS) Josephine struck in October 1996 (Fig. 2). An exception to this is the more than 10 m of vegetation line advance at BEG-08 on Follets Island from 1994 to 1995. Shoreline movement was more variable and probably shifted back and forth during this period at a greater frequency than can be described by these data. Based on these data and field observations after TS Josephine, it is clear that TS Josephine caused the vegetation line retreat and sand volume loss between 1994 and 1997.

Beach profiles before and after TS Frances in 1998

Whereas TS Josephine in 1996 caused 5 to 15 m of vegetation line retreat, TS Frances caused 15 to 25 m of retreat (Fig. 4a). It should be noted that the profiles used here to gauge the

effects of TS Josephine were measured 1 year after the storm, whereas the TS Frances profiles were measured 1 week after the storm. Nevertheless, it is clear that TS Frances had a much greater effect on the beaches than Josephine did. On West Beach from the seawall to west of Galveston Island State Park the foredunes were completely eroded. The foredune and incipient foredune at Galveston Island State Park (BEG-02, Appendix A) were flattened with a portion of the sand washed landward into the picnic area. Father to the west, in the area of GLO-04, piles of vegetated sand in front of the natural foredune were completely eroded, but the foredune survived. Farther to the west at GLO-01, a scarp that had been cut back by Josephine in 1996 retreated an additional 25 m. Next to San Luis Pass at BEG-04, the vegetation line also retreated, but the beach still had more sand than it did in 1997 (Fig. 4c). On Follets Island at BEG-08, the foredune completely eroded, but a prominent foredune ridge that was 50 m landward of the foredune survived (BEG-08 Appendix A).

Storms from 1994 to 1998

Figures 2 and 3 are maps showing the tracks of tropical storms and hurricanes that affected the northwestern Gulf of Mexico from 1994 to 1998. None of the eight storms occurred in 1994. Only TS's Josephine and Frances caused significant beach erosion and property damage on the upper Texas coast, but other storms had tracks just as close or closer to the study area as Josephine and Frances. Figures 5 through 10 are graphs for six of the storms showing wave height and period, and wind speed and direction from NDBC buoy 42035 (Fig. 1), and water level standard deviation (WLSD) from the open-coast tide gauge at the Galveston Pleasure Pier (Fig. 1).

The water level at the tide gauge is computed by smoothing 181 1-second readings. The standard deviation of these 181 readings are higher during high waves which cause high-amplitude water-level variations. Therefore, the WLSD measured by the tide gauge correlates with the wave heights measured by the buoy and can provide a surrogate measurement of wave height. This is especially useful when buoy data are not available.

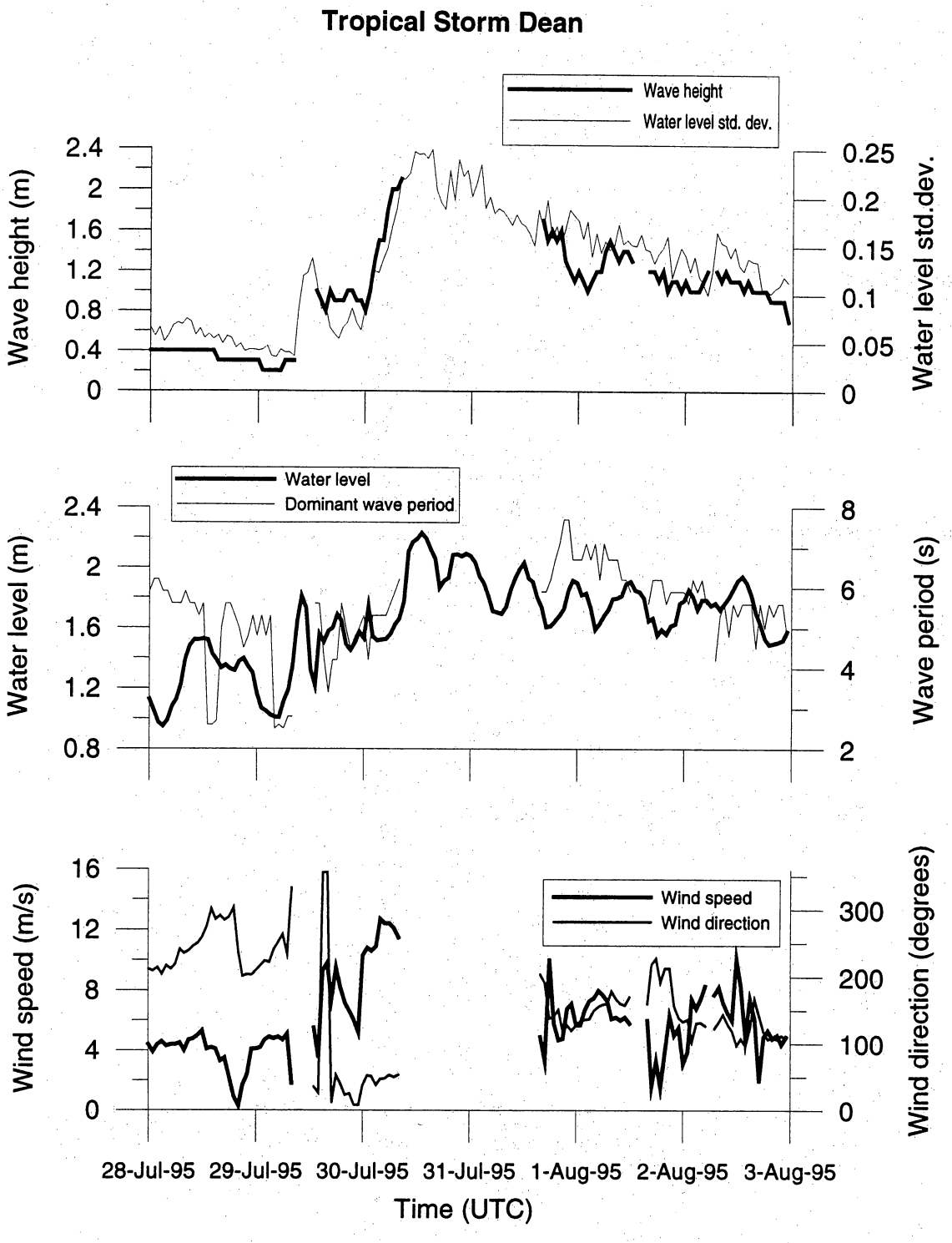

Figure 5. Winds, water levels, and waves during Tropical Storm Dean. Water level and water level standard deviation are from the Pleasure Pier open-coast tide gauge, wave and wind data are from a moored buoy operated by the National Data Buoy Center offshore Galveston Bay. See figure 1 for station locations.

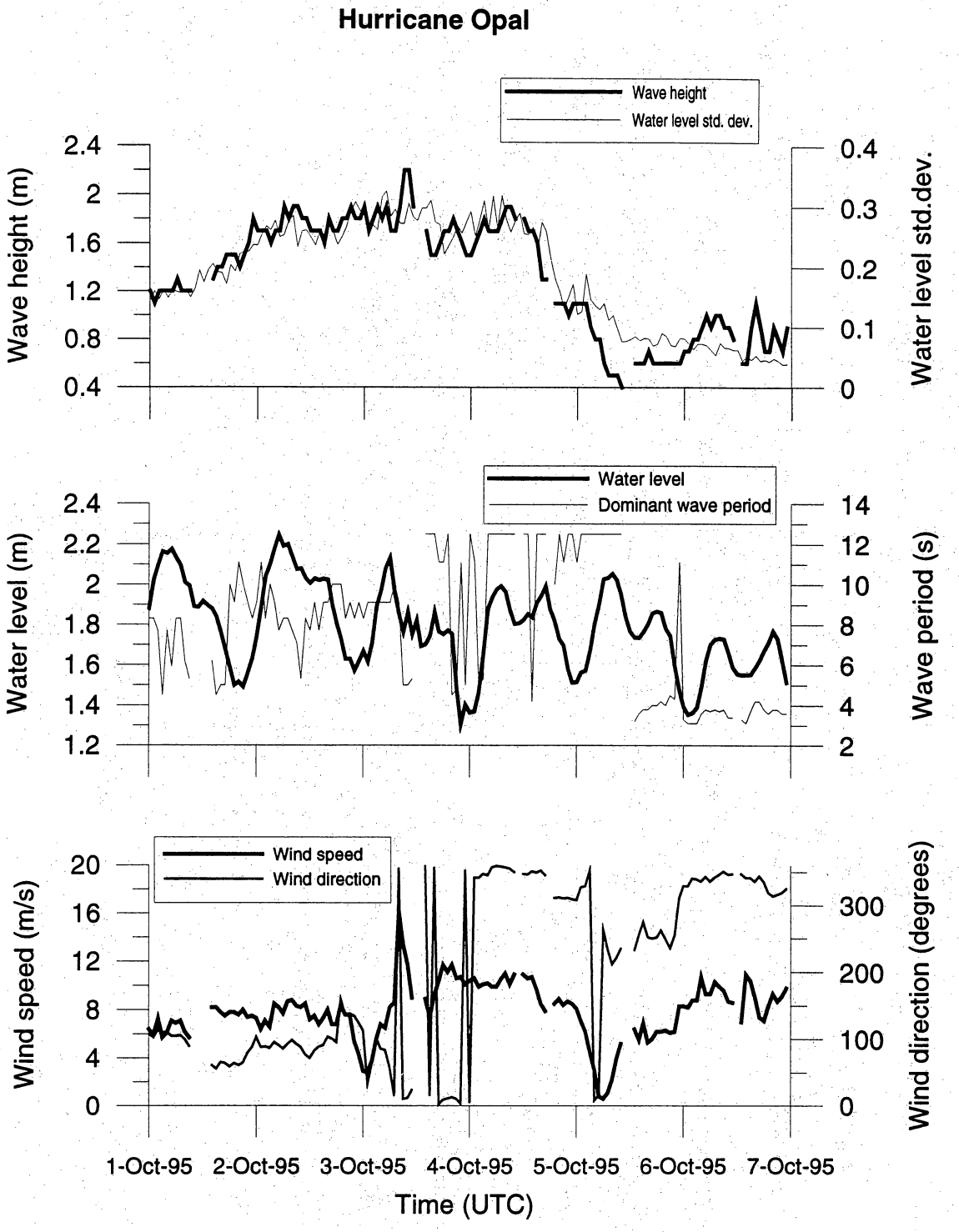

Figure 6. Winds, water levels, and waves during Hurricane Opal. Water level and water level standard deviation are from the Pleasure Pier open-coast tide gauge, wave and wind data are from a moored buoy operated by the National Data Buoy Center offshore Galveston Bay. See figure 1 for station locations.

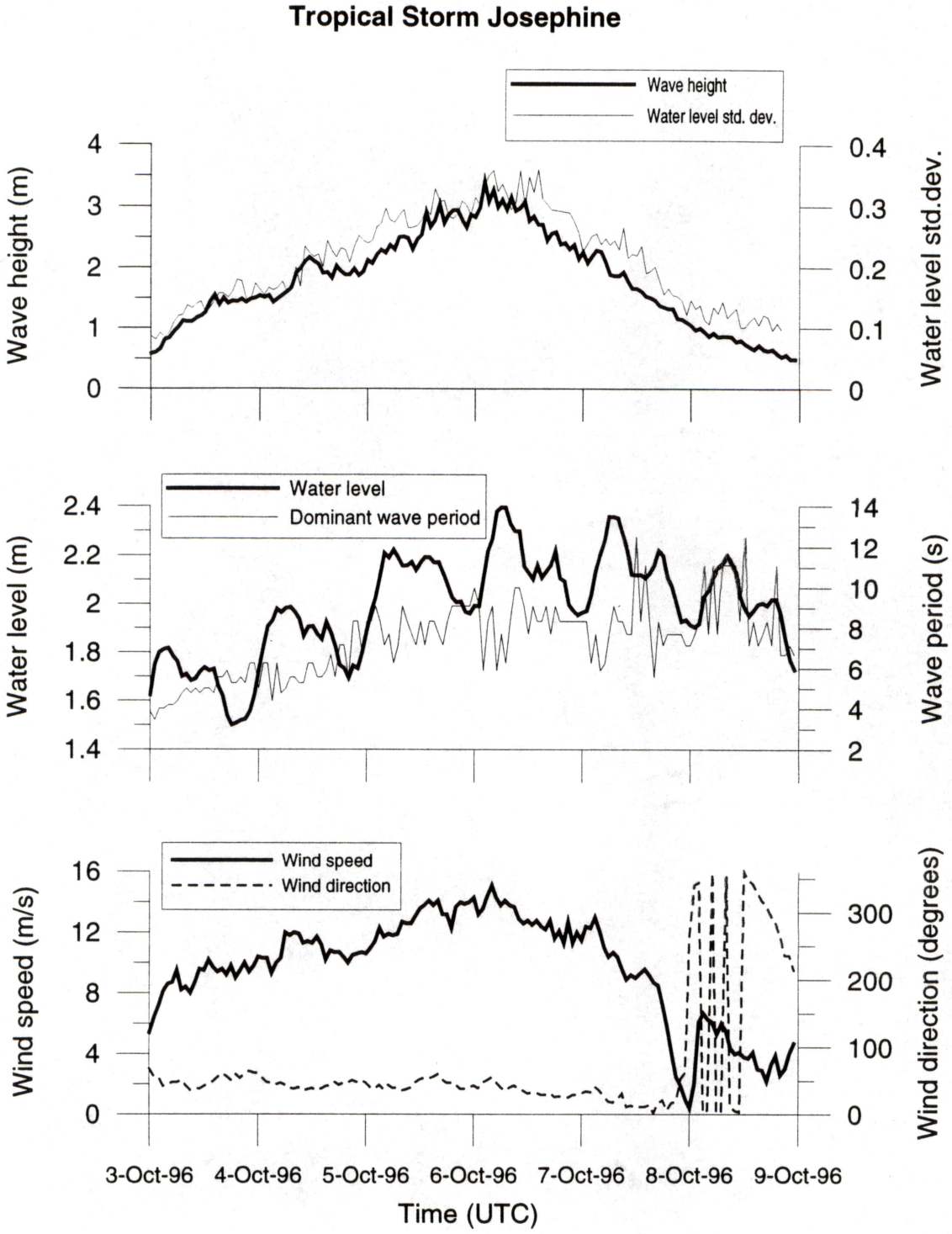

Figure 7. Winds, water levels, and waves during Tropical Storm Josephine. Water level and water level standard deviation are from the Pleasure Pier open-coast tide gauge, wave and wind data are from a moored buoy operated by the National Data Buoy Center offshore Galveston Bay. See figure 1 for station locations.

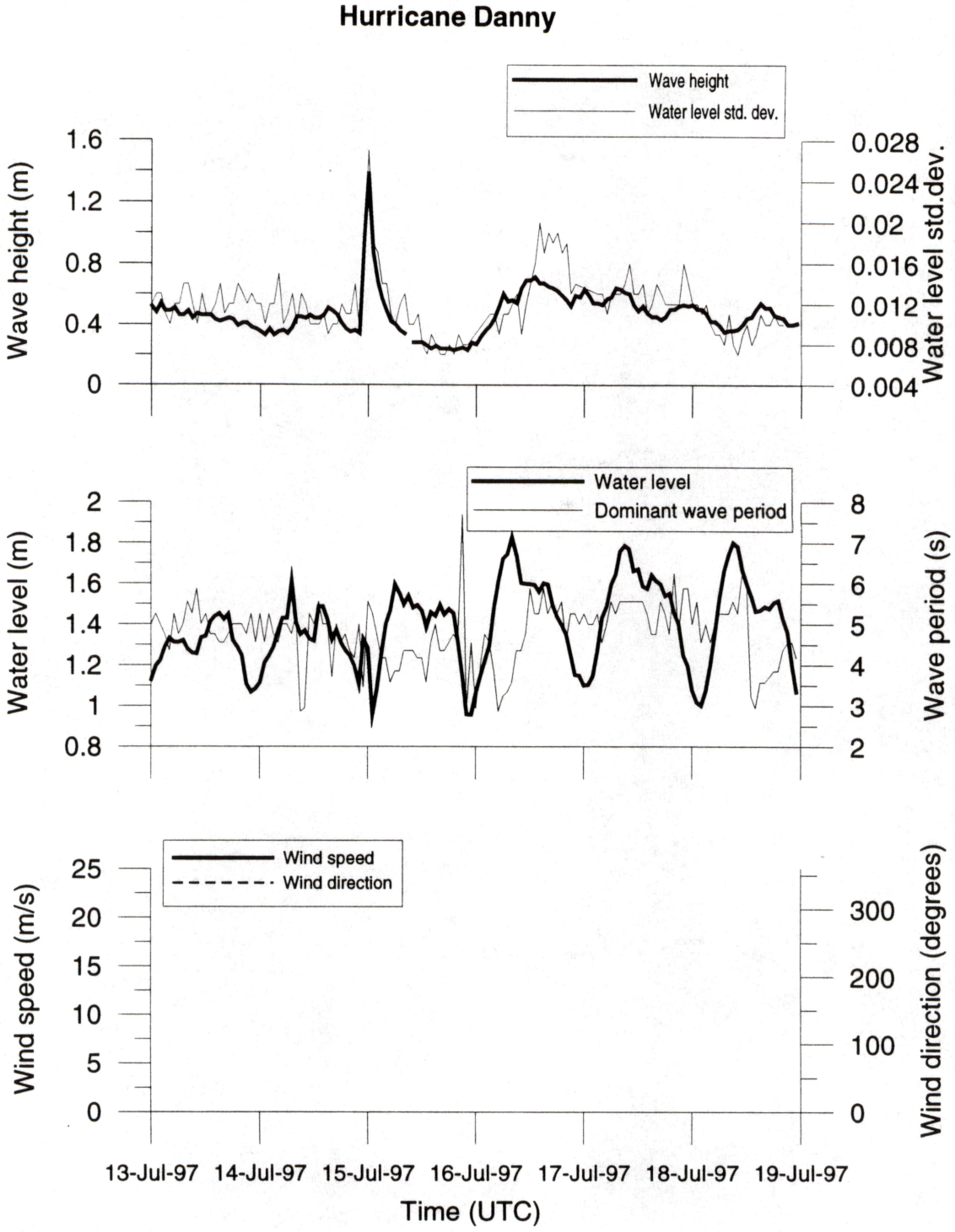

Figure 8. Winds, water levels, and waves during Hurricane Danny. Water level and water level standard deviation are from the Pleasure Pier open-coast tide gauge, wave and wind data are from a moored buoy operated by the National Data Buoy Center offshore Galveston Bay. See figure 1 for station locations.

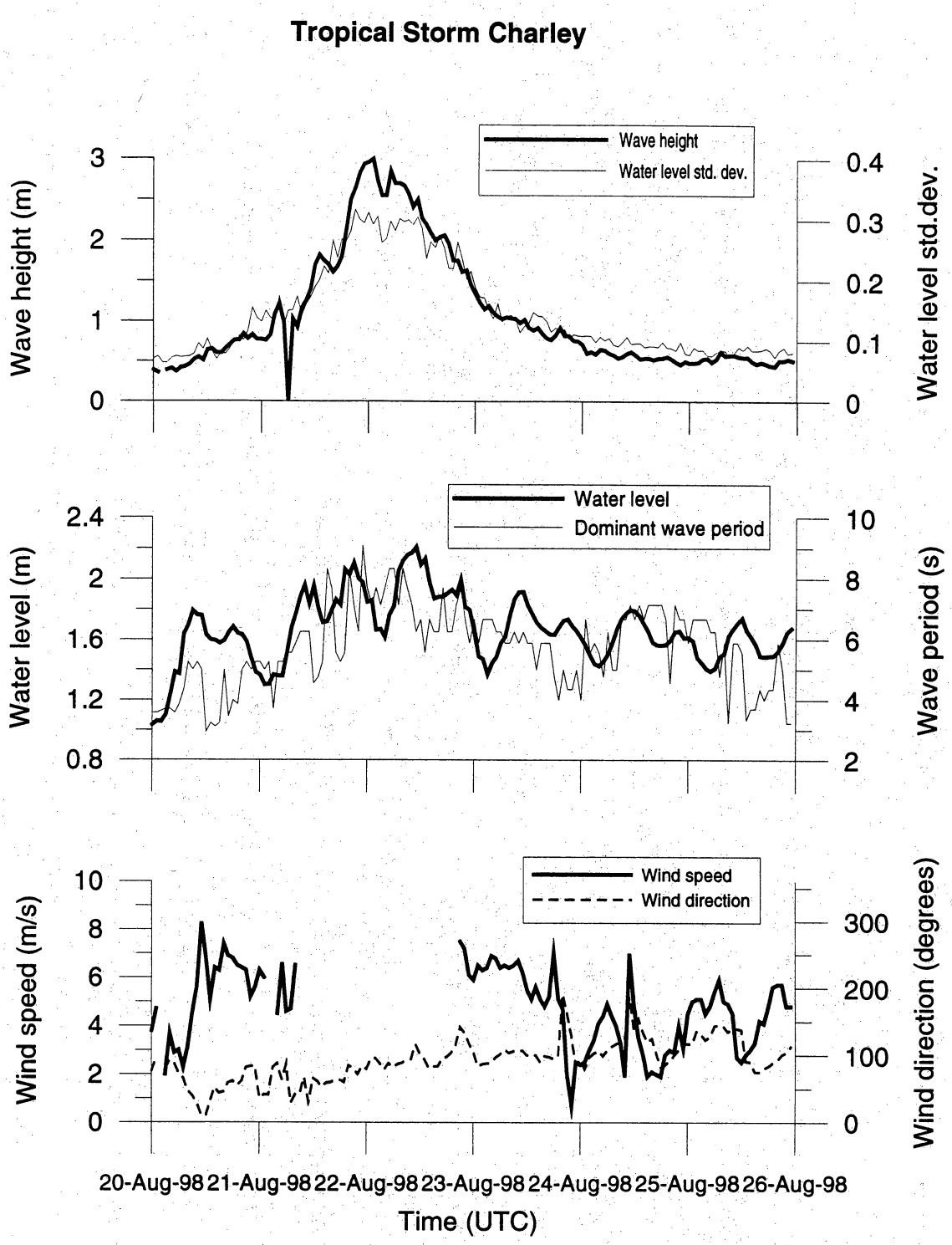

Figure 9. Winds, water levels, and waves during Tropical Storm Charley. Water level and water level standard deviation are from the Pleasure Pier open-coast tide gauge, wave and wind data are from a moored buoy operated by the National Data Buoy Center offshore Galveston Bay. See figure 1 for station locations.

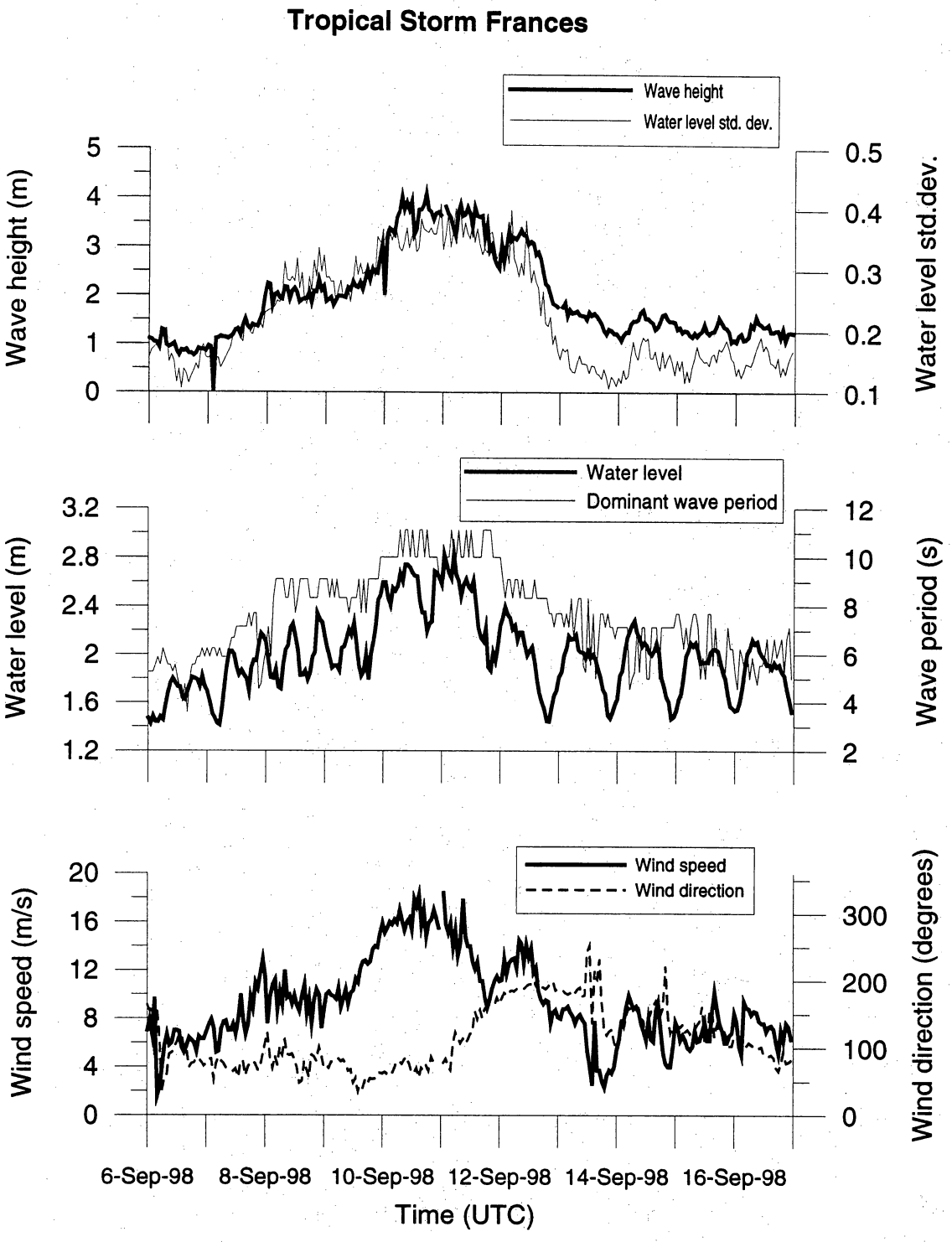

Figure 10. Winds, water levels, and waves during Tropical Storm Frances. Water level and water level standard deviation are from the Pleasure Pier open-coast tide gauge, wave and wind data are from a moored buoy operated by the National Data Buoy Center offshore Galveston Bay. See figure 1 for station locations.

The key parameters of peak water level, peak WLSD, and peak wave height are presented in table 2. For each of these parameters, the average and standard deviations of the hourly readings of the entire time series from 1993 through November 1998 were computed. Table 2 presents the number of hours that the water level, wave height, and WLSD exceeded the value that is three times the standard deviation above the average. These values are considered extreme conditions for this coast.

Table 2: Water levels and wave heights during storms. Water levels were recorded by the Pleasure Pier tide gauge and are referenced to the station datum. Wave heights were recorded by the offshore NDBC buoy #42035. Values for which durations are given are three times the standard deviation above the average of the parameter's time series from 1993 to September 1998. See figure 1 for station locations.

Parameter	TS Dean July 1995	HU Opal October 1995	TS Josephine October 1996	HU Danny July 1997	TS Charley August 1998	TS Frances September 1998
Peak water level (m)	2.23	2.25	2.40	1.83	2.21	2.83
Peak wave height (m)	No data	2.20	3.41	1.39	3.00	4.09
Peak water level standard deviation (WLSD) (m)	0.249	0.326	0.360	0.027	0.317	0.410
Hours water level > 2.18 m	3	4	25	0	1	64
Hours wave height > 2.30 m	No data	0	40	0	16	73
Hours WLSD > 0.26 m	0	40	49	0	23	111

Tropical Storms Josephine and Frances standout from the other storms most notably in the duration of the extreme conditions. Peak water level during Josephine exceeded Dean's, Opal's, and Charlie's water levels by less than 20 cm. However, high-water levels lasted for 25 hours during Josephine versus 4 hours or less for the other storms. The duration of Josephine also allowed high waves to develop. Waves during Josephine were more than 1-m higher than during Dean and Opal and extreme wave heights lasted for 49 hours compared to 0 hours for Dean and Opal. However, extreme WLSD values lasted for 40 hours during Opal, which reflects the long-period swells that arrived at the coast from this distally tracking hurricane. During TS Charley in 1998, waves peaked at 3 m and extreme wave conditions lasted for 16 hours, but the high waves were not coincident with high-water levels. Hurricane Danny in 1997 did not create extreme conditions. Data for Hurricane Earl and TS Hermine (Fig. 3) in 1998 are not presented here, and these storms did not cause significant beach or dune changes.

TS Frances in September 1998 caused large beach and dune changes and created the most extreme conditions of all the storms that affected this coast from 1994 to 1998. Peak water level exceeded the Josephine water level by 43 cm, and extreme water level conditions lasted for 64 hours, more than twice as long as during Josephine. Peak wave height during Frances was 4.09 m and extreme wave heights lasted for 73 hours. Figure 11 is a time series plot of water level, WLSD, and the product of water level and WLSD. High values for the product of WLSD and water level indicate periods of high waves coincident with high-water levels. TS Josephine and Frances are prominent peaks in this plot. Also very evident in the plot are the quiescent conditions that existed during 1994 and 1997.

Discussion

The water level and wave conditions that occurred during TS Josephine appear to be the threshold when significant dune and beach changes occur along the upper Texas coast. The mean higher high water level (MHHW) approximates the elevation of the top of the beach berm. Adding half of the height of the waves to the water level heights relative to MHHW indicates the reach of the storm waves above the pre-storm berm. For Josephine this elevation peaked at 2.27 m and heights above 2.0 m lasted for about 11 hours. This allowed the cutting back or complete erosion of incipient foredunes and vegetated, artificial sand piles formed by

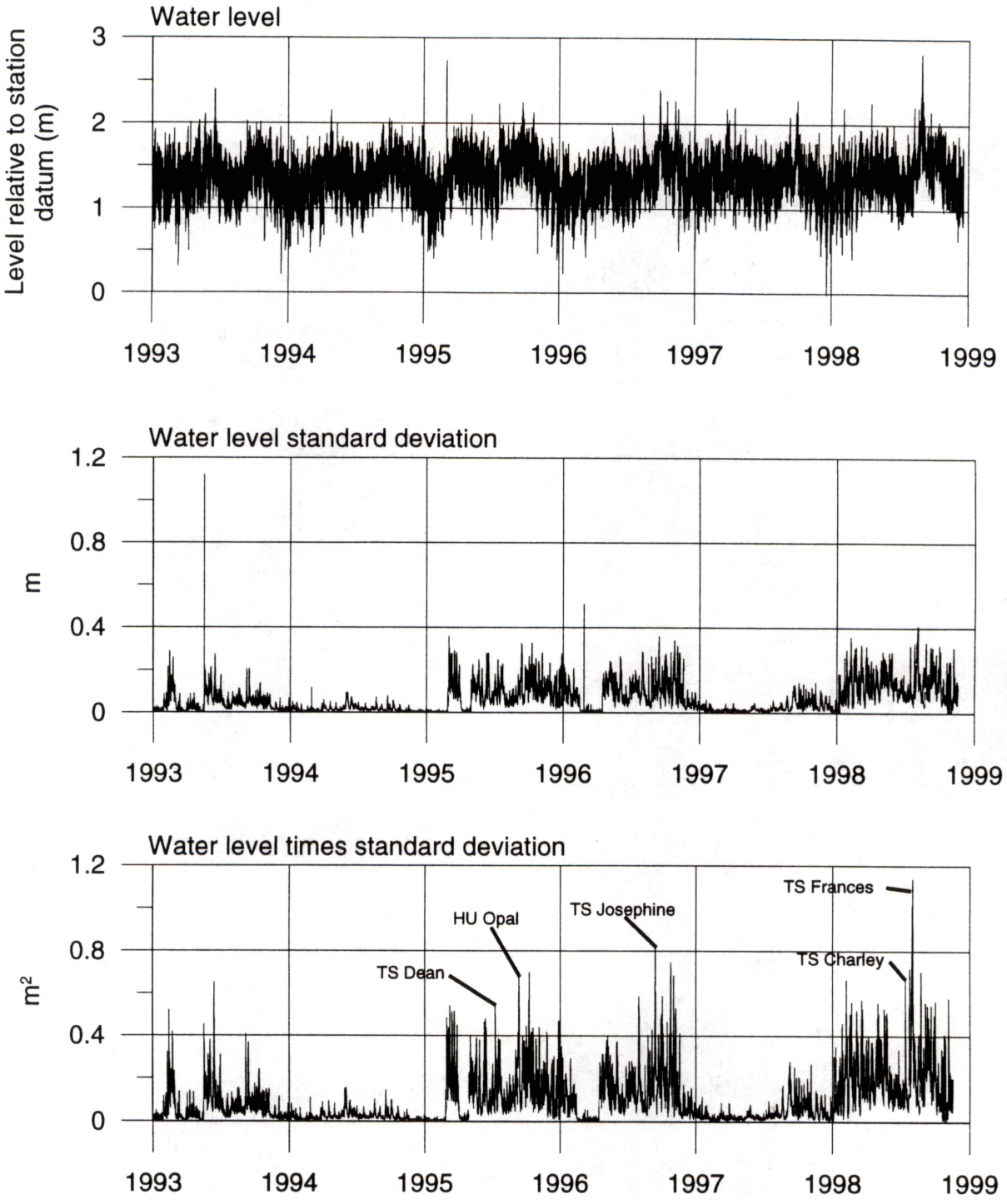

Figure 11. Water level, water level standard deviation (WLSD) and the product of water level and water level standard deviation for the period 1993 through September 1998. Data recorded hourly at the Pleasure Pier tide gauge, see figure 1 for location.

beach scraping. The tops of these incipient foredunes and sand piles were generally 1.5- to 2.0-m above the berm. In areas of relatively high rates of long-term shoreline retreat, such as northeast of San Luis Pass at GLO-01, southwest of the Galveston seawall at GLO-08, BEG-01, and GLO-09, and adjacent to Rollover Pass at GLO-20, 21, and 22, scarps were reactivated by Josephine (see beach profile plots in Appendix A and Fig. 12). At all other locations only the incipient dunes were cut back and the landward primary dunes that were 2.5- to 3.5-m above the berm top were not affected.

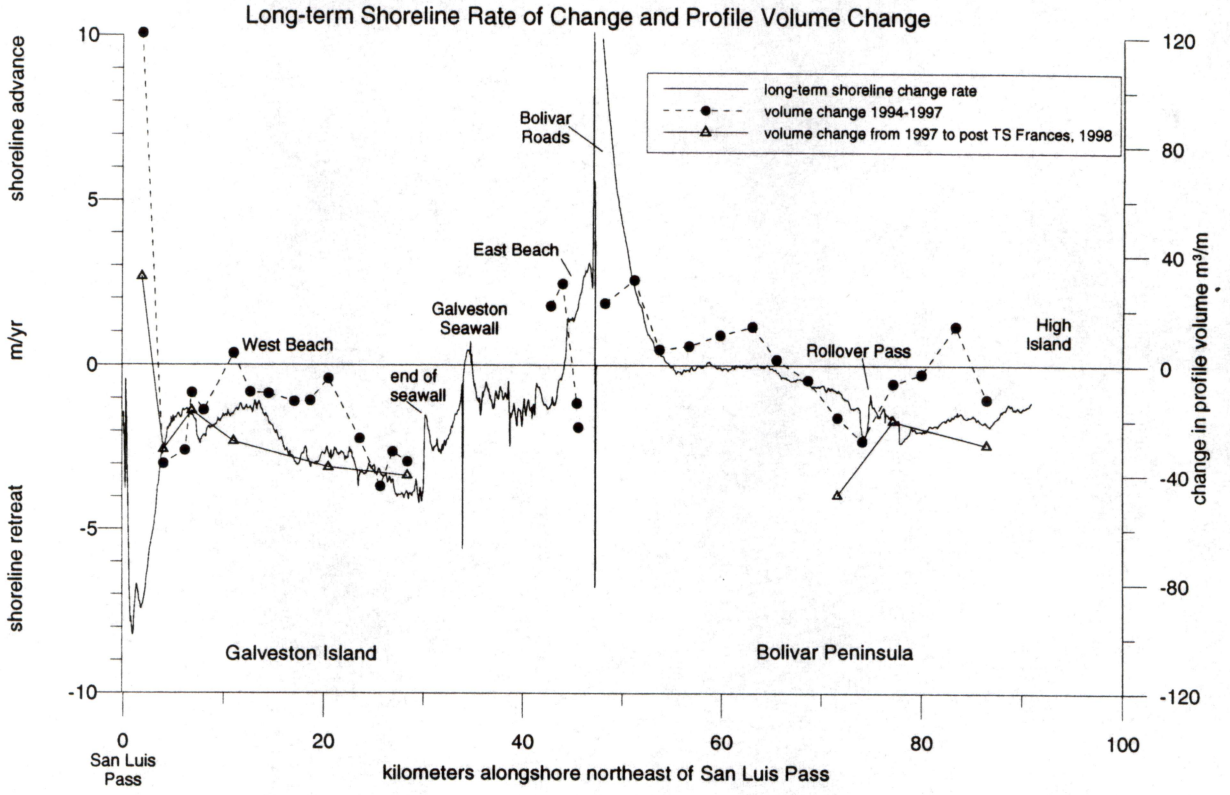

Figure 12. Comparison of long-term shoreline change and profile volume change caused by Tropical Storms Josephine (September 1994 to November 1997) and Frances (November 1997 to September 1998).

TS Frances had a much greater impact on the beaches and dunes than TS Josephine did. The upper reach of the storm waves, computed as above, was 3.0-m above the berm tops and heights greater than 2.0 m lasted 53 hours. This caused extensive scarp retreat in the same areas as Josephine did, but it also completely eroded the primary foredunes along much of West Beach as displayed in the BEG-02 profiles (Appendix A). At BEG-02, the primary foredune

was about 2.7-m above the berm top, and the vegetated dune system was 26-m wide. In the area of relatively low long-term shoreline retreat rates (GLO-04 and BEG-03) (Fig. 12), the incipient foredunes eroded completely but the primary foredunes survived. The primary foredunes in this area are 3.0- to 3.5- m above the berm tops, and the vegetated dune system was 58-m wide before Frances.

The variable heights and widths of the foredunes along this coast made a significant difference in the type of erosion and effects on landward property caused by TS Frances. Where foredunes were less than 3-m above the berm tops and narrower than 30 m, they were completely eroded and overwash occurred. Foredunes higher than 3 m and wider than 30 m protected the landward environment. A future storm with waves reaching just 0.5 m higher than during Frances could cause complete removal of foredunes along all of West Beach.

Overall, TS Josephine caused the greatest change during the storm and for at least one year after the storm where the shoreline is experiencing relatively high rates of long-term retreat (Fig. 12). This correlation is explained by low dunes, no dunes, or the presence of scarps when the storm struck and by a lack of sand for recovery during the year after the storm in areas of high long-term shoreline retreat. The northeast side of San Luis Pass at profile BEG-04 is a notable exception. Long-term shoreline retreat rates here are the highest on Galveston Island, but the beach and foredune grew tremendously from 1994 to 1997. The TABS buoy B (Fig. 1) shows surface currents during Josephine were directed toward the southwest and peaked at over 100 cm/s. This alongshore current indicates that sand eroded during Josephine was transported to the southwest and that some of this sand was added to the beaches at BEG-04. Beaches near San Luis Pass are dynamic because they are affected by shifting tidal channels and shoals. Therefore, it is not expected that the accretion at BEG-04 will continue in the long-term (5+ years).

Conclusions

1. Of the eight tropical storms and hurricanes affecting the northwestern Gulf of Mexico from 1994 to 1998, only Tropical Storm's Josephine in October 1996 and Frances in September 1998 caused significant changes in the dunes and beaches of the upper Texas coast.

2. Conditions generated by TS Josephine appear to have just exceeded the threshold above which significant episodic erosion occurs along the upper Texas coast, particularly in areas with high long-term shoreline erosion rates. Based on the Josephine conditions and other storms that did not cause significant erosion, it is estimated that the threshold conditions are open-coast water levels, as recorded by the Pleasure Pier tide gauge, that exceed 0.9 m above sea level and coincident wave heights that exceed 3 m for at least 12 hours, as recorded by the offshore NDBC buoy #42035. Lower threshold conditions will apply if the beaches and dunes have not fully recovered from a previous storm.

3. TS Frances caused significantly more erosion than TS Josephine did. Vegetation line retreat caused by Josephine was 5 to 15 m along West Beach and for Frances it was 15 to 25 m. Frances also completely eroded foredunes that rose 2.5-m above the berm tops and caused overwash whereas Josephine only removed or cut back 1.5- to 2-m high incipient dunes and sand piles.

4. Preliminary data show that TS Frances did not erode and washover dunes that were more than 3-m above the berm tops or where the dune system was more than about 40-m wide. These areas are on the west end of Bolivar Peninsula, and an area on West Beach 11 to 14 km northeast of San Luis Pass where long-term shoreline retreat rates are relatively low. Additional data will be collected in 1999 to define better the effects of TS Frances.

5. TS Josephine was 500 km south of Galveston Bay when peak water levels and wave heights occurred early on October 6, 1996 (Fig. 2). Maximum wind speed at this time was only 30 kts. Coastal residents and managers should note that such a weak and distally tracking storm can cause significant beach and dune changes and concomitant property damage and management issues.

6. Real-time data on water level and wave heights are available for the Galveston area, and emergency responders could monitor these data during a storm and get an indication of the damage to expect. Officials should also be aware of the present conditions of the beach and dune system along the coast in order to anticipate the effects of the next storm.

AIRBORNE LASER TERRAIN MAPPING SURVEYS

Introduction

As part of this project, we mapped topography along the southeast Texas coast using an airborne laser altimeter. This technique is capable of 15-cm accuracy with data spacing of less than 5 m. The work is in conjunction with our National Aeronautic and Space Administration (NASA) grant and is a joint effort between the Bureau, The Center for Space Research (CSR) of the University of Texas at Austin, the Texas Aircraft Pooling Board, STARLINK Inc. of Austin, Texas, and Optech Inc. of Ontario Canada, the maker of the laser altimeter system. The goal of the Airborne Laser Terrain Mapping (ALTM) mission was to (1) improve the development of digital elevation models (DEM's) in low-relief coastal areas, (2) evaluate and apply ALTM for monitoring beach and foredune volume, (3) evaluate and apply ALTM for mapping the shoreline position, and (4) evaluate and apply ALTM for assessing shoreline susceptibility to storm washover. We will acquire at least one more ALTM survey of the upper coast shoreline during our current NASA grant.

Methods

For these surveys, we installed an Optech Inc. ALTM-1020 laser altimeter in a Cessna 206 single-engine aircraft operated by the Texas State Aircraft Pooling Board. The Optech ALTM-1020 system combines a pulsed, solid-state laser, an inertial motion unit (IMU), and a geodetic GPS receiver in a compact and modular configuration. The IMU (accelerometers and gyroscopes) monitors the aircraft attitude, and the GPS receiver provides aircraft position data. Rotating optics in the instrument's sensor head scans the laser across the ground, illuminating a swath under the aircraft typically 200- to 400-m wide. The laser pulses up to 5,000 times per second. We adapted the aircraft, originally modified for vertical aerial photography, to the Optech instrument in about four hours with the assistance of State aircraft maintenance technicians. For accurate, differential aircraft positioning we operated an Ashtech Z-12 GPS receiver in the aircraft and Trimble 4000SSi GPS receivers on the ground. To provide accurate navigation for the pilot we installed a Starlink DNAV-212 differential GPS system (DGPS), which uses DGPS corrections broadcast by the U.S. Coast Guard. DNAV-212 positions were transferred to a Starlink LB-3 cockpit lightbar that

computed flightlines and displayed flightline corrections. GeoLink® software running on a laptop computer provided real-time plotting of aircraft position on a background map. Detailed specifications of the ALTM-1020 instrument are in Appendix C.

We conducted ALTM missions along the southeast Texas coast in November 1997 and August and September 1998 (Figure 13). We mapped the southwest half of Bolivar Peninsula on November 8, 1998. In 3.5 hours we covered more than 163 km^2. From August 6, 1998 to August 9, 1998, the survey of Bolivar Peninsula was completed. In August we also acquired data along the Galveston Island shoreline. On September 10, Tropical Storm Frances caused 20 to 30 m of shoreline retreat, completely eroded foredunes, and severely damaged many structures along the southeast Texas coast. On September 17, we conducted an ALTM survey of the shoreline from Sabine Pass to the Brazos River (200 km), an area surrounding San Luis Pass, and several shore-normal transects for TOPSAR calibration (Figure 13). For comparison with ALTM data, detailed beach profiles (topographic transects oriented normal to the shoreline) were measured within three days of the ALTM flights using an Electronic Total Station (ETS). We also conducted extensive kinematic GPS surveys along roads and beaches. These data are used to calibrate and check the laser altimeter data for accuracy.

Optech Inc. is performing the initial processing of the data to compute x, y, and z data points of the ground/vegetation. The Bureau is computing aircraft GPS trajectories for comparison with Optech-computed GPS trajectories and for use in the ground point solutions. The Bureau is also determining the position of the GPS ground reference stations with respect to a local tidal datum and comparing kinematic GPS road surveys and beach profile surveys to estimate the accuracy of ALTM surveys. We are also using the road surveys to determine the bias error of each ALTM survey so that they may be adjusted to allow temporal comparisons. The Bureau is constructing Digital Elevation Models and topographic profiles.

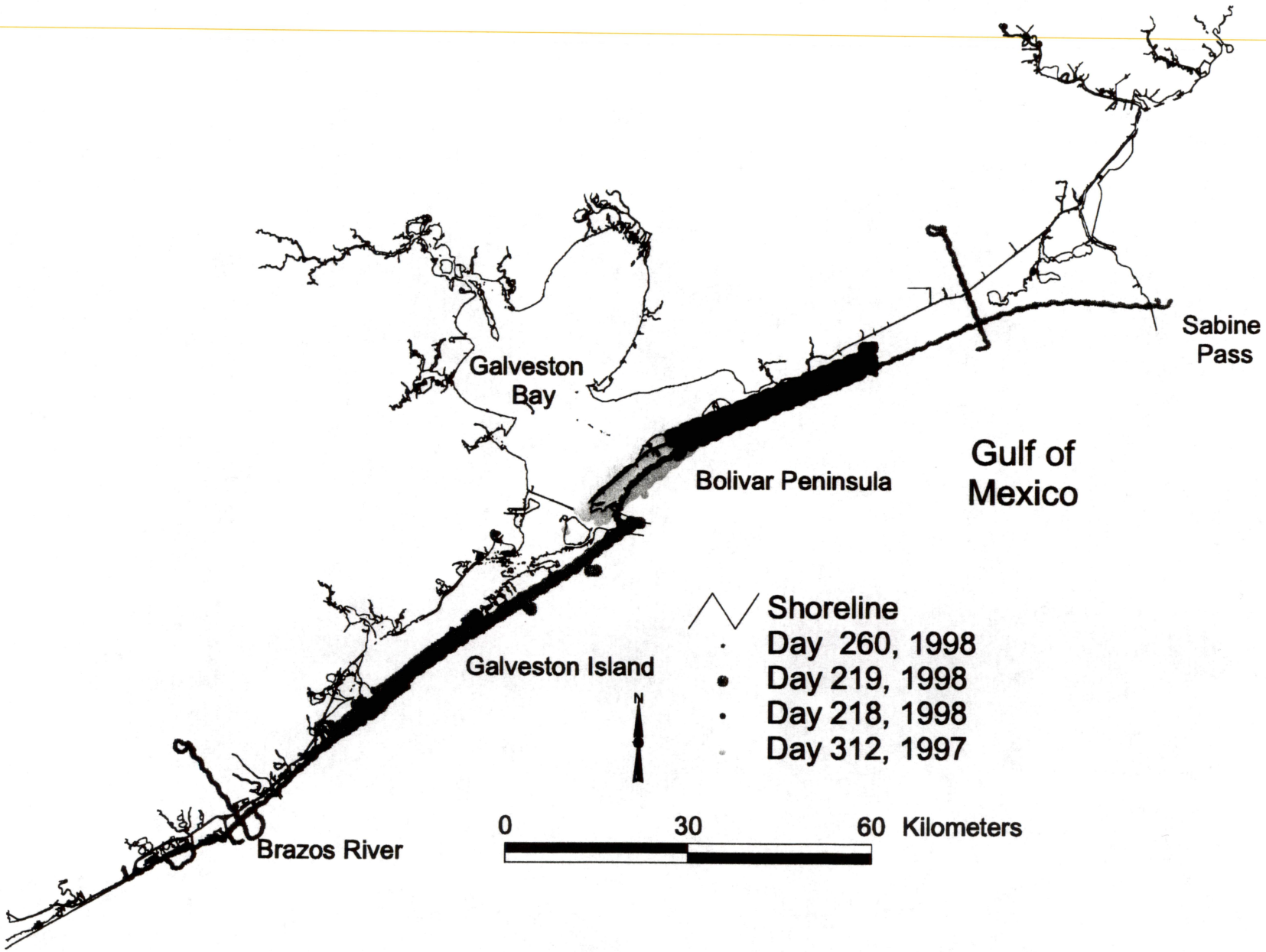

Figure 13. Location of ALTM surveys on the southeast Texas coast.

Preliminary Results

Our results show that we can efficiently and accurately acquire beach and dune surveys along hundreds of kilometers of coast. Vertical precision is 8 to 15 cm (Root Mean Square Error). Absolute accuracy is also 8 to 15 cm after subtracting a bias error determined by comparing ALTM data with road surveys. Data point spacing for these surveys is 2 m, and the mapping swath width is about 200 m, which covers the beach, foredune, secondary dunes, and structures. Further details are presented in the articles and abstracts in the appendices of this report. Following are several highlights of our results to date.

Accurately mapping shoreline position and calculating rates of shoreline change has been a problem addressed by coastal geologists for decades. Usually, shoreline position is mapped using vertical aerial photographs. The shoreline is interpreted and drawn on the photograph and then transferred to a base map for comparison with earlier shorelines. Typically, the boundary between wet and dry sand on the beach, which is displayed as a tonal contrast on the photographs, is used as the shoreline. This boundary, however, is affected by recent water level and wave activity and may not be a reliable indicator of shoreline position. There is also error introduced to the shoreline position when it is transferred to the base map. Because ALTM surveys are GPS based, there is no need for transferring data to a base map. Furthermore, we can use a contour line as the shoreline, eliminating the ambiguity present in the wet sand/dry sand boundary. Figure 14 shows a shoreline swath of ALTM data in the vicinity of Rollover Pass on Bolivar Peninsula. A contour map was constructed from this swath of data and is shown in Figure 14 with one contour highlighted along the beach. Our results show that a single swath of ALTM data appears adequate to define a contour line as the shoreline. The GPS-based ALTM data, however, are produced as heights above the ellipsoid and what should be mapped as the shoreline is an elevation that is related to local sea level. We are continuing research to adjust the ALTM data to be relative to local sea level and, therefore, to significant beach morphology features such as scarps, or berm crests.

Figure 15 is a DEM of a portion of Bolivar Peninsula. This DEM was generated from over 14 million ALTM data points acquired in November 1997. The grid size is 5 by 5 m. The DEM shows all the significant natural features of this low-relief area including

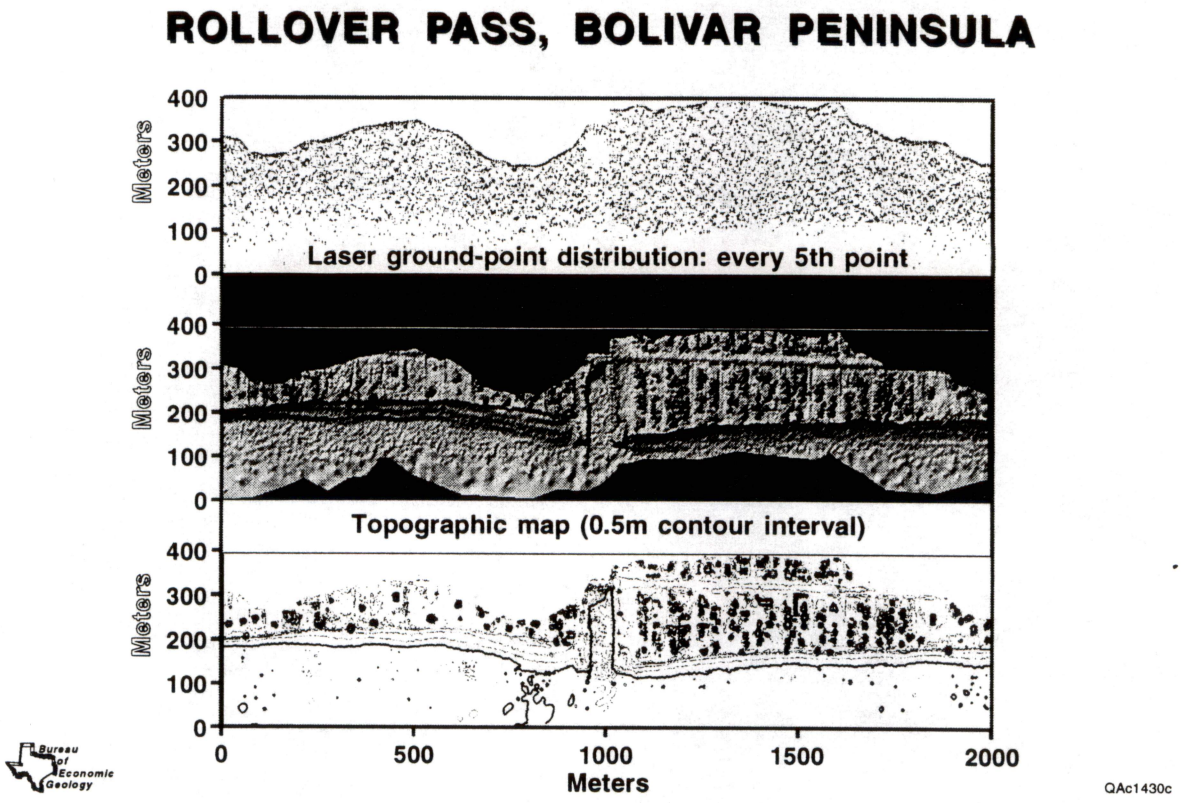

Figure 14. ALTM swath of the shoreline in the vicinity of Rollover Pass on Bolivar Peninsula. The Gulf of Mexico is at the bottom. Top is a Map of every 5th data point. Middle is a shaded relief view with artificial sun angle from the top. Bottom is a contour map with one contour line highlighted along the beach.

foredunes, beaches, and a subtle ridge and swale topography. Cultural features, such as houses, dredge spoil, and roads are also readily apparent. Detailed comparisons of ALTM and ground survey data are presented in Appendix C where it is noted that vegetation causes less agreement with the ground-surveyed beach profiles than with the road surveys. Optech has a proprietary computer program that is designed to remove data points from vegetation and structures leaving only the ground surface represented. We are experimenting with the output of this program and investigating other ways to remove vegetation. The effect of vegetation on DEM's and specifically on dune sand volume calculations will be an area of research during the second year of the NASA project.

Figure 16 is a comparison between ground-surveyed beach profiles and beach profiles constructed from two swaths of ALTM data before and after Tropical Storm Frances. Data points that fall within 2 m on each side of the profile line form the ALTM profiles. Points interpreted on the ALTM profiles as ground points agree to within 15 cm of the ground-surveyed points. A significant discrepancy between the ALTM and ground profile occurs on the berm and beachface for one of the ALTM passes before Tropical Storm Frances (Fig. 16a). We think this discrepancy was caused by a spot of oil on the window of the laser altimeter, which caused anomalous data points in the portion of the data swath directly under the aircraft. For one of the ALTM passes, the anomalous data occurred offshore and did not affect the beach data. Relatively thick vegetation on the landward side of the primary foredune is evident in the ALTM data. Here, some of the laser shots reflected from the top of the vegetation and some penetrated the vegetation and reflected from the ground. The laser energy does not penetrate water; thus the water surface is apparent on the ALTM profiles. Other differences between the ALTM and ground surveys are caused by natural variation to each side of the profile. This is particularly evident in the post-Frances profile where a picnic shelter was measured (Fig. 16b). It is apparent that ALTM can measure beaches and dunes with enough accuracy and detail to make significant advances in mapping the foredunes and beaches, assessing the coast for susceptibility to storm damage, and measuring the effects of storms.

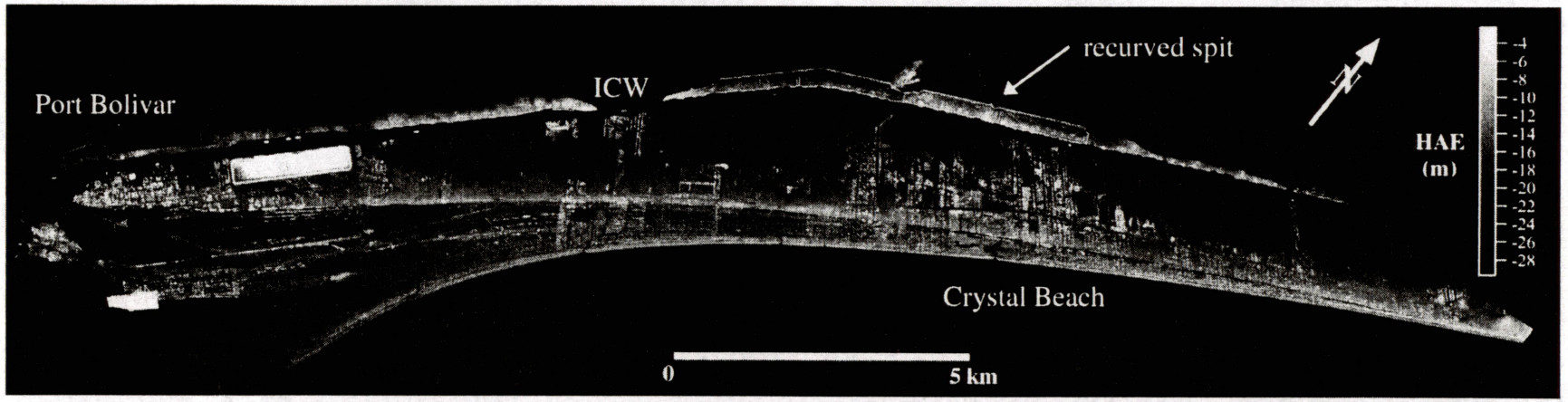

Figure 15. ALTM topographic image of Bolivar Peninsula. The Gulf of Mexico is on the bottom. This 5 by 5 m Digital Elevation Model (DEM) is constructed from over 14 million laser data points acquired in November 1997.

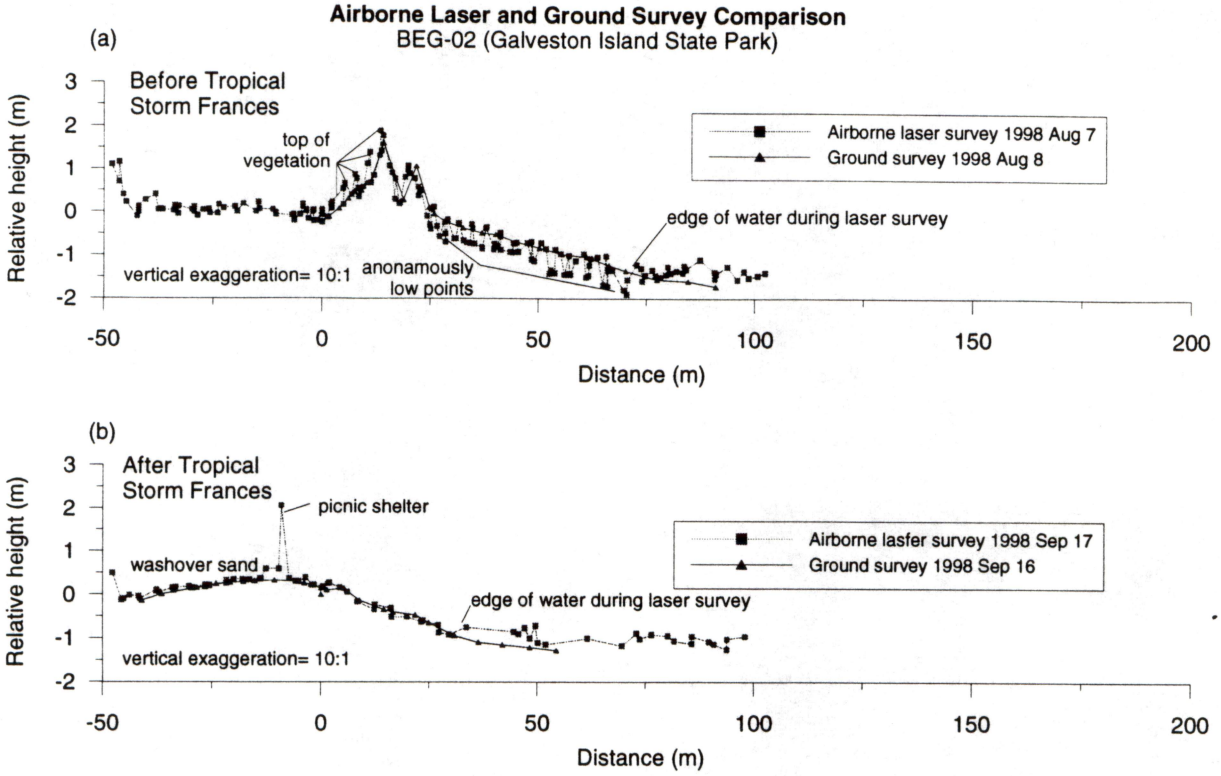

Figure 16. Beach profile comparisons of ALTM (airborne laser terrain mapping) and ground surveys at Galveston Island State Park, profile BEG-02: (a) before Tropical Storm Frances; (b) after Tropical Storm Frances.

The Bolivar Peninsula DEM was "textured" with a color infrared, digital, orthophoto that has a resolution of 2.5 m. A 3-dimensional, stereo model was created for interactive viewing (Figure 17). Vertical exaggeration of the detailed topography and the land cover information provided by the orthophoto allows the delineation of the seaward and landward boundaries of the foredune system. These boundaries are significant in coastal management plans because foredunes are often allotted special protection. Once the horizontal and vertical boundaries of the foredune are determined, the volume of sediment may be calculated. Hence, a "snapshot" of the amount of sediment stored in the protective foredune system may be obtained for 100's of kilometers of shoreline. This information may be used to help determine the legal "value" of the foredune, as part of a sediment budget determination, and

Figure 17. ALTM Digital Elevation Model of a portion of Bolivar Peninsula textured with a color infrared digital orthophoto. Vegetation shows in various shades of red. Barren areas, such as the beach and roads, are grayish and white in color. White buildings and dark red trees show as highly exaggerated protrusions. Vertical exaggeration is about 15 times. The top shows a view toward the north with the Gulf of Mexico on the right. The bottom is an enlargement that distinctly shows the beach, foredunes, secondary dunes, and subtle ridge and swale topography.

to map hazardous areas that are prone to washover and enhanced erosion during storms. This work will continue in the second year of the NASA project.

Future Research

(1) We will continue analysis of the effect of vegetation on ALTM surveys, particularly on the effect vegetation has on dune sand volume and morphology measurements.

(2) Foredune volume will be calculated along the southeast Texas coast using the ALTM survey. This work will establish a general procedure that others may follow for this type of calculation.

(3) The shoreline will be mapped along the southeast Texas coast using the ALTM survey in conjunction with beach profile measurements. This work will establish a general procedure that others may follow for this type of mapping. We will also compute the rate of shoreline change through comparison with earlier shorelines.

(4) Weather and wave data will continue to be compiled and analyzed.

(5) Wave refraction analysis will continue.

(6) Integration of ALTM DEM's with other remote sensing data such as digital orthophotos, airborne multispectral, and airborne synthetic aperture radar data will continue.

(7) The next survey of the southeast Texas coast is tentatively scheduled for September 1999. This survey will include ALTM, ground beach profile measurements, and bathymetric surveys.

Appendix A
Beach profile plots ordered geographically from west to east.

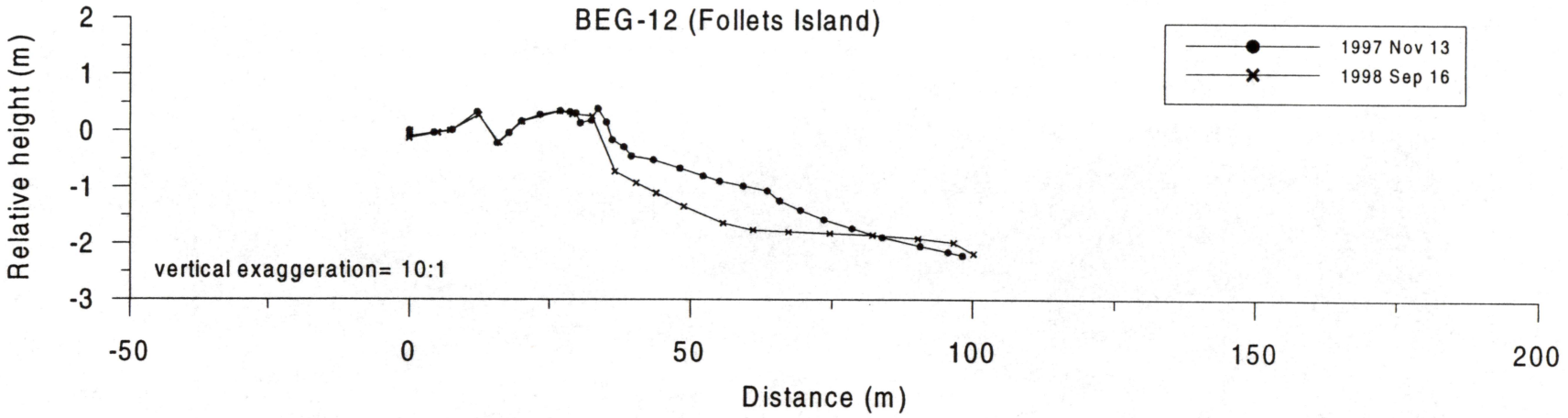
BEG-12 (Follets Island)
1997 Nov 13
1998 Sep 16
Relative height (m)
2
1
0
-1
-2
-3
vertical exaggeration= 10:1
-50
0
50
100
150
200
Distance (m)

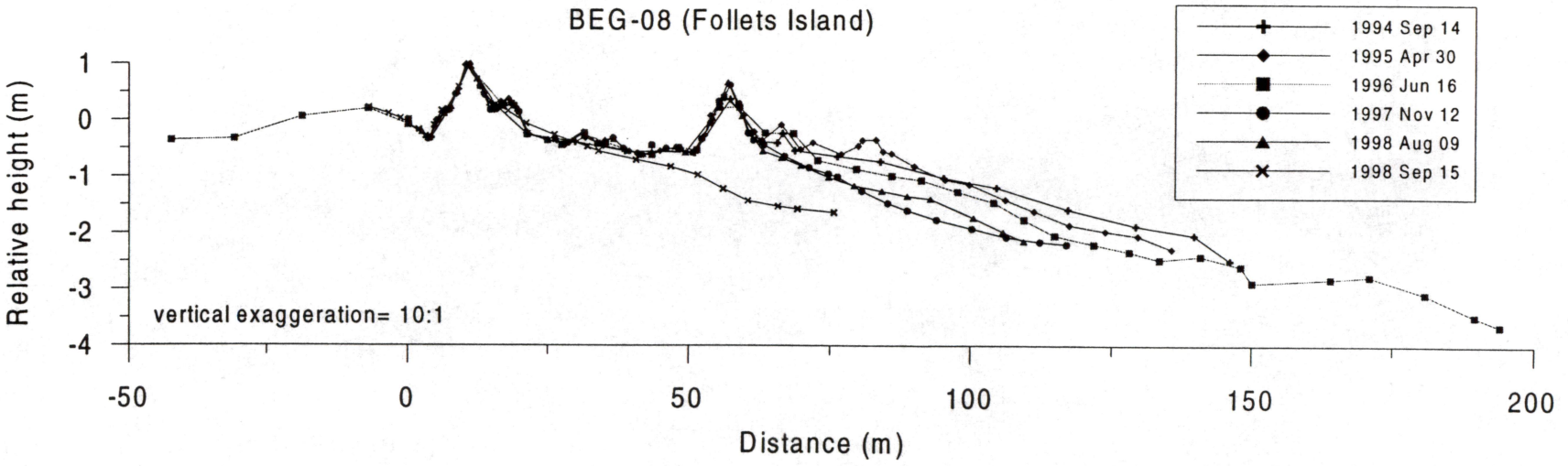
BEG-08 (Follets Island)
1994 Sep 14
1995 Apr 30
1996 Jun 16
1997 Nov 12
1998 Aug 09
1998 Sep 15
Relative height (m)
1
0
-1
-2
-3
-4
vertical exaggeration= 10:1
-50
0
50
100
150
200
Distance (m)

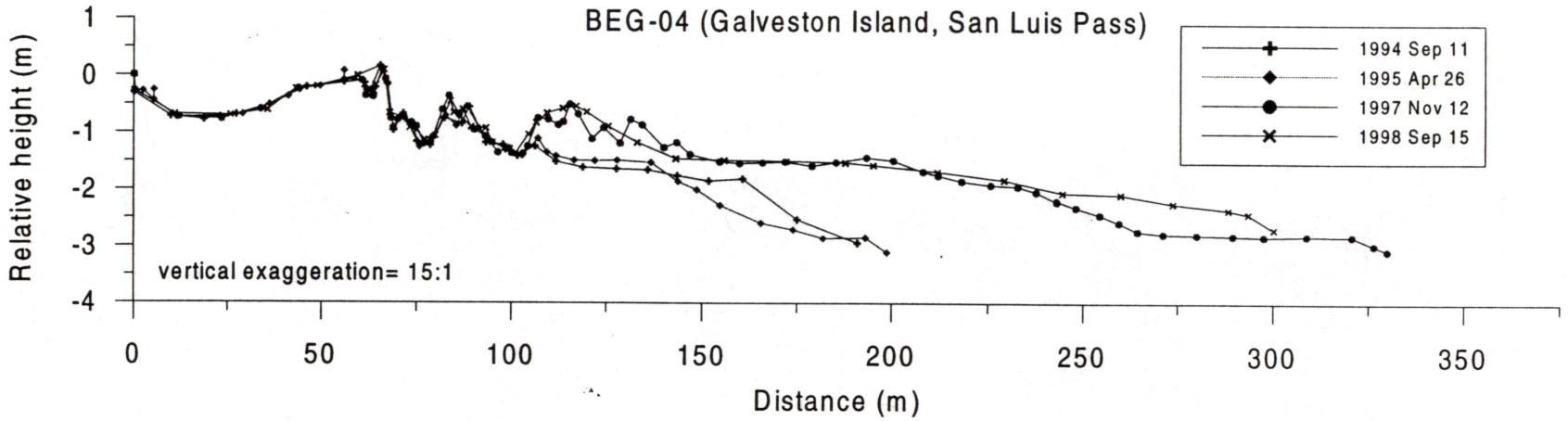
BEG-04 (Galveston Island, San Luis Pass)
1994 Sep 11
1995 Apr 26
1997 Nov 12
1998 Sep 15
Relative height (m)
vertical exaggeration= 15:1
Distance (m)

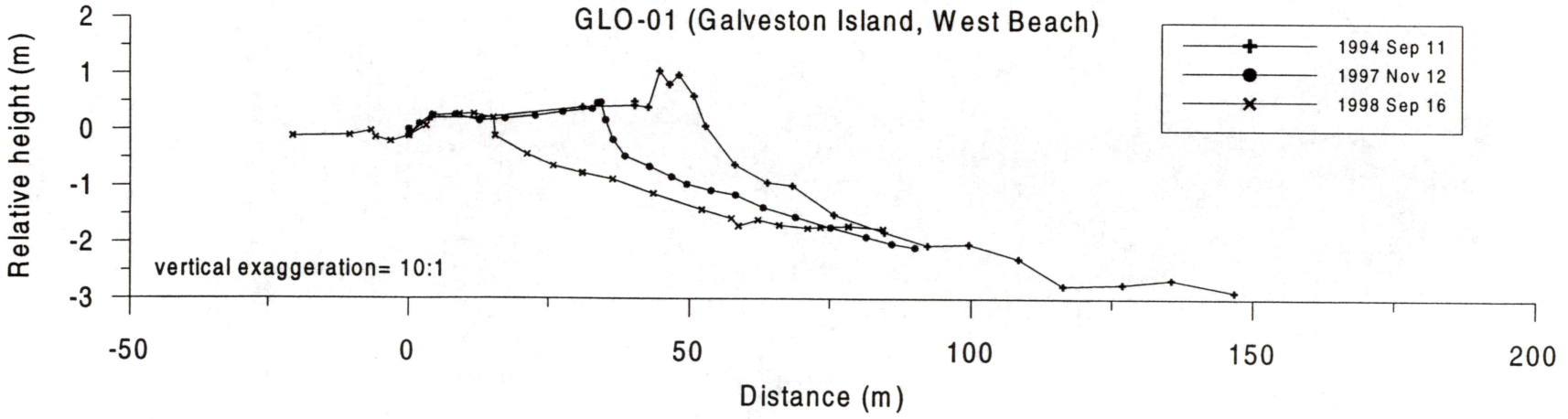
GLO-01 (Galveston Island, West Beach)
1994 Sep 11
1997 Nov 12
1998 Sep 16
Relative height (m)
vertical exaggeration= 10:1
Distance (m)

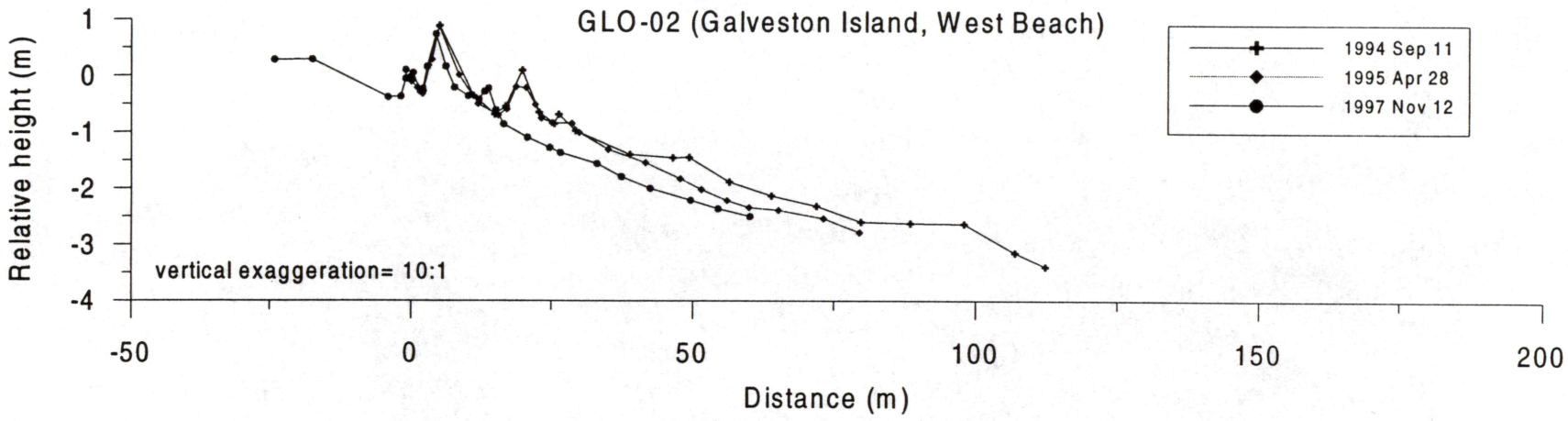
GLO-02 (Galveston Island, West Beach)
1994 Sep 11
1995 Apr 28
1997 Nov 12
Relative height (m)
1
0
-1
-2
-3
-4
vertical exaggeration= 10:1
-50
0
50
100
150
200
Distance (m)

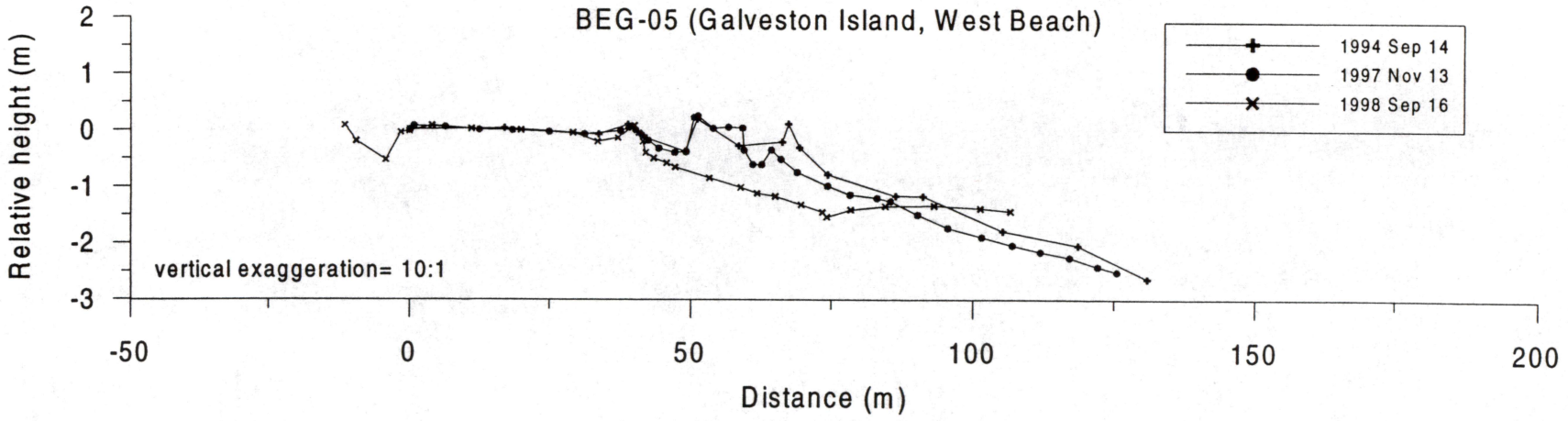
BEG-05 (Galveston Island, West Beach)
1994 Sep 14
1997 Nov 13
1998 Sep 16
Relative height (m)
2
1
0
-1
-2
-3
vertical exaggeration= 10:1
-50
0
50
100
150
200
Distance (m)

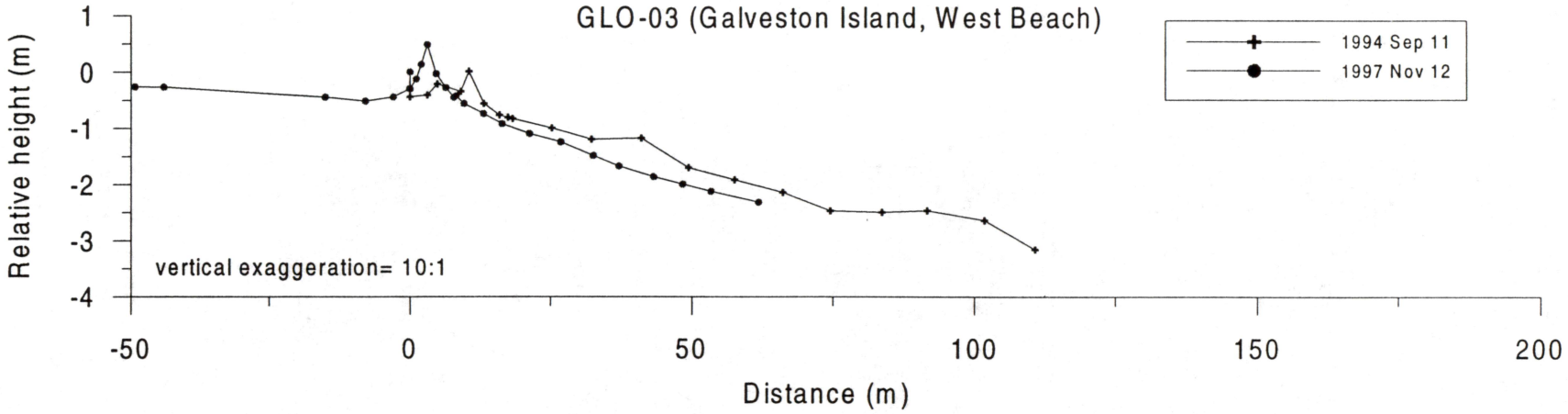
GLO-03 (Galveston Island, West Beach)
1994 Sep 11
1997 Nov 12
Relative height (m)
1
0
-1
-2
-3
-4
vertical exaggeration= 10:1
-50
0
50
100
150
200
Distance (m)

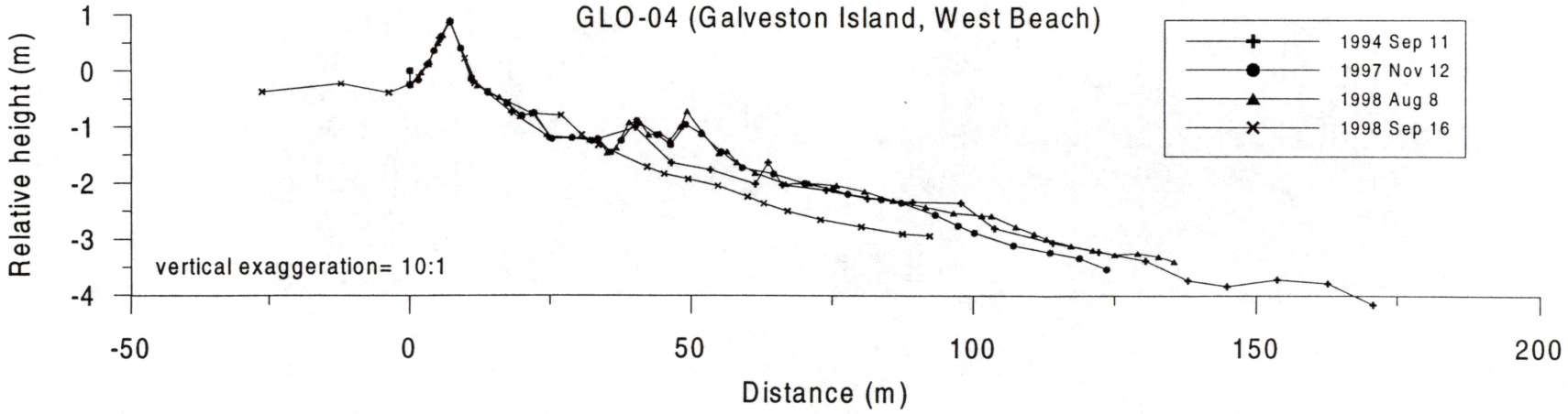
GLO-04 (Galveston Island, West Beach)
1994 Sep 11
1997 Nov 12
1998 Aug 8
1998 Sep 16
Relative height (m)
1
0
-1
-2
-3
-4
vertical exaggeration= 10:1
-50
0
50
100
150
200
Distance (m)

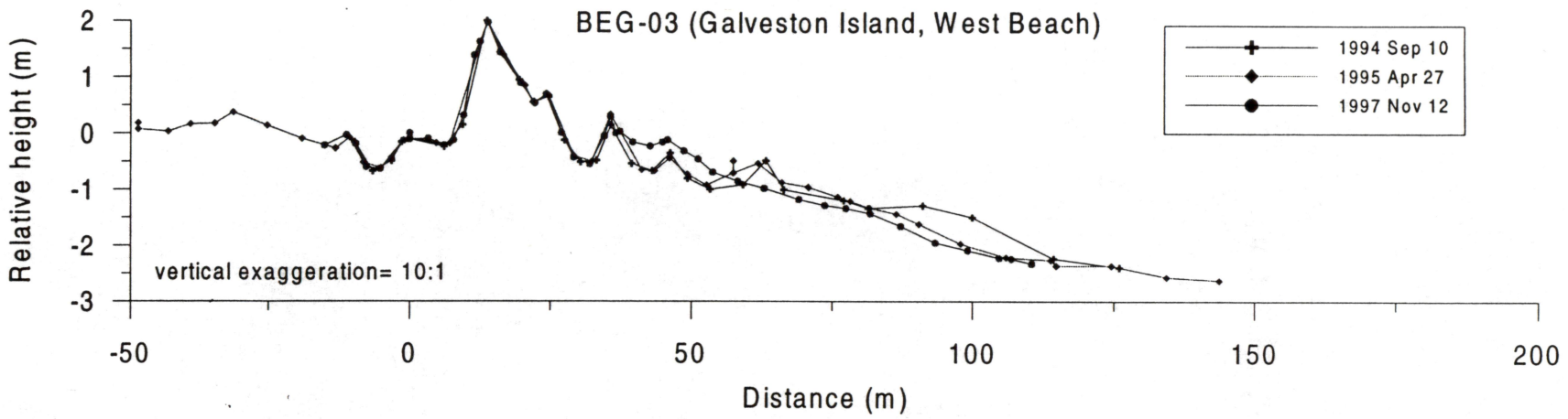
BEG-03 (Galveston Island, West Beach)
1994 Sep 10
1995 Apr 27
1997 Nov 12
Relative height (m)
2
1
0
-1
-2
-3
vertical exaggeration= 10:1
-50
0
50
100
150
200
Distance (m)

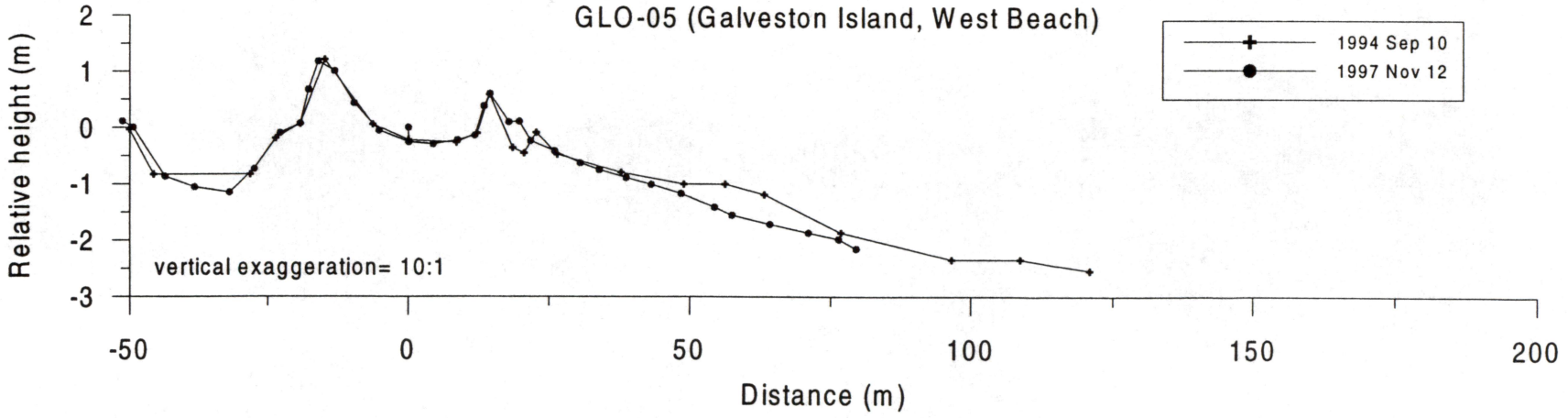
GLO-05 (Galveston Island, West Beach)
1994 Sep 10
1997 Nov 12
Relative height (m)
2
1
0
-1
-2
-3
vertical exaggeration= 10:1
-50
0
50
100
150
200
Distance (m)

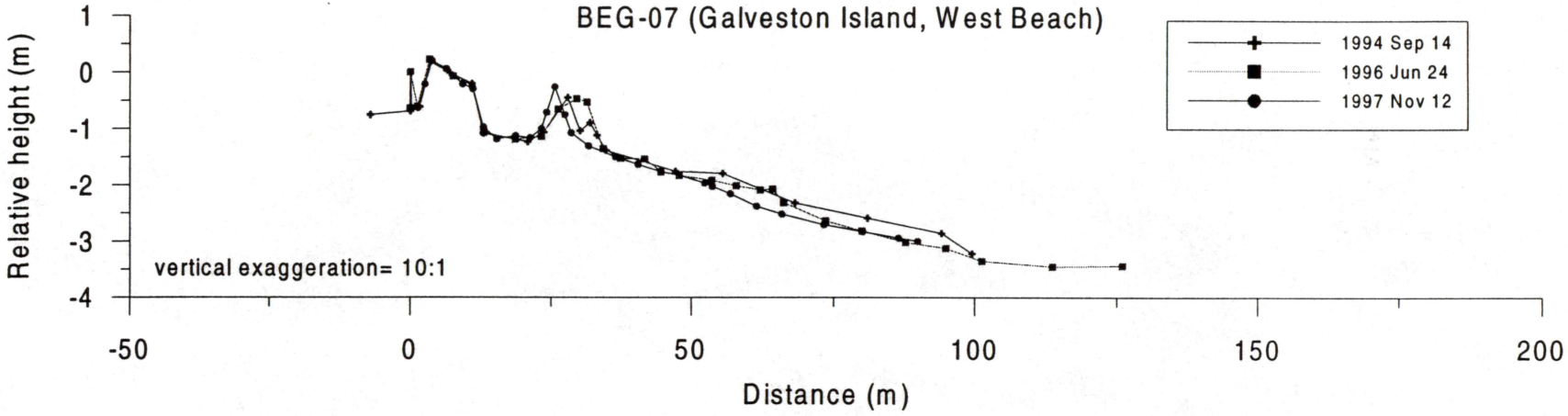
BEG-07 (Galveston Island, West Beach)
1994 Sep 14
1996 Jun 24
1997 Nov 12
Relative height (m)
1
0
-1
-2
-3
-4
vertical exaggeration= 10:1
-50
0
50
100
150
200
Distance (m)

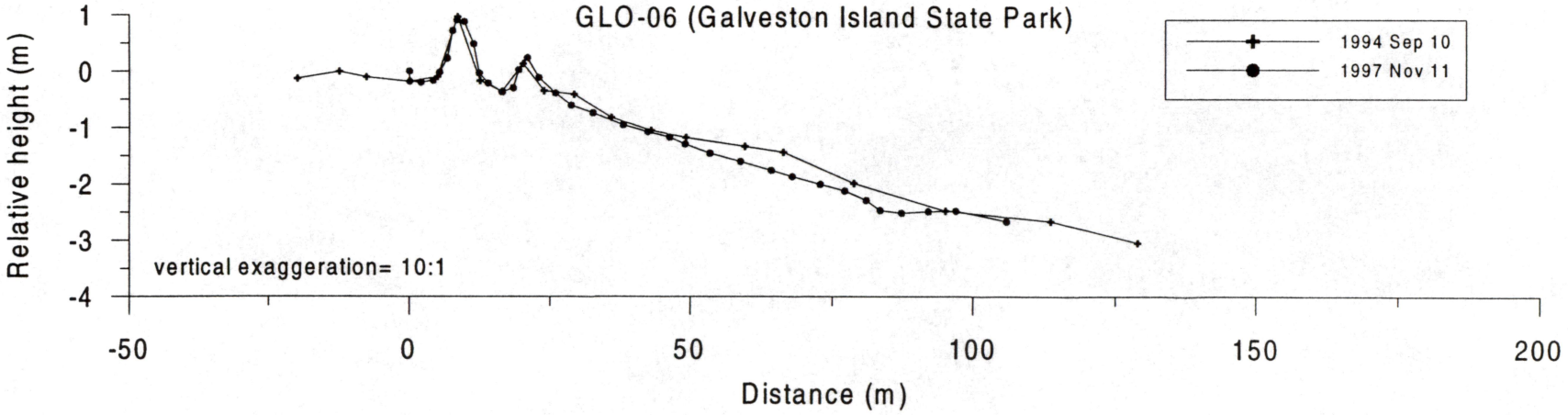
GLO-06 (Galveston Island State Park)
1994 Sep 10
1997 Nov 11
Relative height (m)
1
0
-1
-2
-3
-4
vertical exaggeration= 10:1
-50
0
50
100
150
200
Distance (m)

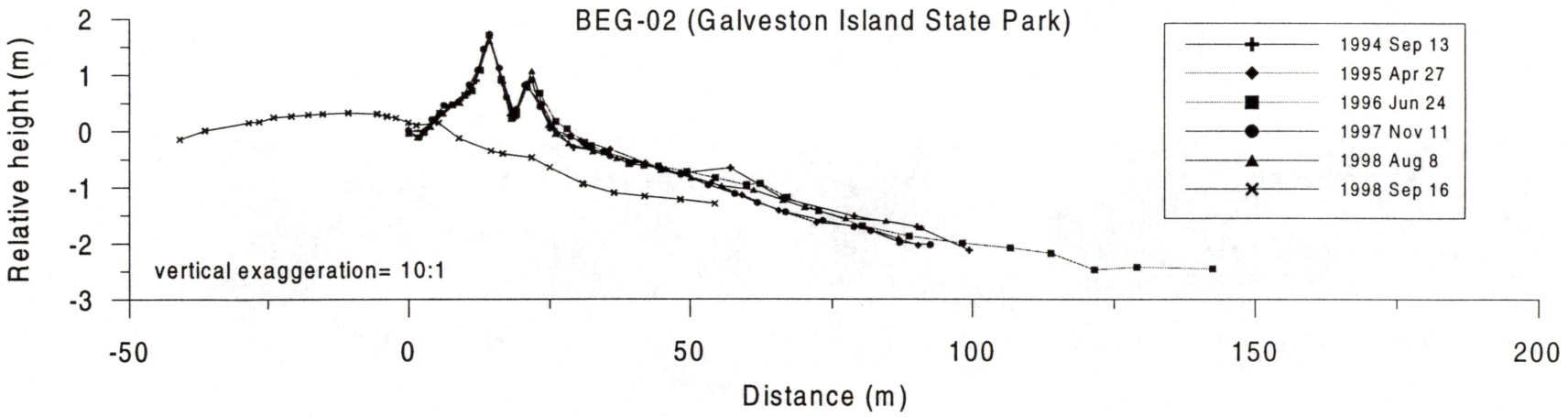
BEG-02 (Galveston Island State Park)
Relative height (m)
2
1
0
-1
-2
-3
vertical exaggeration= 10:1
-50
0
50
100
150
200
Distance (m)
1994 Sep 13
1995 Apr 27
1996 Jun 24
1997 Nov 11
1998 Aug 8
1998 Sep 16

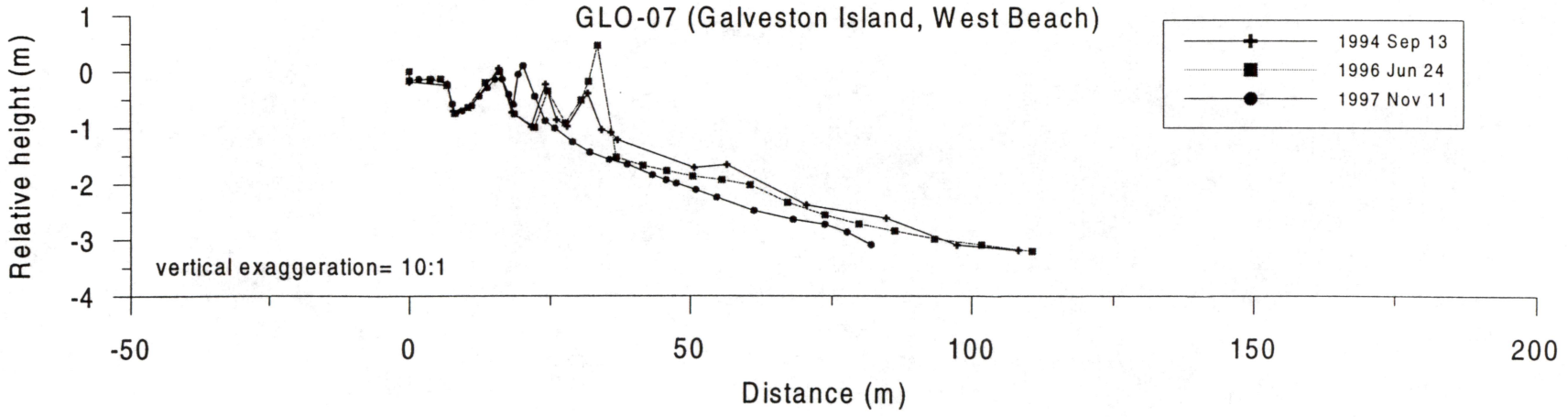
GLO-07 (Galveston Island, West Beach)
Relative height (m)
1
0
-1
-2
-3
-4
vertical exaggeration= 10:1
-50
0
50
100
150
200
Distance (m)
1994 Sep 13
1996 Jun 24
1997 Nov 11

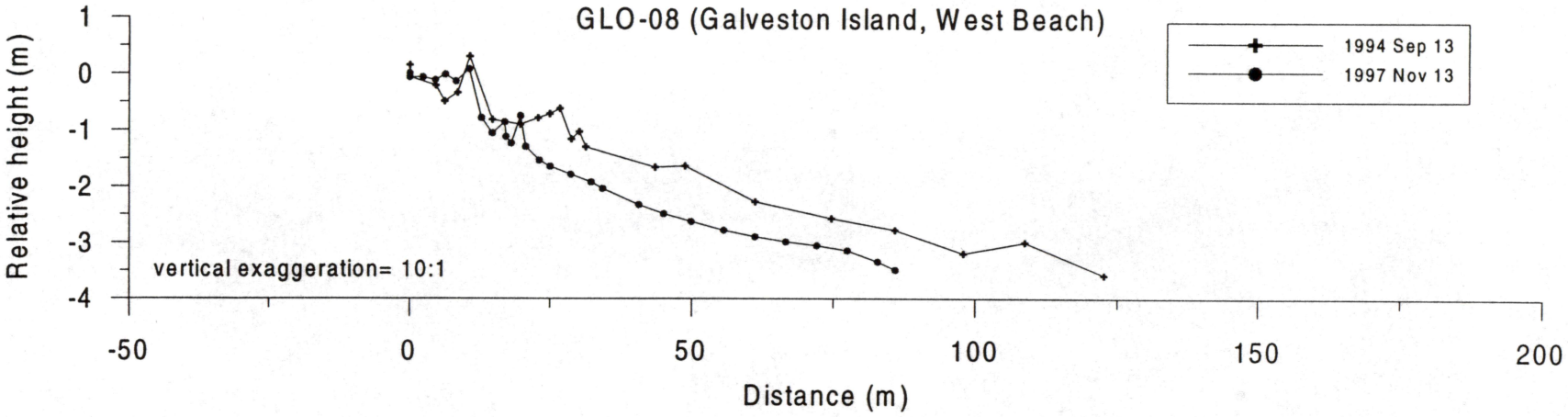
GLO-08 (Galveston Island, West Beach)
1994 Sep 13
1997 Nov 13
Relative height (m)
1
0
-1
-2
-3
-4
vertical exaggeration= 10:1
-50
0
50
100
150
200
Distance (m)

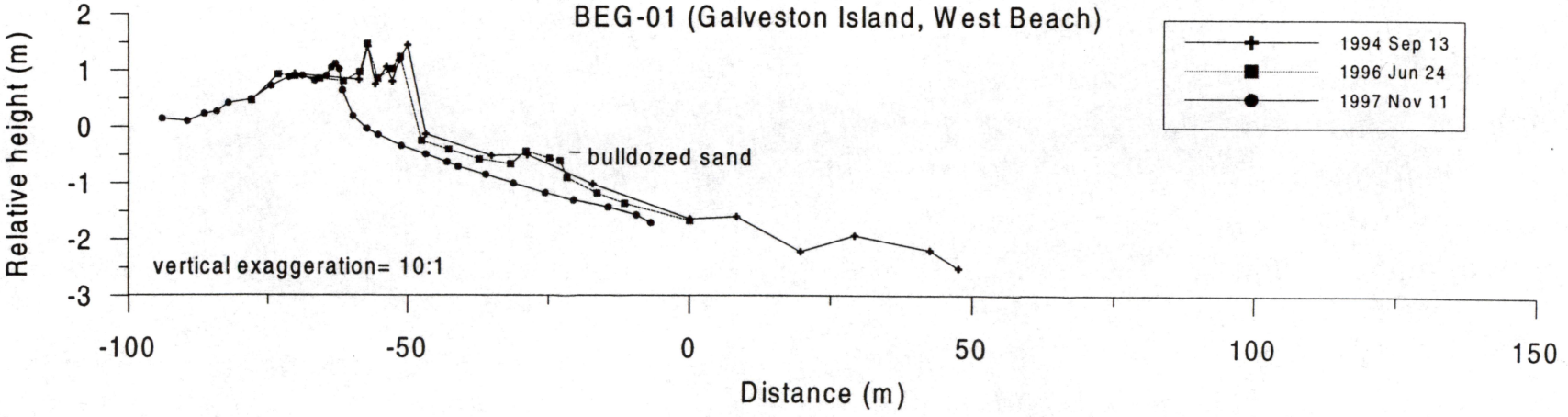
BEG-01 (Galveston Island, West Beach)
1994 Sep 13
1996 Jun 24
1997 Nov 11
Relative height (m)
2
1
0
-1
-2
-3
bulldozed sand
vertical exaggeration= 10:1
-100
-50
0
50
100
150
Distance (m)

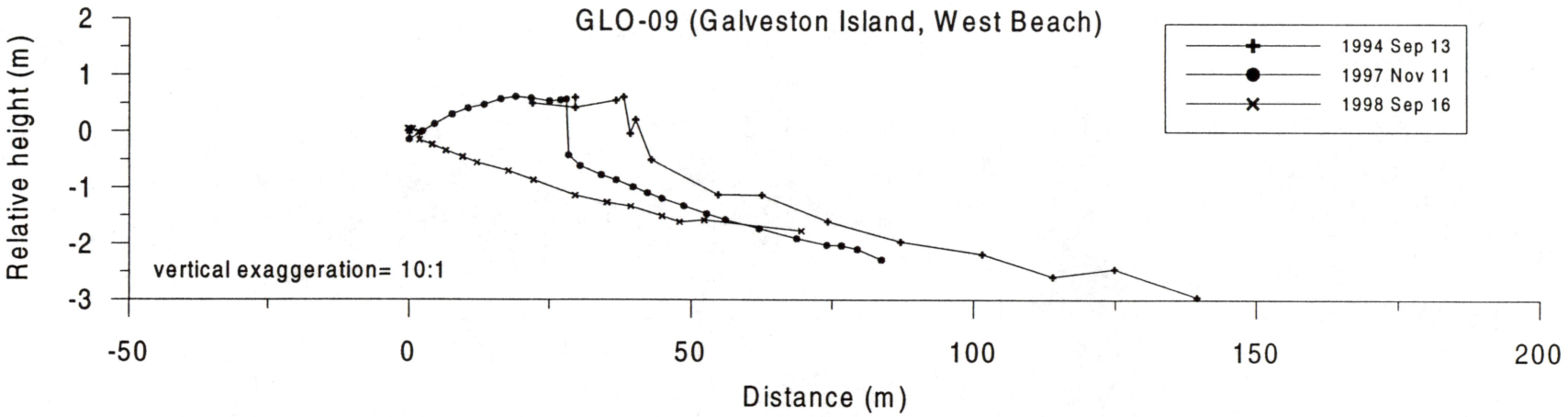
GLO-09 (Galveston Island, West Beach)
1994 Sep 13
1997 Nov 11
1998 Sep 16
Relative height (m)
2
1
0
-1
-2
-3
vertical exaggeration= 10:1
-50
0
50
100
150
200
Distance (m)

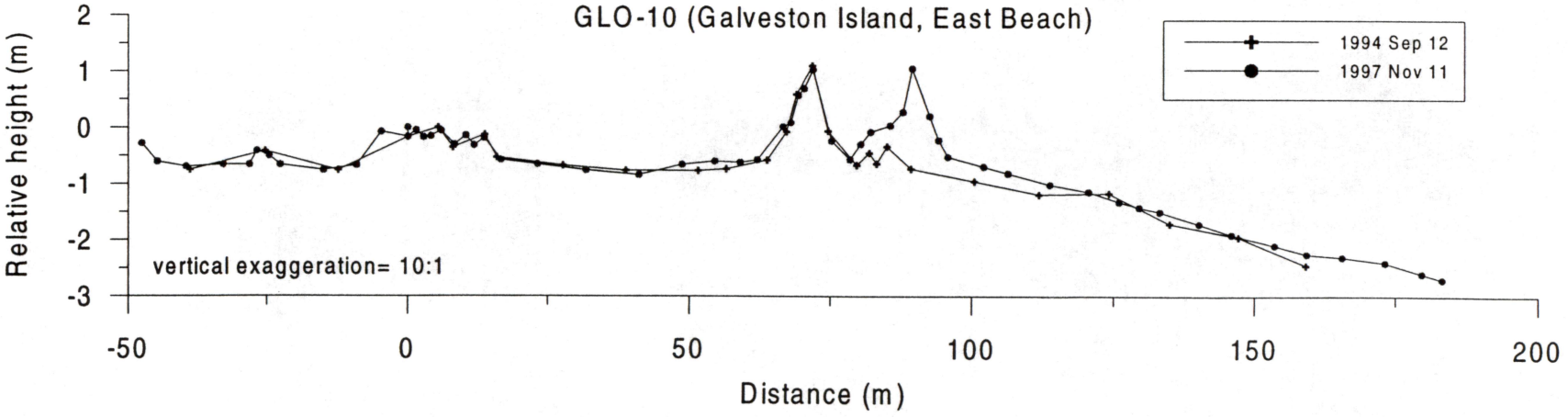
GLO-10 (Galveston Island, East Beach)
1994 Sep 12
1997 Nov 11
Relative height (m)
2
1
0
-1
-2
-3
vertical exaggeration= 10:1
-50
0
50
100
150
200
Distance (m)

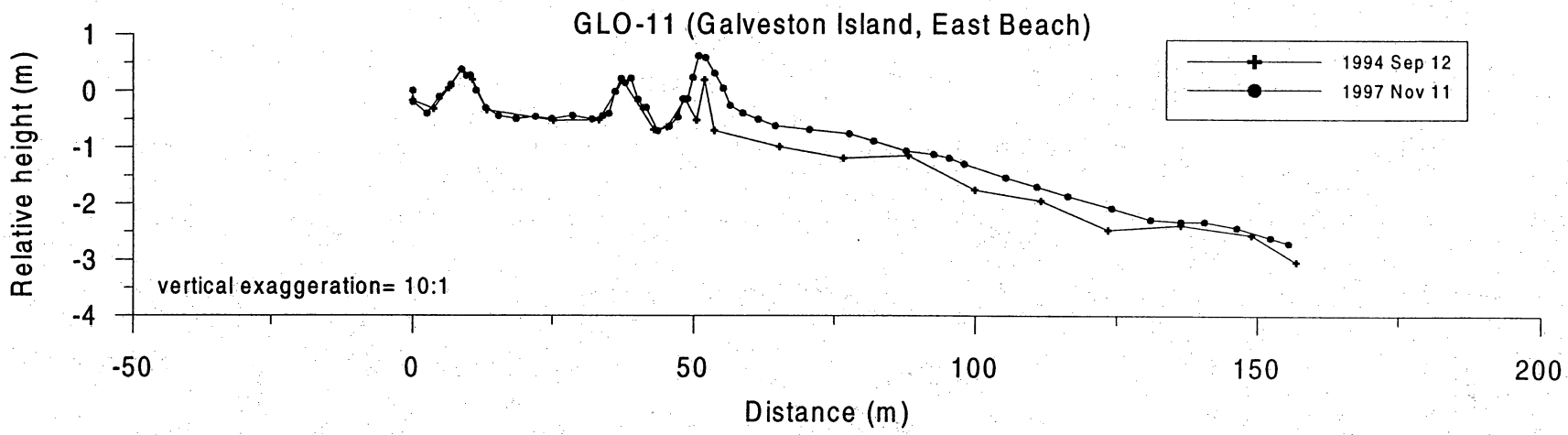
GLO-11 (Galveston Island, East Beach)
1994 Sep 12
1997 Nov 11
Relative height (m)
1
0
-1
-2
-3
-4
vertical exaggeration= 10:1
-50
0
50
100
150
200
Distance (m)

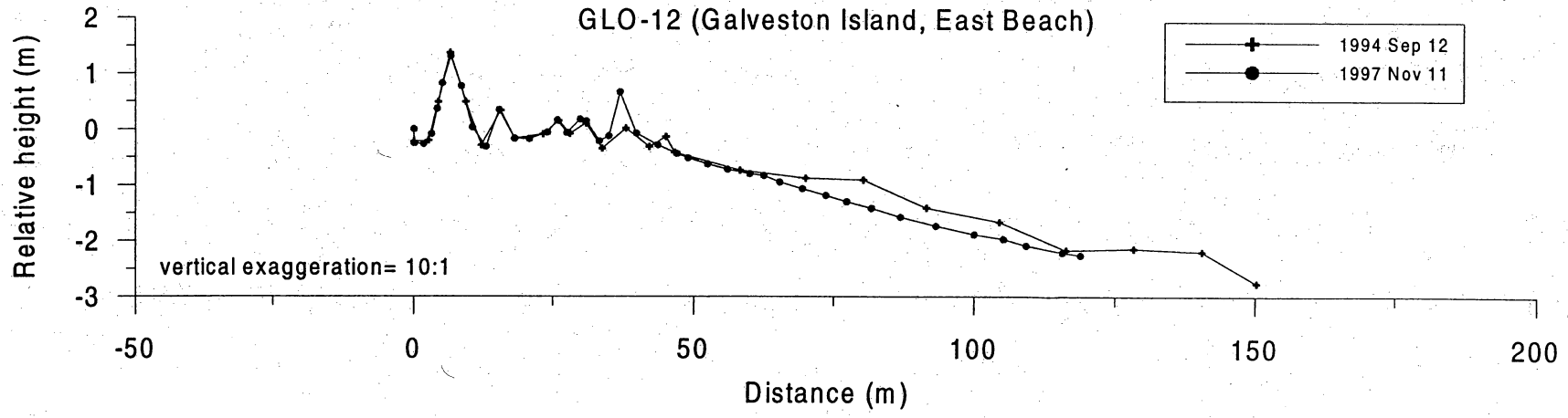
GLO-12 (Galveston Island, East Beach)
1994 Sep 12
1997 Nov 11
Relative height (m)
2
1
0
-1
-2
-3
vertical exaggeration= 10:1
-50
0
50
100
150
200
Distance (m)

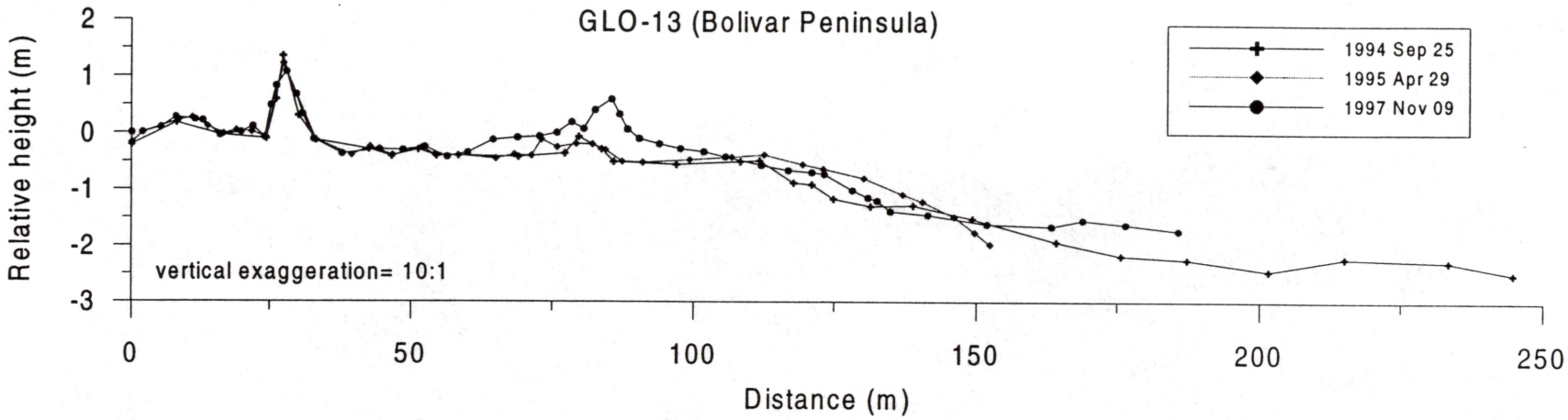
GLO-13 (Bolivar Peninsula)
1994 Sep 25
1995 Apr 29
1997 Nov 09
Relative height (m)
2
1
0
-1
-2
-3
vertical exaggeration= 10:1
0
50
100
150
200
250
Distance (m)

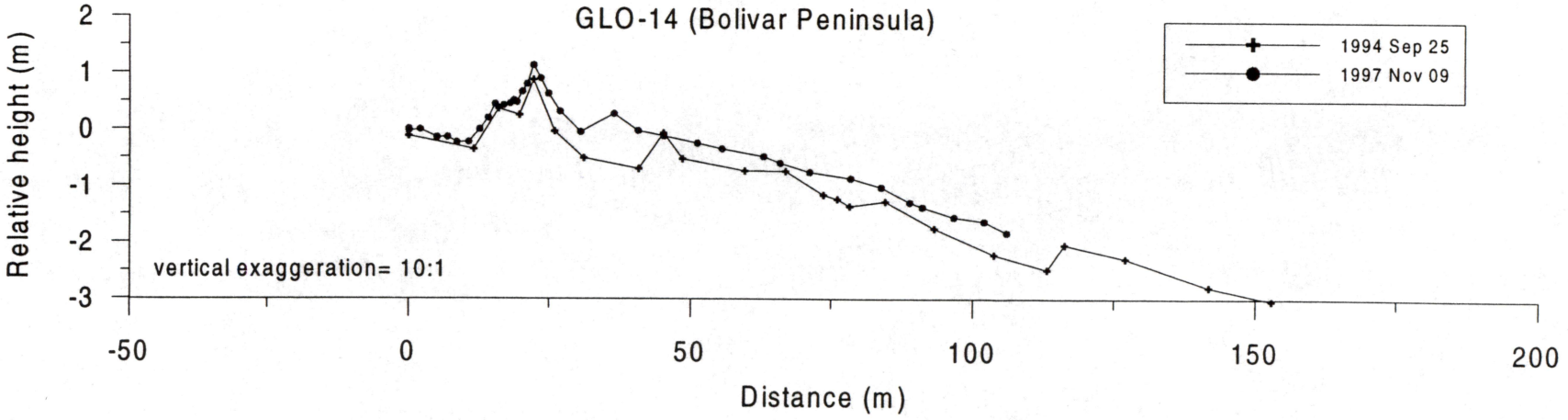
GLO-14 (Bolivar Peninsula)
1994 Sep 25
1997 Nov 09
Relative height (m)
2
1
0
-1
-2
-3
vertical exaggeration= 10:1
-50
0
50
100
150
200
Distance (m)

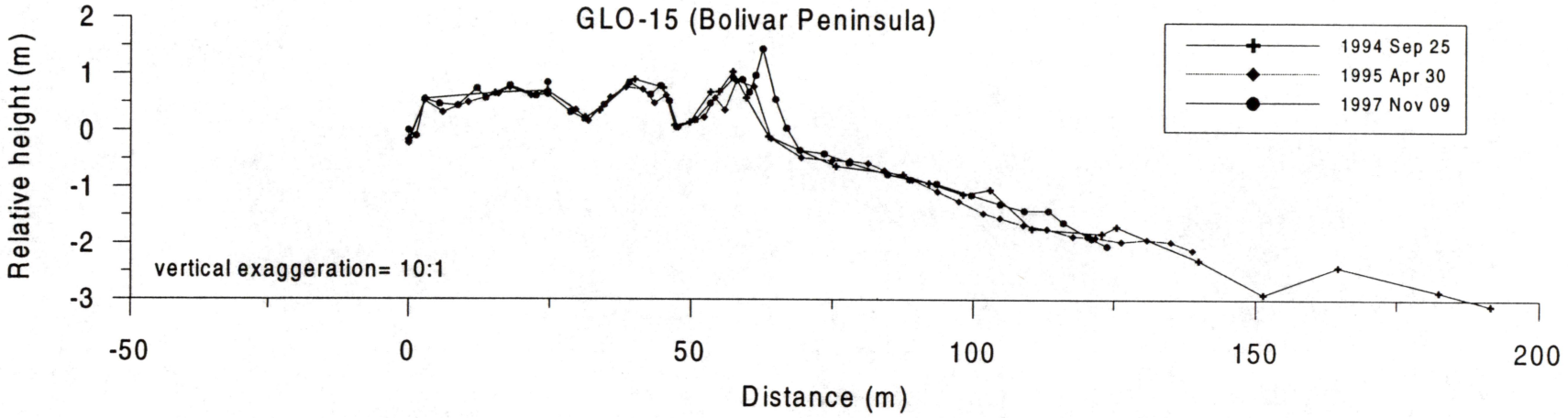
GLO-15 (Bolivar Peninsula)
1994 Sep 25
1995 Apr 30
1997 Nov 09
Relative height (m)
2
1
0
-1
-2
-3
vertical exaggeration= 10:1
-50
0
50
100
150
200
Distance (m)

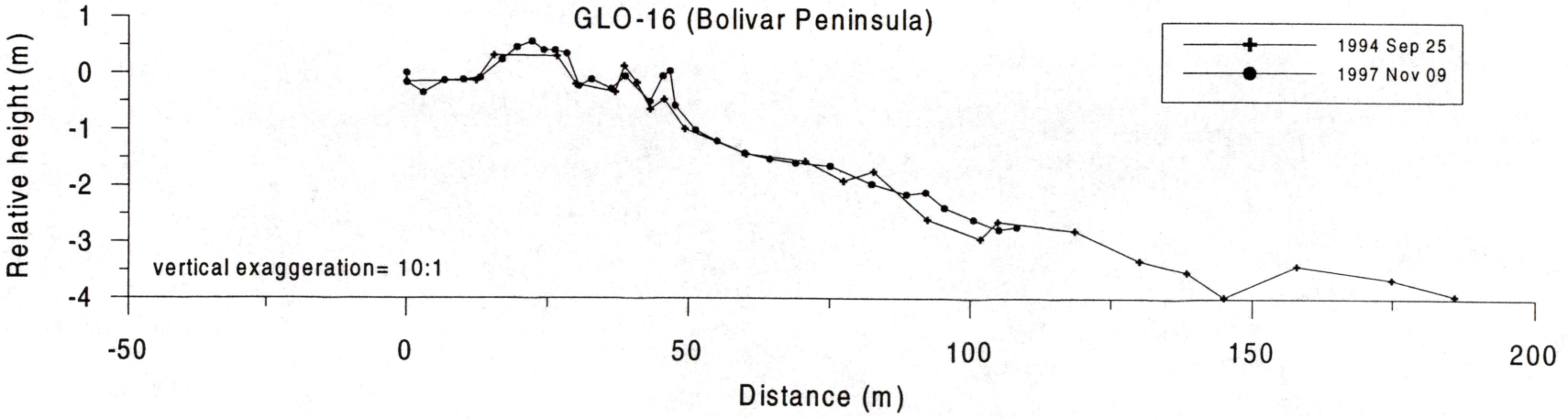
GLO-16 (Bolivar Peninsula)
1994 Sep 25
1997 Nov 09
Relative height (m)
1
0
-1
-2
-3
-4
vertical exaggeration= 10:1
-50
0
50
100
150
200
Distance (m)

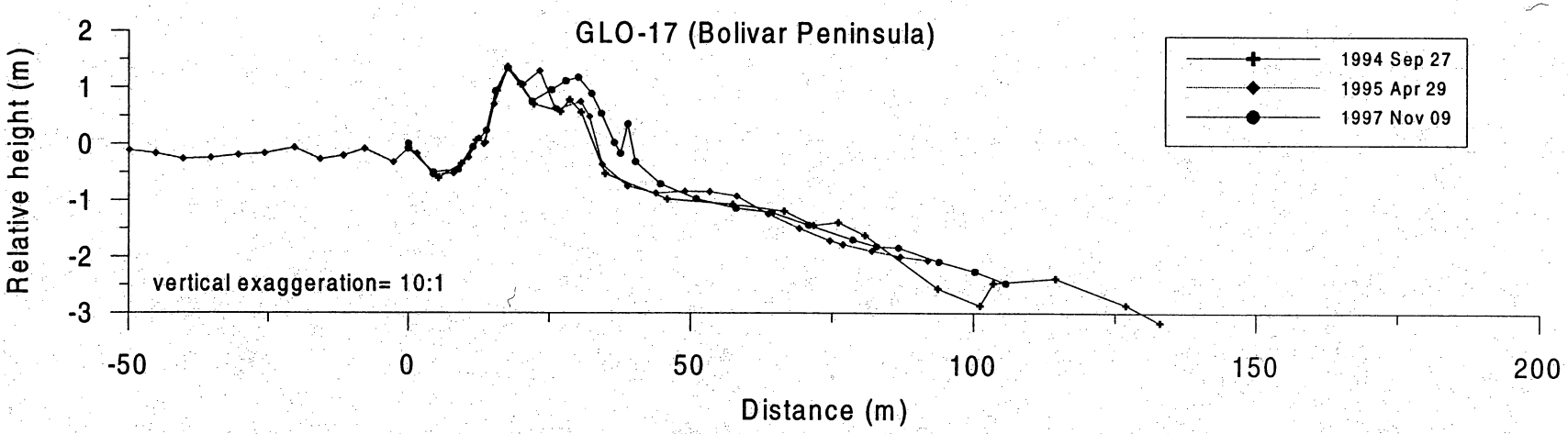
GLO-17 (Bolivar Peninsula)
1994 Sep 27
1995 Apr 29
1997 Nov 09
Relative height (m)
2
1
0
-1
-2
-3
vertical exaggeration= 10:1
-50
0
50
100
150
200
Distance (m)

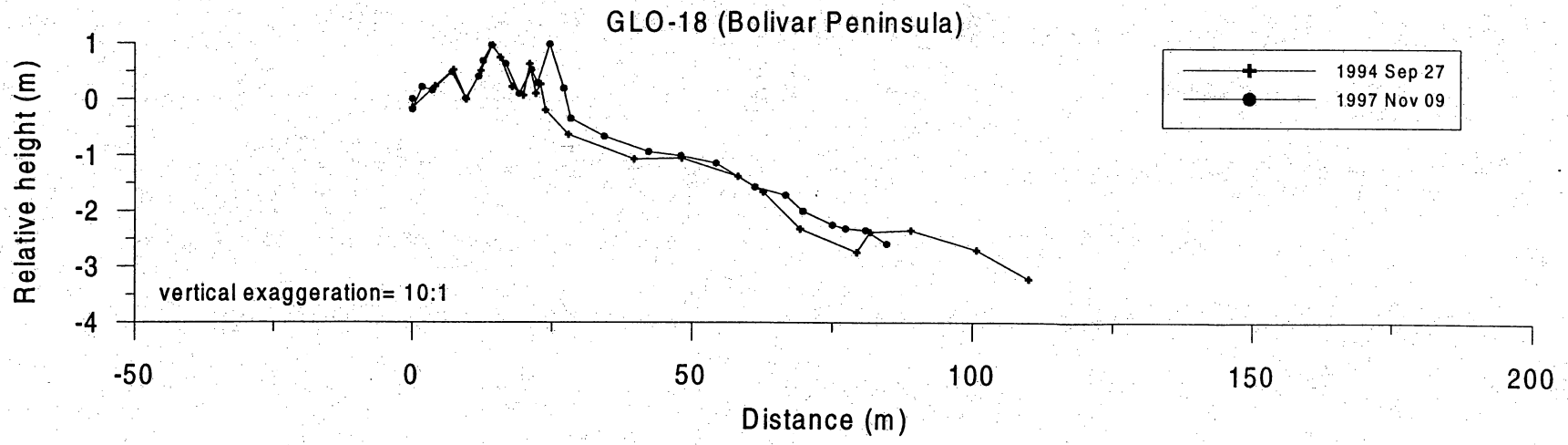
GLO-18 (Bolivar Peninsula)
1994 Sep 27
1997 Nov 09
Relative height (m)
1
0
-1
-2
-3
-4
vertical exaggeration= 10:1
-50
0
50
100
150
200
Distance (m)

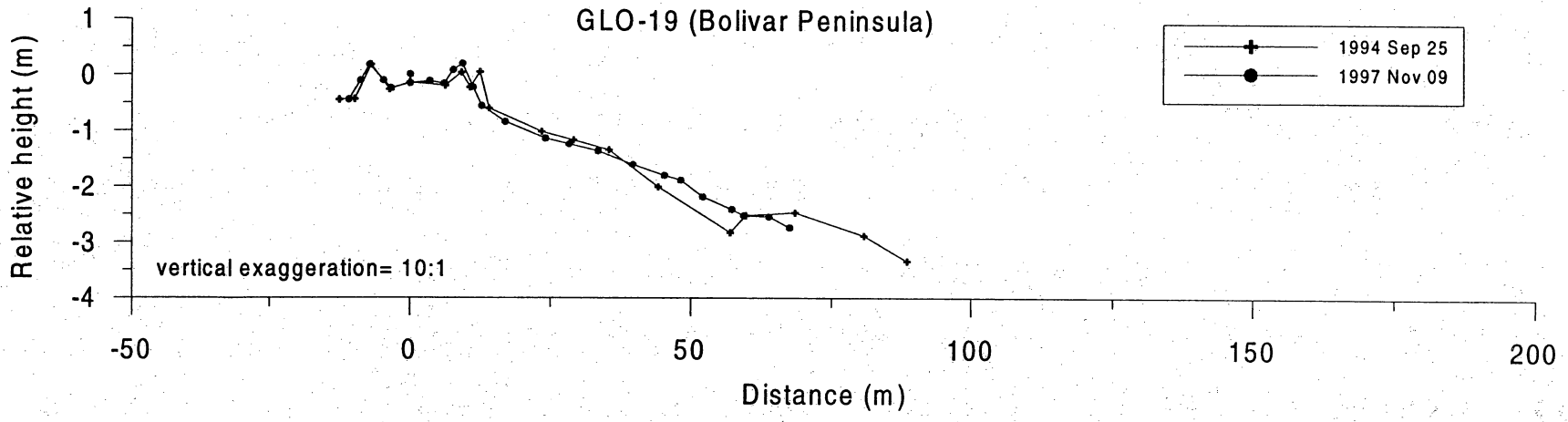
GLO-19 (Bolivar Peninsula)
1994 Sep 25
1997 Nov 09
Relative height (m)
1
0
-1
-2
-3
-4
vertical exaggeration= 10:1
-50
0
50
100
150
200
Distance (m)

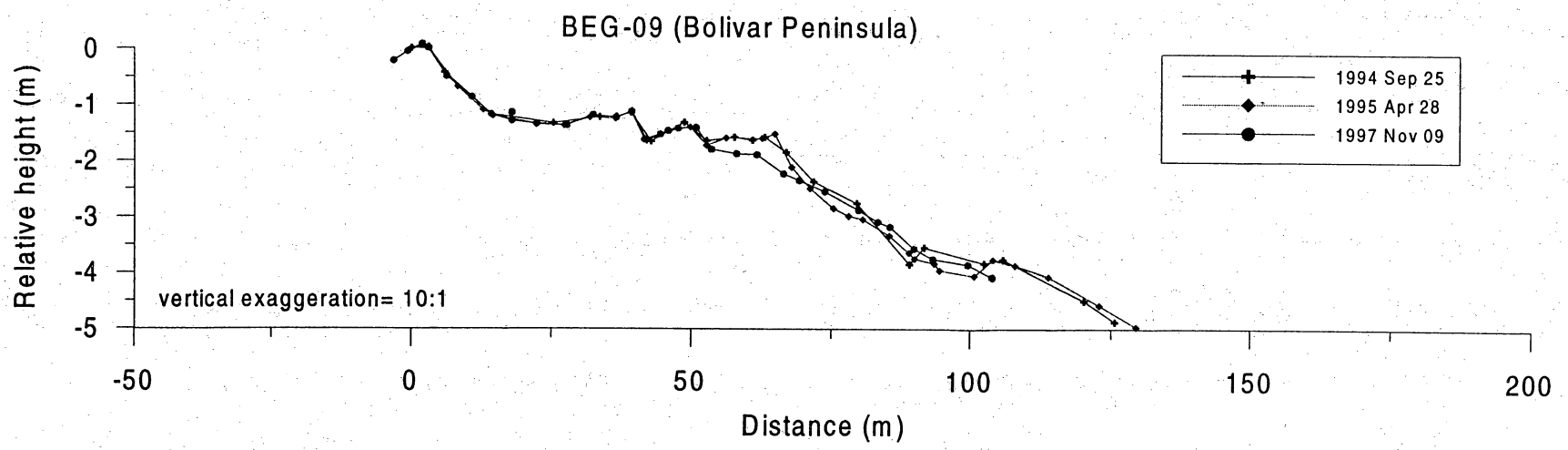
BEG-09 (Bolivar Peninsula)
1994 Sep 25
1995 Apr 28
1997 Nov 09
Relative height (m)
0
-1
-2
-3
-4
-5
vertical exaggeration= 10:1
-50
0
50
100
150
200
Distance (m)

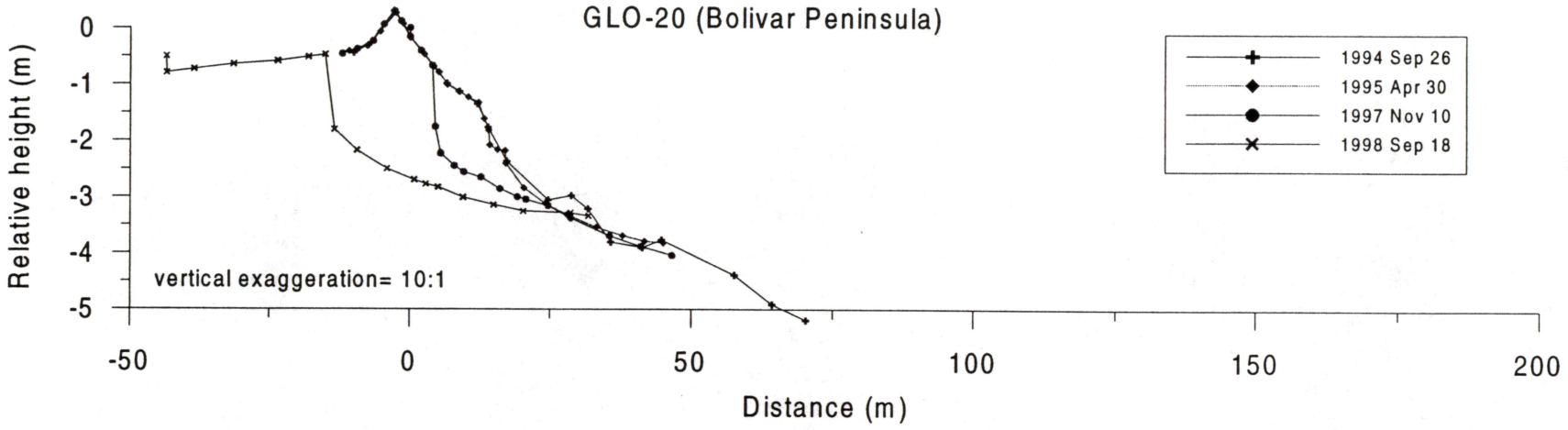
GLO-20 (Bolivar Peninsula)
Relative height (m)
0
-1
-2
-3
-4
-5
vertical exaggeration= 10:1
-50
0
50
100
150
200
Distance (m)
1994 Sep 26
1995 Apr 30
1997 Nov 10
1998 Sep 18

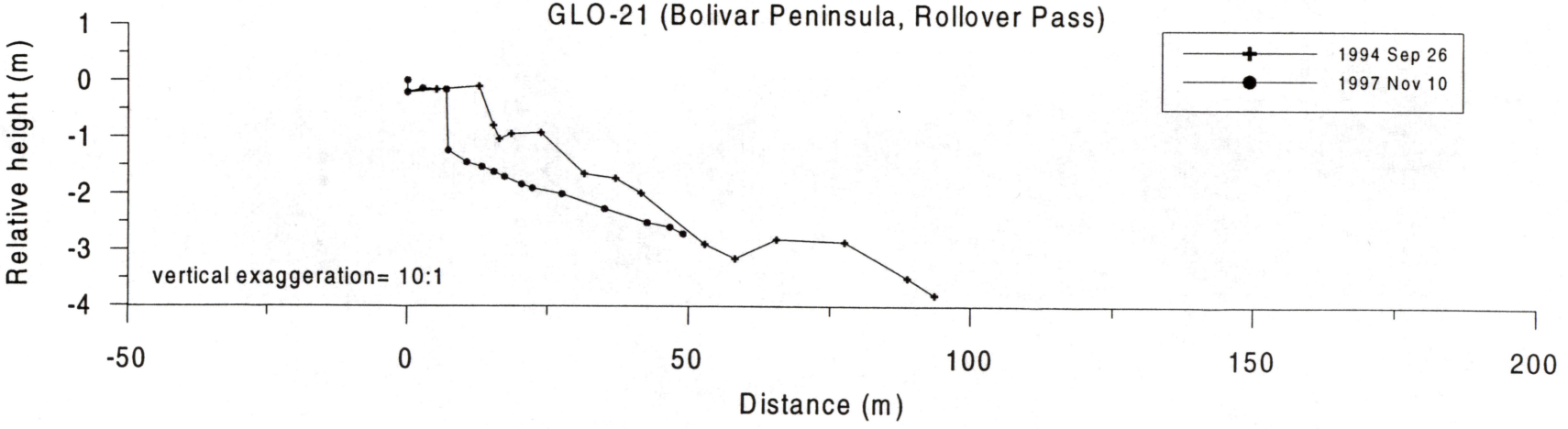
GLO-21 (Bolivar Peninsula, Rollover Pass)
Relative height (m)
1
0
-1
-2
-3
-4
vertical exaggeration= 10:1
-50
0
50
100
150
200
Distance (m)
1994 Sep 26
1997 Nov 10

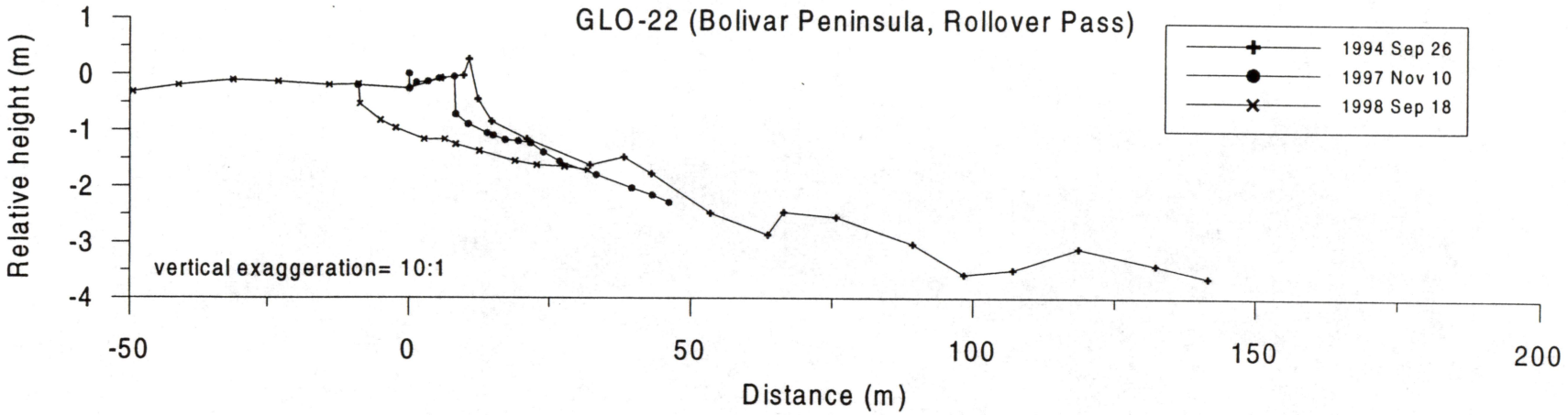
GLO-22 (Bolivar Peninsula, Rollover Pass)
1994 Sep 26
1997 Nov 10
1998 Sep 18
Relative height (m)
1
0
-1
-2
-3
-4
vertical exaggeration= 10:1
-50
0
50
100
150
200
Distance (m)

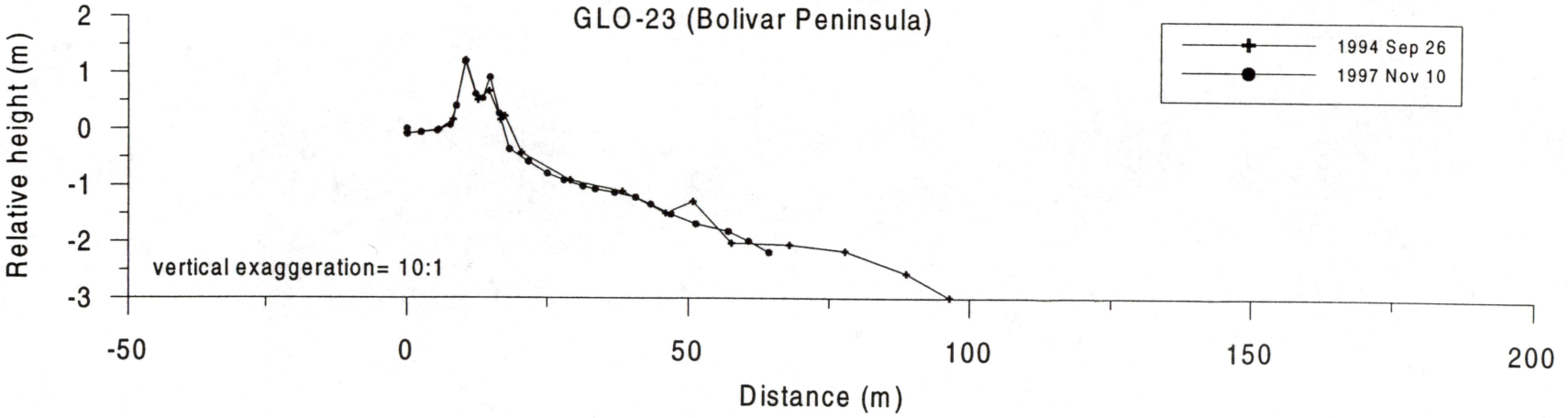
GLO-23 (Bolivar Peninsula)
1994 Sep 26
1997 Nov 10
Relative height (m)
2
1
0
-1
-2
-3
vertical exaggeration= 10:1
-50
0
50
100
150
200
Distance (m)

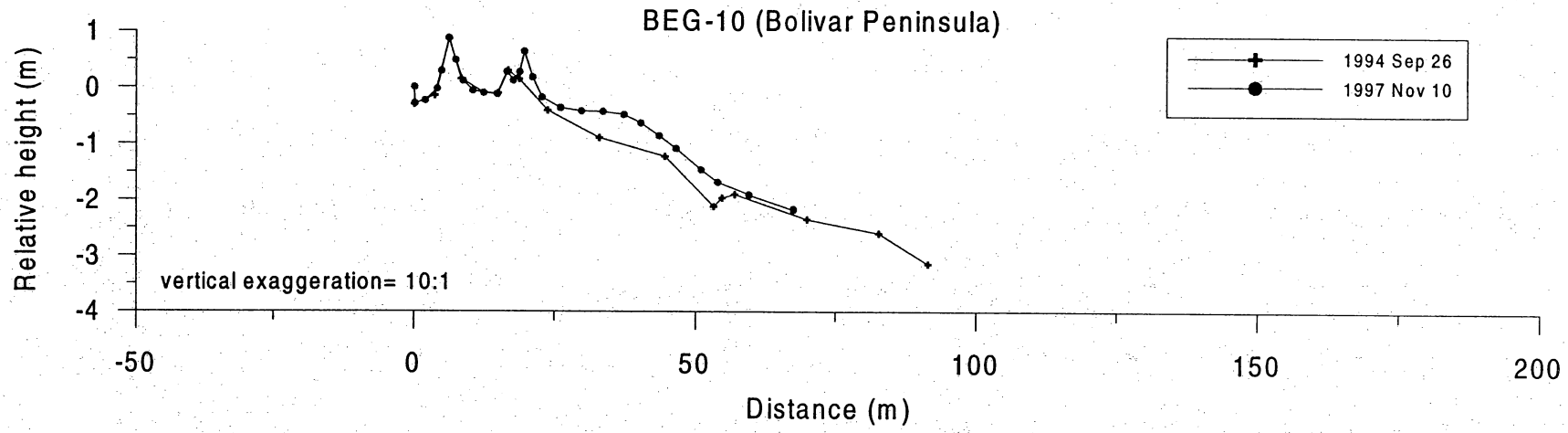
BEG-10 (Bolivar Peninsula)
1994 Sep 26
1997 Nov 10
Relative height (m)
1
0
-1
-2
-3
-4
vertical exaggeration= 10:1
-50
0
50
100
150
200
Distance (m)

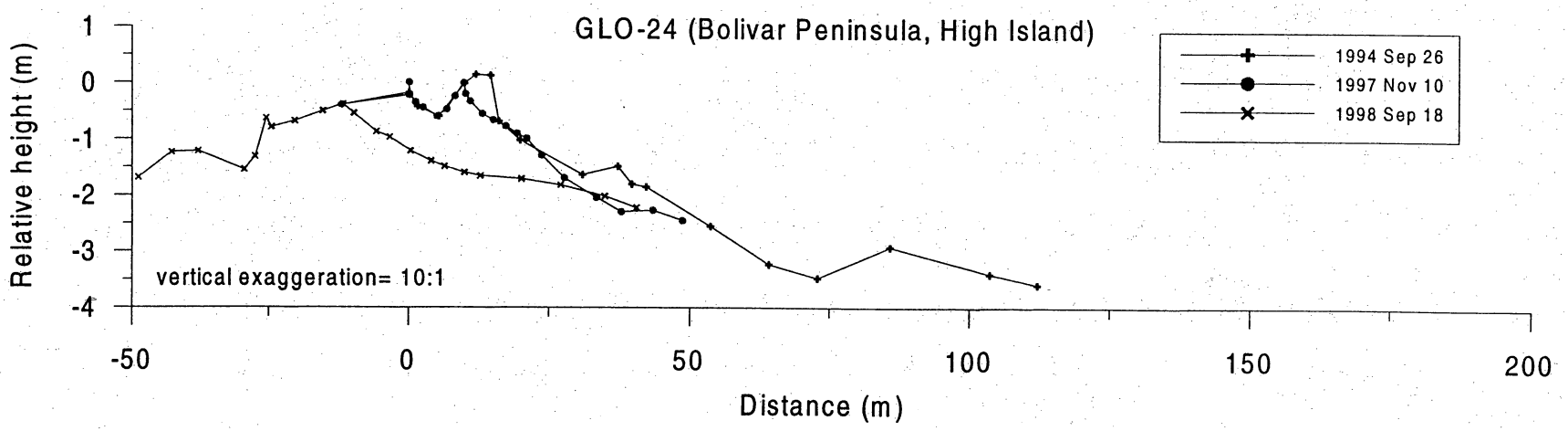
GLO-24 (Bolivar Peninsula, High Island)
1994 Sep 26
1997 Nov 10
1998 Sep 18
Relative height (m)
1
0
-1
-2
-3
-4
vertical exaggeration= 10:1
-50
0
50
100
150
200
Distance (m)

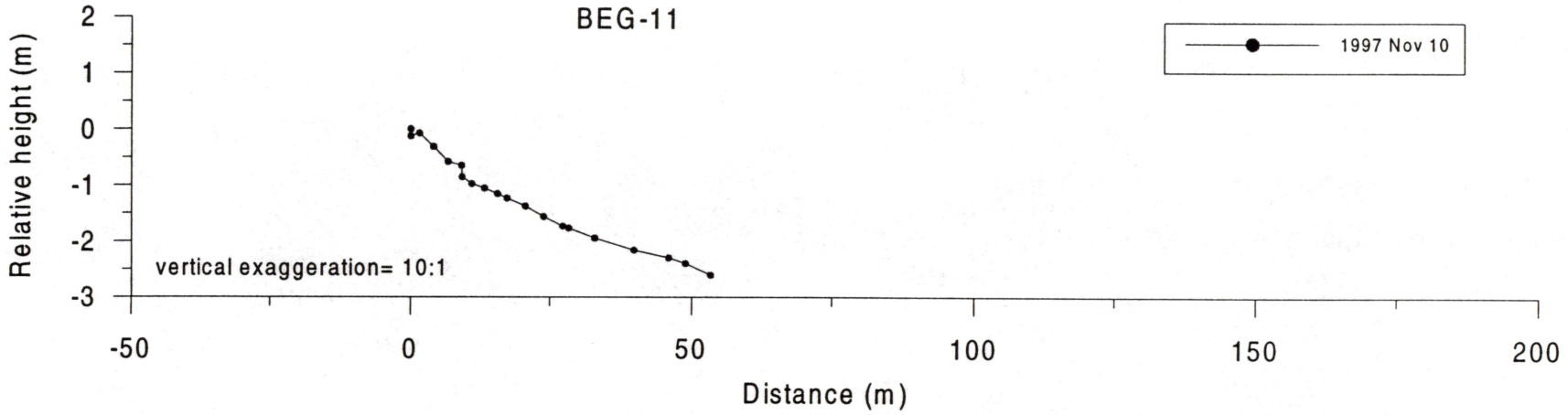
BEG-11
1997 Nov 10
Relative height (m)
2
1
0
-1
-2
-3
vertical exaggeration= 10:1
-50
0
50
100
150
200
Distance (m)

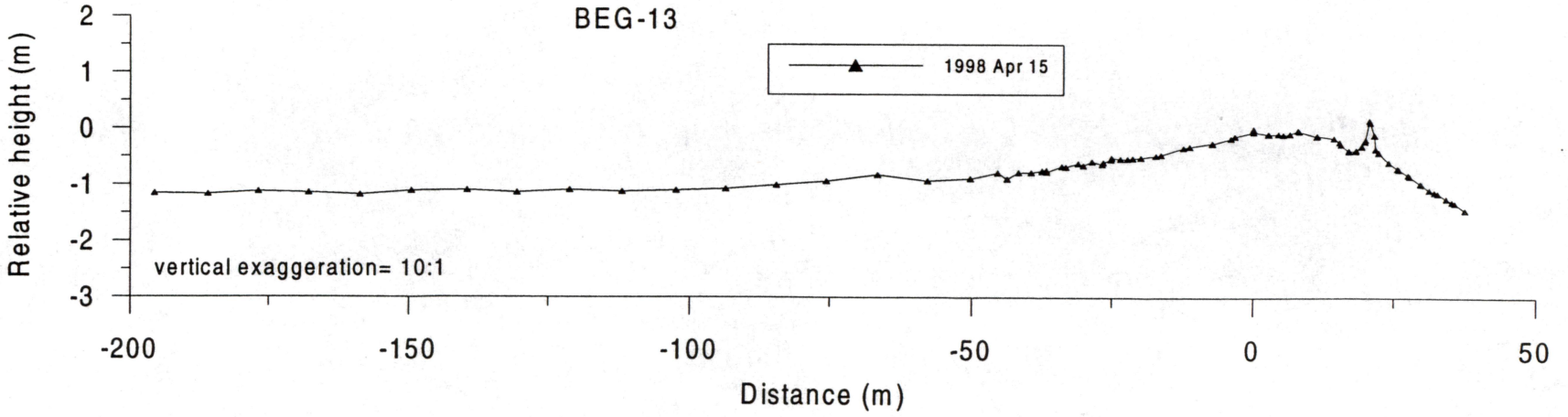
BEG-13
1998 Apr 15
Relative height (m)
2
1
0
-1
-2
-3
vertical exaggeration= 10:1
-200
-150
-100
-50
0
50
Distance (m)

Appendix B
Article published as a "Highlight" article in Photogrammetric Engineering & Remote Sensing, April 1998, p. 246-253.

Engineering Applications of Airborne Scanning Lasers: Reports From the Field

BILL BUTELJUS

Several organizations and private enterprises have undertaken some challenging and unique mapping projects during 1996 and 1997. What distinguishes these projects from standard surveying and mapping operations is that they were performed with scanning airborne laser systems. The focus of these operations is to provide digital elevation information to engineers, scientists and commercial users to perform engineering-related tasks.

THANKS TO PIONEERING efforts by NASA and the ATM (Airborne Terrain Mapper) group at Wallops Island, airborne laser scanning has long been established as a topographic research tool. In the last five years, the airborne remote sensing sector has seen this technology emerge as an extremely rapid and highly accurate terrain-mapping tool. This development has spawned innovative solutions to difficult mapping problems. While there are only a few commercial manufacturers of such systems and little more than a handful of operators of airborne laser scanners, the use of these systems is growing quickly.

The following article discusses some of the innovative uses of airborne scanning lasers as applied to engineering projects. The focus will be on several samples of reports provided by commercial operators and researchers in the fields of Highway, Coastal and Power Line Engineering.

Dr. William E. Carter
& Dr. Ramesh L. Shrestha
University of Florida
Department of Civil Engineering

Introduction

The basic concepts of airborne laser terrain (ALTM) mapping are simple. A pulsed laser is optically coupled to a beam director which scans the laser pulses over a "swath" of terrain, usually centered on, and co-linear with, the flight path of the aircraft in which the system is mounted. The round trip travel times of the laser pulses from the aircraft to the

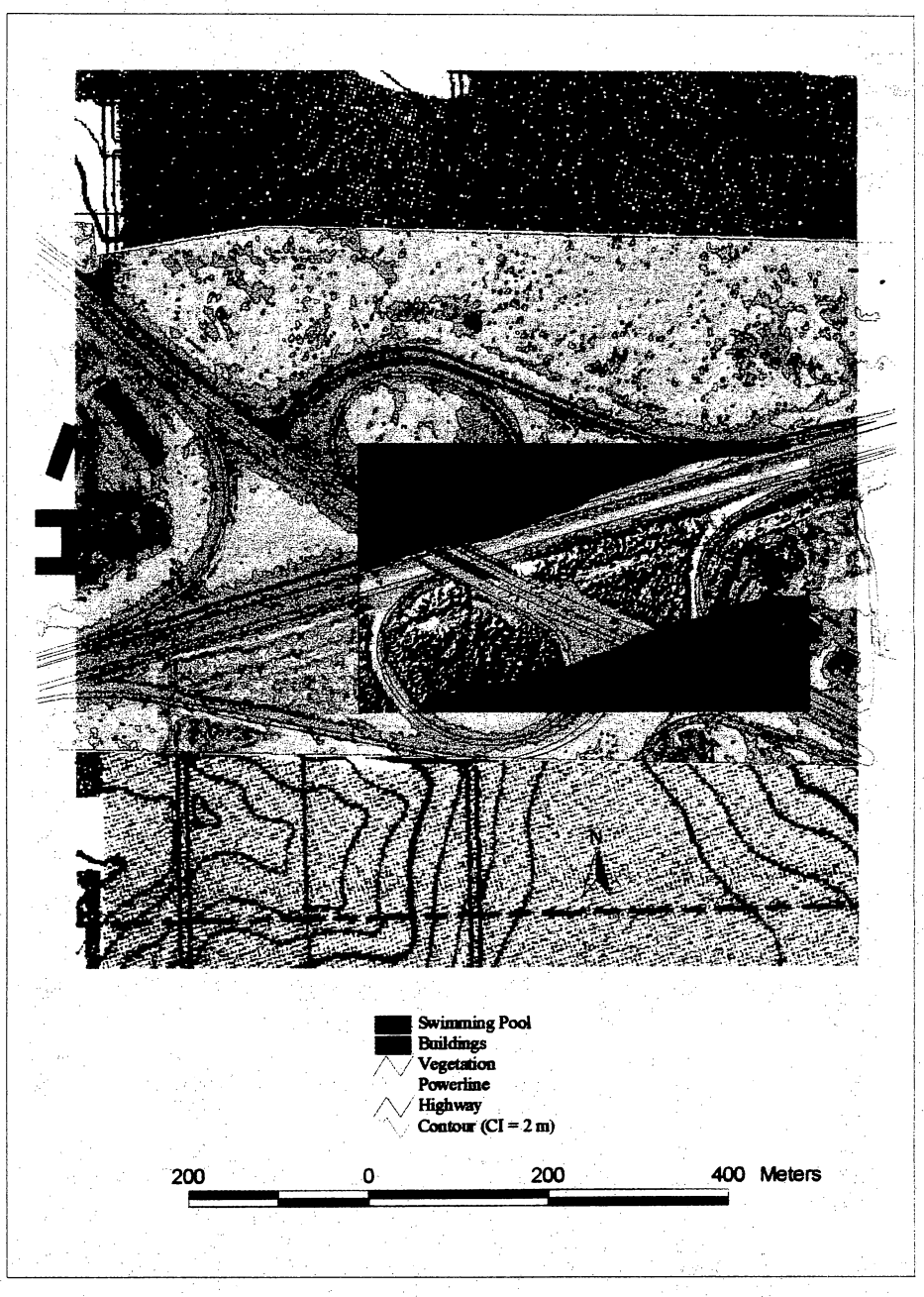

FIGURE 1. The intersection of Interstate Highway 1-10 and State Highway 63 near Tallahassee, FL, mapped by a team of University of Florida researchers and Optech personnel in November 1996.

ground (or objects such as buildings, trees, power lines) are measured with a precise interval timer and the time intervals are converted into a range of measurements using the velocity of light. The position of the aircraft at the epoch of each measurement is determined by phase difference kinematic Global Positioning System (GPS). Rotational positions of the beam director are combined with aircraft roll, pitch and heading values determined with an inertial navigation system, and the range measurements to obtain vectors from the aircraft to the ground points. When these vectors are added to the aircraft locations they yield accurate coordinates of points on the surface of the terrain.

Solid state lasers are now available that can produce thousands of pulses of light per second, each pulse having a duration of a few nanoseconds (10-9 seconds). Light travels approximately 30 centimeters in one nanosecond. By accurately timing the round trip travel time of the light pulses from the laser to a reflecting surface it is possible to determine the distance from the laser to the surface, typically with a precision of one centimeter or better. Errors in the location and orientation of the aircraft, the beam director angle, atmospheric refraction model, and several other sources degrade the coordinates of the surface points to 5 to 10 centimeters, in the current state of the art systems. The width of the "swath" covered in a single pass of the aircraft depends on the scan angle of the laser ranging system and the airplane height. Typical operating specifications permit flying speeds of 200 to 250 kilometers per hour (55 to 70 meters per second), flying heights of 300 to 3,000 meters, scan angles up to 20 degrees, and pulse rates of 2,000 to 25,000 pulses per second. These parameters can be selected to yield a measurement point every few meters, with a footprint of 10 to 15 centimeters, providing enough information to create a digital terrain model (DTM) adequate for many engineering applications, including the design of drainage systems, the alignment of highways, the determination of volumes of earth works, and the design of coastal structures.

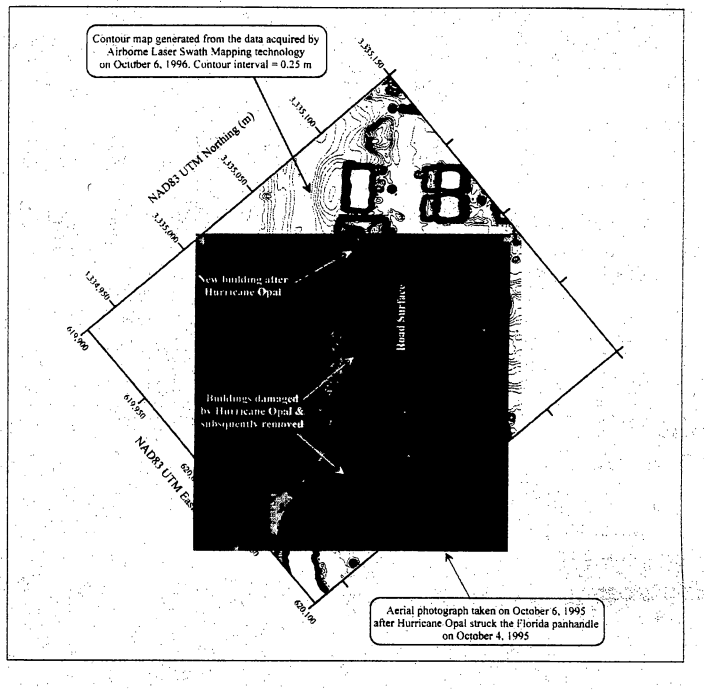

FIGURE 2. An example of one product produced from the data covering a few hundred meters of beach area in which a number of buildings were severely damaged.

Highway Engineering

ALTM is particularly well suited to mapping lineal areas such as the right of ways of highways. The aircraft can be flown directly along the centerline of the highway, resulting in the mapping only of the area of interest, and providing a digital terrain map with high spatial resolution, capturing information about the pavement, drainage system, and vegetation.

Figure 1 at the intersection of Interstate Highway 1-10 and State Highway 63 near Tallahassee, Florida, mapped by a team of University of Florida researchers and Optech personnel in November 1996. A digitized version of the US Geological Survey quad sheet (based on 1967 photography and revised in 1976 to include some new photography collected by Florida state agencies) was overlaid with a strip of 0.5 meter resolution digital photographs collected as part of the University research program in 1997. Features such as the edges of pavement and buildings were delineated using the 1997 digital photography, and a DTM created from the laser swath mapping data was then overlaid on a portion of the digital photograph to show how these various types of data can be combined into a single product that can be used by highway engineers.

Coastal Engineering

On October 4, 1995, Hurricane Opal struck the panhandle region of Florida doing severe damage to the beaches and buildings. In October 1996 researchers from the University of Florida, supported by Optech personnel, surveyed the beach area using an Optech 1020 ALTM system, mounted in a Florida Department of transportation aircraft. More than 200 kilometers of shoreline were mapped twice, in opposite directions of flight, in just over two hours. Figure 2 is an example of one product produced from the data covering a few hundred meters of beach area in which a number of buildings were severely damaged.

The laser data were used to generate a contour map, which is shown as an overlay on an aerial photograph taken on October 6, 1995, just two days after the storm. In the thirteen months between the date of the photograph and the date of the laser contour map two of the more severely damaged buildings were torn down and a new building was erected on previously undeveloped beachfront

property. The laser contour map provides footprints of the buildings at the time of the survey, and surface of the land after removal of the storm damaged buildings.

Eugene Medvedev
Head of Remote Sensing Dept.
Opten Limited, Moscow, Russia

We have been watching with great interest the activities of airborne scanning lasers since the First International Airborne Remote Sensing Conference in Strasbourg in September 1994. In the summer of 1997 we had the opportunity to become more closely acquainted with Optech Inc. after our company Opten Ltd., whose major area of business is the design and installation of fiber optic communication lines, purchased the laser sensor ALTM 1020 for power transmission line precision surveys. We started with a large airborne survey project along Ulan-Ude - Blagoveshensk line and within 10 days surveyed over 5,000 km of transmission lines using a local Mi-8 helicopter. Complete installation of on-board equipment only took us two days.

Trying to determine the exact location of each support tower is extremely difficult. Available information about the towers and their location and also as-built drawings, are either very scarce or altogether non-existent. Therefore, the complete Trans-Siberian powerline corridor needed to be surveyed to obtain detailed information regarding the tower locations. In addition to tower location, accurate topographic information about the terrain in proximity to the lines and towers was required to establish routes to the towers as well as possible encroachment by vegetation. Figure 3 shows a profile view of a section of powerline corridor. Clearly visible are the "conductors" as well as parts of the tower structure. Below the lines and towers are vegetation and terrain. The data in this image are the results of a "decimation" process applied to the data set. All points were first classified as "vegetation," "terrain," "wires," or "intersection points" (support towers). Then a "removal" algorithm is applied that eliminates approximately 70-90% of all points, leaving the majority of points that fall on the terrain below the wires, the wires themselves, or the towers.

The results of laser scanning are especially impressive when compared with traditional methods of power lines survey. Along with tremendous productivity — around 500-600 km per day, the method also provides accuracy of 15-20 cm for ground objects' geometric parameters, that is completely unattainable for traditional stereo photogrammetric methods. Here we have first gotten the opportunity to directly analyze the 3-dimensional observance that significantly increased efficiency of survey results interpretation and consequent topical decoding.

The other remote sensing methods that were tested and evaluated were aerial photo, thermal IR, SAR, high-resolution video and low-altitude digital aerial photo. A combination of airborne laser scanning and video seems to be the most reliable and efficient means of gathering digital elevation and imagery information about the lines and towers.

The reason Opten requires this detailed geographic information about the towers, is that the shield or "ground" wire will be replaced on the powerline with specially shielded high-speed fiber optic communication cable. Since fiber optic cable is quite expensive, a substantial savings is realized by having precise information regarding the location and height of existing lines and towers. This allows "cut-lengths" to be prepared at the factory and then delivered directly to the installation site without additional alteration of the cable, other than splicing.

We certainly do not limit application of the technology to only power lines surveys. ALTM applications, along with modern digital airborne cameras for creating general-purpose topographic maps, appear to hold much prospect. Such an approach shall first allow us to make labor intensive and expensive processes like orthorectification and photomaps synthesis completely automatic.

Roberto Gutierrez
& James C. Gibeaut
UT Bureau of Economic Geology
Melba Crawford, Solar Smith,
UT-Center for Space Research

Over the last three years, the Bureau of Economic Geology (BEG) and Center for Space Research (CSR) at the University of Texas at Austin have monitored Galveston Island and Bolivar Peninsula on the Texas Gulf coast. With the support of the NASA Topography and Surface Change Program, the BEG and CSR are developing new techniques for studying coastal processes using

FIGURE 3. A profile view of a section of powerline corridor. Clearly visible are the "conductors" as well as parts of the tower structure. Below the lines and towers are vegetation and terrain. The data in this image are the results of a "decimation" process applied to the data set.

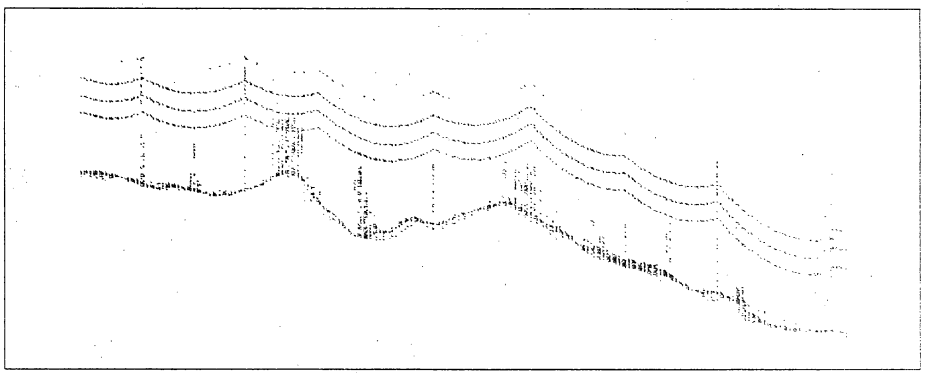

conventional ground surveys, ground Global Positioning System (GPS) surveys, and NASA's Topographic Airborne Synthetic Aperture Radar (TOPSAR). This fall our research group began using airborne laser terrain mapping (ALTM). On November 8, 1997, we flew over Galveston Island and Bolivar Peninsula with an Optech ALTM-1020 airborne laser terrain mapping system. With the instrument installed in a single-engine Cessna 206 (Figure 4), we mapped over 163 sq. km in one day with a laser ground point spacing of 2 to 6 m. The Optech engineers processed the raw data on a laptop computer and had a preliminary ALTM data set available the next day.

ALTM data from adjacent flightlines over Bolivar Peninsula were merged together without any adjustments and then gridded to create a smooth digital terrain model (DTM). Figure 5 is a shaded relief topographic image of the Port Bolivar area, the west end of Bolivar Peninsula. This image has a spatial resolution of five meters and is constructed from approximately 3.2 million laser ground points distributed over the 5 km x 7 km area. Vegetation and cultural features (roads, buildings, ships, jetties) are clearly discernible in the topographic image. The Intracoastal Waterway with barge traffic is visible along the upper left-hand edge of the image.

Identifiable geomorphic features include the shoreline, beach and foredunes, a series of accretionary spits, relict beach ridges, and small tidal creeks. A kinematic, differential GPS ground survey was conducted across the west end of Bolivar Peninsula; note the line A to A' on the topographic image. Figure 6 is a plot comparing the ground GPS survey (+) to the topography measured by the ALTM laser system (o). The laser profile is noisier than the GPS, nevertheless, the ALTM profile closely matches the ground GPS profile in all significant details.

Figure 7 is an oblique, hand-held aerial photograph of Fort Travis, a 100-year-old fortification on Bolivar Peninsula. This photo was taken during the ALTM flight. Figure 8 is a three-dimensional, elevation contour plot of Fort Travis computed from the laser DTM. The contour interval is 0.5 m and vertical exaggeration is 2X. This contour plot demonstrates the near-photographic resolution of airborne laser terrain mapping. The low seawall around the fortification is discernible, and roads, trees, and small buildings are all recognizable on the plot and easy to correlate with the identical features on the photograph.

In Figure 9, the dunes and seawall are visible, looking in an easterly direction along the Galveston city shorefront. Figure 10 is a three-dimensional, elevation contour plot of the Galveston city shorefront derived from a single, 300m-wide mapping swath flown at an altitude of 470 m

FIGURE 4. An Optech ALTM-1020 airborne laser terrain mapping system was installed in this single-engine Cessna 206 to map over 163 sq. km in one day over Galveston Island and Bolivar Peninsula.

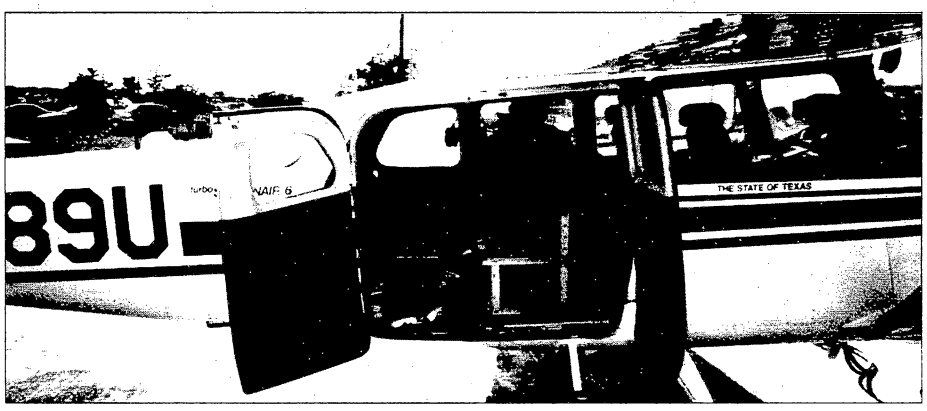

(AGL). The contour interval is 0.25 m and the vertical exaggeration is 2x. On the left are shorefront buildings in downtown Galveston; in the center are Seawall Boulevard (with cars) and the Galveston seawall. Projecting from the seawall is a low groin and various hotels and restaurants on piers. Contour lines in front of the seawall define a gently sloping artificial beach and more chaotic contour lines seaward of the beach reflect wave heights in the surf zone.

Our experience with the ALTM system convinces us that airborne laser mapping has the potential to revolutionize coastal geology and engineering. Until now, observations of coastal processes have been restricted to either detailed surveys at widely distributed points along a coastline or regional studies using maps, aerial photography, or remote sensing systems of relatively low resolution. Airborne laser mapping combines the resolution of ground surveys with large area coverage. The accuracy of GPS positioning and the high resolution of airborne laser mapping will allow us to compare coastal surveys conducted years apart and identify areas of change. By monitoring such changes, we will be able to delineate areas at risk from storms, land subsidence, and beach erosion with unprecedented accuracy. With detailed geomorphologic information we can estimate sediment transport rates along the entire Texas Gulf coast and relate variations in wind and wave regime, currents, and river flow to coastal patterns of beach accretion or erosion.

Conclusion

Employing airborne scanning lasers as terrain and object mapping tools will continue to grow as an aid in the analysis carried out by scientists and engineers. For example, Figure 11 is a DTM of a spillway structure. Gathering data about the condition of constructions that are engineered to prevent flooding disasters is imperative to maintaining these structures.

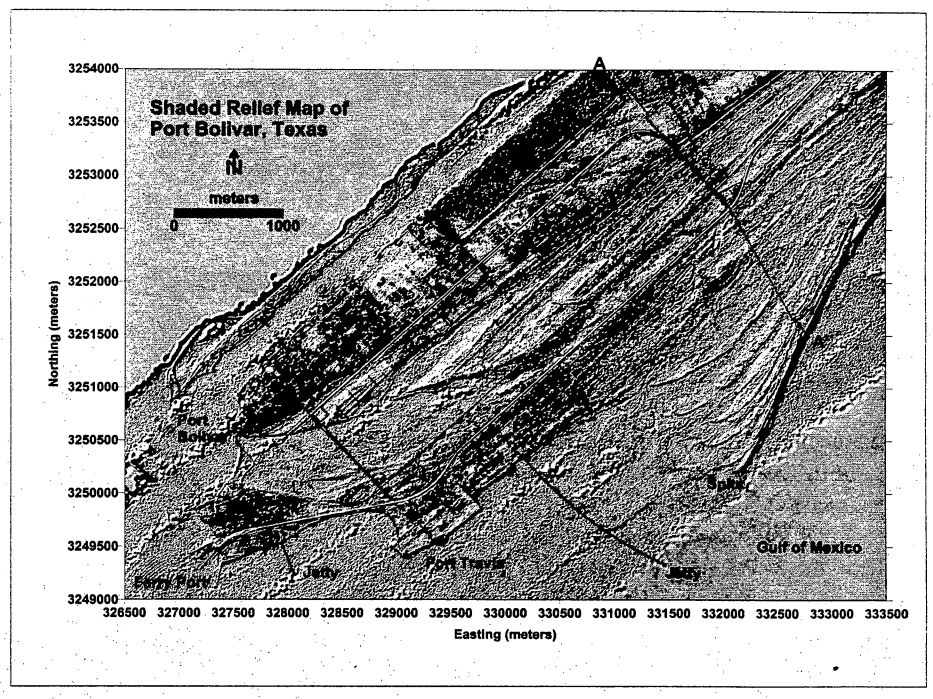

FIGURE 5 (ABOVE). A shaded relief topographic image of the Port Bolivar area, the west end of Bolivar Peninsula.

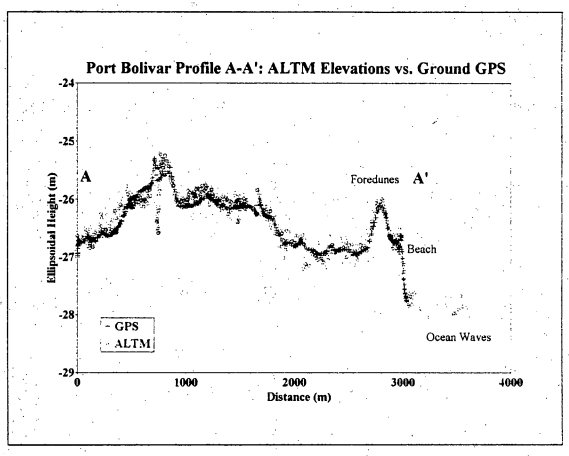

FIGURE 6 (RIGHT). A plot comparing the ground GPS survey (+) to the topography measured by the ALTM laser system (o).

FIGURE 7 (BELOW). An oblique, hand-held aerial photograph of Fort Travis, a 100 year-old fortification on Bolivar Peninsula. This photo was taken during the ALTM flight.

Laser scanning can be used more effectively than many standard methods since it can be mobilized rapidly and provide data almost instantaneosly. Following a storm event, engineers often need to acquire data at night or in poor weather. This means that almost all other methods of remote sensing cannot fulfil the requirement. Laser scanners can be flown in the dark and in bad weather, thereby providing a powerful remote sensing tool.

In an effort to gather elevation data about the 40% of land that is below sealevel, the Rijkswaterstaat in Holland has recently mandated that the entire country be mapped using airborne laser scanners. The engineers in the Rijkswaterstaat certainly know the benefit of having detailed knowledge about the terrain elevation in their flood-prone environment.

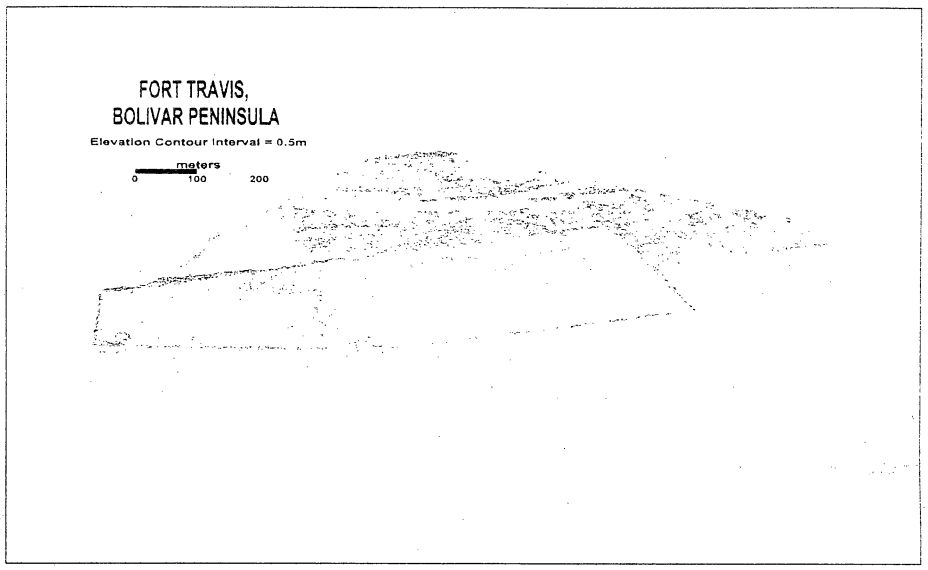

References

Carter, W.E., R.L. Shrestha, P.Y. Thompson, and R.G. Dean, *Project LASER Final Report*, University of Florida, pp. 27, April 4, 1997.

Milbert, D.S., *Computing GPS-Derived Orthometric Heights with Geoid90 Height Model*, Presented at ACSM Fall Meeting, GIS/LIS, Atlanta, GA, 1991.

BILL GUTELIUS is an ALTM Product Specialist at Optech, Inc. He can be reached by e-mail at billg@optech.ists.ca.

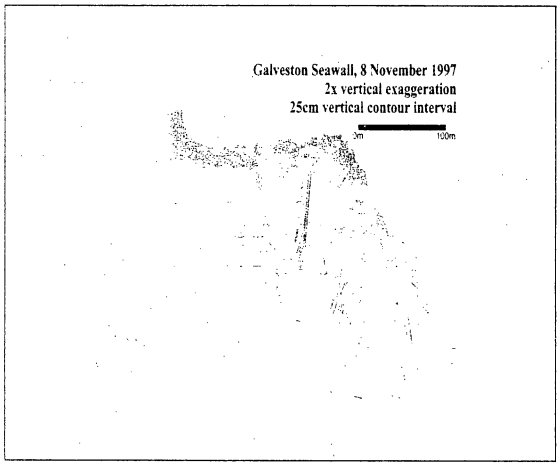

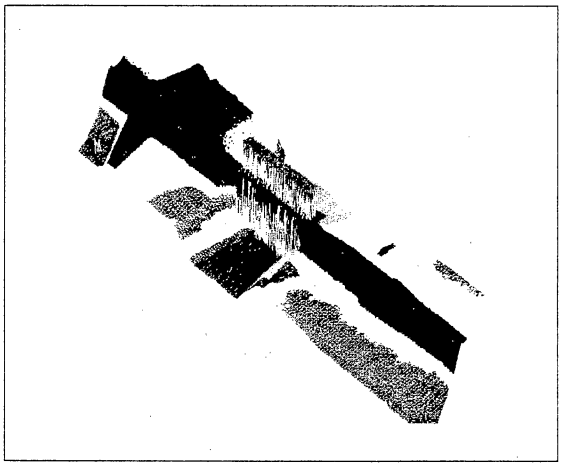

FIGURE 8 (TOP). **A three-dimensional, elevation contour plot of Fort Travis computed from the laser DTM.**

FIGURE 9 (ABOVE). **The dunes and seawall from an easterly direction along the Galveston city shorefront.**

FIGURE 10 (FAR LEFT). **A three-dimensional, elevation contour plot of the Galveston city shorefront.**

FIGURE 11 (LEFT). **A DTM of a spillway structure.**

Appendix C

Article published in the Proceedings of the Fifth International Conference on Remote Sensing for Marine and Coastal Environments, 5-7 October 1998, San Diego, California, USA, p. I236-I243.

(The poster derived from this paper won the "Best of Session" award.)

AIRBORNE LASER SWATH MAPPING OF GALVESTON ISLAND AND BOLIVAR PENINSULA, TEXAS*

[1]Roberto Gutiérrez, [1]James C. Gibeaut, [2]Melba M. Crawford, [1]Matthew P. Mahoney, [2]Solar Smith
[1]Bureau of Economic Geology and [2]Center for Space Research, The University of Texas at Austin
Austin, Texas, U.S.A.
William Gutelius, Donald Carswell, Elise MacPherson
Optech Inc.
North York, Ontario, Canada

ABSTRACT

In November 1997 The University of Texas at Austin and Optech surveyed Galveston Island and Bolivar Peninsula on the Texas Gulf Coast using an airborne laser swath mapping system, the Optech ALTM-1020. With the ALTM-1020 installed in a small aircraft we mapped more than 163 km^2 in one day with a laser ground point spacing of 2 to 6 m. We merged laser data from multiple flightlines to create a high-resolution, digital terrain model (DTM). Vegetation and cultural features are clearly discernible in the DTM. Geomorphic features identifiable in the DTM include the shoreline, beach and foredunes, a series of accretionary spits, beach ridges, and small tidal creeks. Comparisons with ground surveys indicate that the laser DTM matches ground truth in all significant details and measures topography with a precision of about 0.15 m.

1.0 INTRODUCTION

The Bureau of Economic Geology (BEG) and Center for Space Research (CSR) at The University of Texas at Austin are using high-resolution airborne topographic mapping technologies in the study of barrier systems. Our current emphasis is on the integration of multisensor data sets. These include conventional ground surveys, Global Positioning System (GPS) surveys, the NASA/Jet Propulsion Laboratory Airborne Synthetic Aperture Radar, and, most recently, airborne laser terrain mapping (ALTM). Airborne laser systems have been used for terrain mapping for several years [Krabill and others, 1984; Krabill and others, 1995], and recent applications have focused on beach surveying [Armstrong and others, 1996; Carter and Shretha, 1997]. Here we describe a laser mapping system developed by Optech, Inc., and discuss the potential of ALTM to provide high-resolution topographic data in a timely and cost-effective manner. Because coastal monitoring requires the accurate, temporal sampling of shoreline features, we examine the precision and repeatability of ALTM measurements. We also discuss the applications of ALTM data in the study of coastal geomorphology using Bolivar Peninsula as an example.

2.0 STUDY AREA

Bolivar Peninsula and Galveston Island are Holocene barrier landforms that lie at the southwest end of the Galveston Bay system, separating it from the Gulf of Mexico (Figure 1). Galveston Island is a high-profile barrier island composed of a prograding sequence of Recent deposits [Morton and McGowen, 1980]. The island is assumed to have originated from an emergent bar during the standing sea-level stage in approximately 2-3 m of water. The island's sands are as much as 15 m thick and progressively thin from east to west in the direction of longshore transport [Cole and

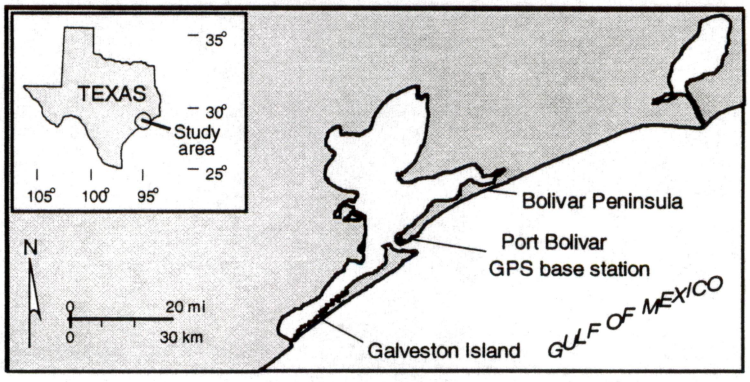

Figure 1. Galveston Bay Study Area.

* Presented at the Fifth International Conference on Remote Sensing for Marine and Coastal Environments, San Diego, California, 5-7 October 1998

Anderson, 1982]. Northeast of Galveston Island is Bolivar Peninsula. Bolivar Roads, a large tidal inlet, separates the peninsula from the island. Bolivar Peninsula is assumed to have formed through spit accretion. The peninsula's early stage of development is represented by a series of recurved, spit ridges, washover features, and washover-associated channels on the landward side of the peninsula. Two large, fan-shaped features on the landward side of the peninsula are composed of thin sand and mud interlaminae interpreted as overwash and/or flood-tidal deposits. These early geomorphic features indicate southwest migration [Siringan and Anderson, 1993]. A later developmental stage is represented by a series of beach ridges that parallel the modern shoreline. These latter ridges are slightly concave-seaward, diverge to the southwest, and have recurved ends [Siringan and Anderson, 1993].

3.0 METHODS

The Optech ALTM-1020 system combines a pulsed, solid-state laser, an inertial motion unit (IMU), and a geodetic GPS receiver in a compact and modular configuration. The IMU (accelerometers and gyroscopes) monitors the aircraft attitude, and the GPS receiver provides aircraft position data. Rotating optics in the instrument's sensor head scans the laser across the ground, illuminating a swath under the aircraft. We installed the ALTM system in a single-engine Cessna 206 from the Texas State Aircraft Pooling Board. We adapted the aircraft, originally modified for vertical aerial photography, to the Optech instrument in about eight hours with the assistance of State aircraft maintenance technicians. See Figure 2. For accurate, differential aircraft positioning we operated an Ashtech Z-12 GPS receiver in the aircraft and a Trimble 4000SSi GPS receiver on the ground. To provide accurate navigation for the pilot we installed a Starlink DNAV-212 differential GPS system (DGPS), which uses DGPS corrections broadcast by the U.S. Coast Guard, in the aircraft. DNAV-212 positions were transferred to a Starlink LB-3 cockpit lightbar that computed flightlines and displayed flightline corrections.

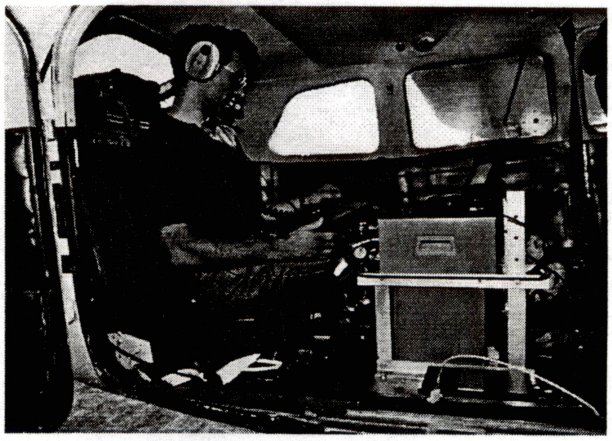

Figure 2. ALTM-1020 Installed in Cessna 206.

On 8 November 1997 we flew 34 flightlines over Bolivar Peninsula and Galveston Island collecting 3.5 hours of ALTM data. In the morning we flew the first two flightlines normal to the peninsula at an altitude of 470 m above ground level (AGL) and then 21 flightlines parallel to the peninsula at an altitude of 750 m AGL. In the afternoon we flew 12 additional flightlines parallel to the peninsula at 750 m AGL. The last two flightlines were flown along the Gulf shoreline down the length of Bolivar Peninsula and the northern half of Galveston Island at an altitude of 470 AGL. The illuminated laser footprint on the ground was approximately 0.12 to 0.19 m in diameter for these altitudes. For all flightlines we set the ALTM-1020 at a laser pulse rate of 2000 Hz and a scan angle of ±20° from nadir. The aircraft speed was 46 meters per second (90 kts). The resulting ground swaths had a width of 340-540 m with 30% overlap. The ALTM-1020 can operate at laser pulse rates up to 5000 Hz, but because of technical problems we could not acquire accurate data at rates above 2000 Hz. Nonetheless, we were able to map more than 163 km^2 in one day (40 km^2 per hour) with a horizontal data spacing of 2 to 6 m.

All laser, GPS, and IMU data reduction was done using the Optech GBPP processing software. Optech used GPS data from the aircraft Ashtech Z-12 and the Trimble 4000SSi ground station to compute a L1 phase solution for the aircraft's trajectory. They adjusted and corrected the laser ranges for scan geometry and aircraft attitude, then merged the range data with the aircraft trajectory to create a sequence of X, Y, Z ground points. Optech then transformed the ground points into Universal Transverse Mercator (UTM) coordinates and heights above the WGS-84 reference ellipsoidal (HAE).

4.0 RESULTS

To help evaluate the ALTM data we conducted GPS ground surveys along 50 km of roads on Bolivar Peninsula. Sorting through all the morning ALTM flightlines and the GPS road surveys we identified 1,760 GPS and ALTM laser points that were horizontally separated by less than 1 m. The GPS ground surveys were done kinematically

using a GPS antenna on a vehicle; therefore the road elevations are averaged over the vehicle's approximately 3 × 2 m footprint. Table 1 describes the mean elevation difference (δe) between the road elevations determined by ground GPS and by ALTM. Table 1 also shows the associated standard deviations (σ), the number of elevation pairs, and the approximate aircraft altitude for the ALTM data. The histograms (Figure 3A) for the GPS-ALTM δe indicate that the ALTM elevation errors have a simple, symmetric, non-Gaussian distribution about a well-defined mean δe. This comparison between ALTM and ground GPS surveys indicates that the ALTM elevation errors contain an elevation bias (mean δe) and a noise component (σ). The ALTM elevation bias includes the laser instrument calibration error, the atmospheric refraction of the laser path between the aircraft and the ground, and the GPS height errors due to tropospheric delay. The magnitude of atmospheric effects in the ALTM bias is indicated by the decrease in mean δe from 0.184 to 0.145 cm as the aircraft altitude drops from 750 to 470 m AGL. The noise component in the ALTM data is the sum of random errors in laser range measurements, in the GPS aircraft positioning, and in the measurements of the scan angle or aircraft attitude. The δe for the ALTM road surveys includes measurements from nine different flightlines and from different points across each mapping swath. Therefore we interpret the associated σ values of 0.12 and 0.15 m as representing the RMS error of the entire ALTM-1020 system including the supporting geodetic GPS equipment.

Table 1. Differences in Road Elevation Between GPS Ground Surveys and ALTM

Number of flightlines over surveyed roads	mean HAE difference (δe) m	σ m	number of points	aircraft altitude m AGL
Eight morning flightlines	**-0.184**	**0.152**	**1760**	**750**
One afternoon flightline	**-0.145**	**0.124**	**495**	**470**

Table 2. Elevation Differences Between Overlapping ALTM Flightlines

Overlapping flightline pairs	mean HAE difference (δe) m	σ m	number of points	aircraft altitude m AGL
1-2	**0.001**	**0.121**	**463**	**470**
11-12	**-0.022**	**0.217**	**348**	**750**
12-13	**0.051**	**0.208**	**412**	**750**
13-14	**0.048**	**0.212**	**345**	**750**

The 30% overlap between flightlines allowed us to compare the elevations measured by successive ALTM mapping swaths. We examined those portions of flightlines 1, 2, 11, 12, 13, and 14 that mapped the peninsula's barrier flat, a region with few trees or buildings and very low relief. In the overlap between flightlines we identified pairs of laser ground points that were horizontally separated by less than 0.10 m. After culling out elevation outliers, large elevation differences (1-12 m) for the same ground location caused by differential foliage penetration, we computed the mean elevation difference (δe) between adjacent flightlines. We also computed the standard deviation (σ) of these elevation differences. Table 2 describes the δe and σ for overlapping flightlines 1-2, 11-12, 12-13, and 13-14. The δe histogram for overlapping flightlines 1-2 (Figure 3B) shows an ALTM elevation error distribution very similar to the GPS-ALTM δe histogram. The δe histograms for overlapping flightlines 11-12, 12-13, and 13-14 are more complex. The δe represents the variation in ALTM elevation bias from flightline to flightline. In the overlap area between adjacent flightlines, measurement errors in the laser geometry are exaggerated. Flying at 750 m AGL with the laser scan angle set at ±20° from nadir, a measurement error of 0.05° in the scan angle or in the aircraft roll results in a 0.24-m elevation error at the edges of the mapping swath. Decreasing the aircraft altitude to 470 m reduces the elevation error at the swath edges to 0.15 m. Therefore the δe between the overlapping edges of two adjacent mapping swaths is a measure of the accuracy of the IMU and the optical scanning system. The σ in Table 2 indicate that the IMU and optical scanning components in the ALTM system have a combined accuracy of about 0.025° to 0.05°.

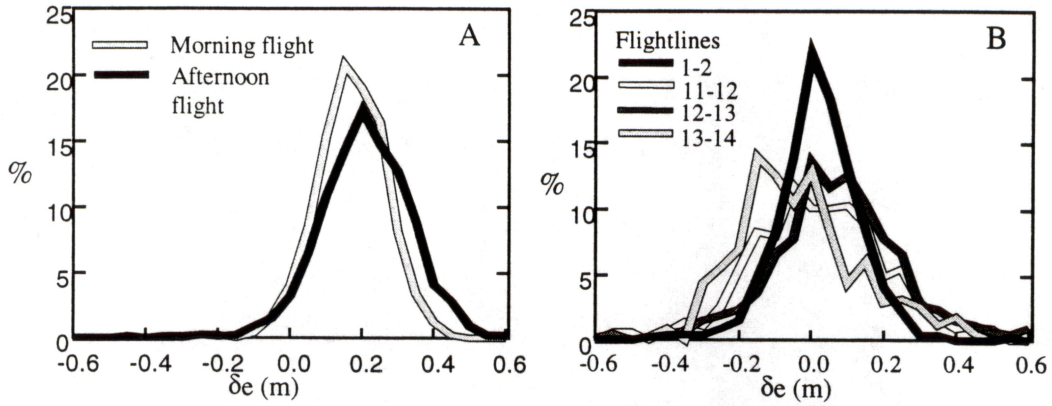

Figure 3. A. Histogram of δe for ALTM and Ground GPS Road Elevations
B. Histograms of δe for overlapping pairs of ALTM flightlines.

We merged the ALTM data, approximately 14.4 million data points, from all flightlines and gridded them to create a digital terrain model. The DTM has a 5 × 5 m horizontal resolution and provides an extremely detailed image of the peninsula, Figure 4. The only significant gaps in the DTM occur over areas of open water. Little or no laser energy returned off water unless the beam was aimed within ±5- 6° of nadir or the water surface had sufficient roughness. Major cultural features in the DTM include the Intracoastal Waterway (ICW) and two towns, Port Bolivar and Crystal Beach. The history of the peninsula is apparent in the topographic variations mapped by ALTM. A large, recurved spit is visible in the middle of the peninsula, cutting across the ICW and a composite washover fan. This spit and fan are relicts from the early, migratory phase of the peninsula's development. Ridge and swale topography running through the center of the peninsula represents a more recent accretionary phase. The highest natural feature in the DTM is a 3-m-high beach ridge running along the center of the peninsula from Port Bolivar through Crystal Beach. This ridge is truncated by the shoreline at the extreme right of the image.

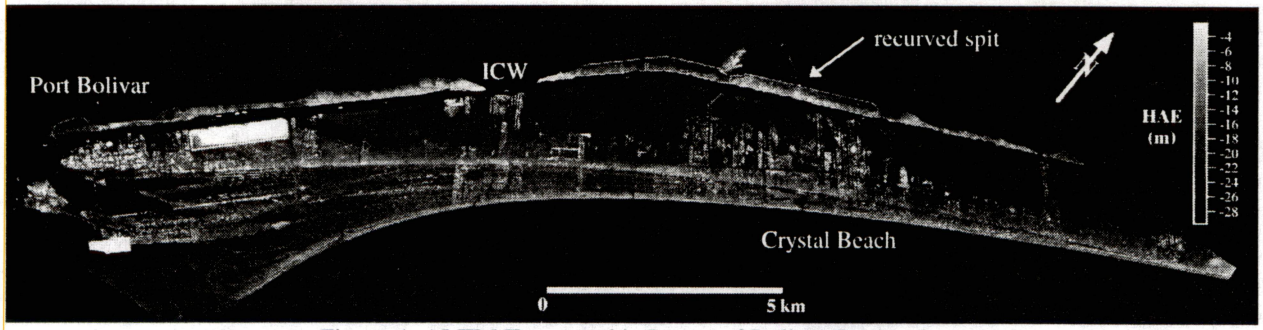

Figure 4. ALTM Topographic Image of Bolivar Peninsula.

Figure 5 is a shaded-relief topographic image of the Port Bolivar area on the west end of Bolivar Peninsula. The image, which covers a 7 × 5 km area, has a spatial resolution of 5 m and is constructed from 3.8 million ALTM laser points. The ICW with barge traffic is visible along the upper left-hand edge of the image. Vegetation and cultural features (roads, buildings, and jetties) are clearly discernible. A large rectangular pile of dredge spoil forms a topographic high to the northeast of Port Bolivar. Identifiable geomorphic features include the shoreline, beach and foredunes, recurved spits, beach ridges, and small tidal creeks. The recurved spits and tidal flats immediately northeast of the North Jetty are the current site of peninsular accretion with as much as 5 m of seaward advance per year [Morton, 1997]. In the center of the peninsula are a series of straight ridge and swale features that represent accretion along the peninsula prior to the construction of the Bolivar Roads' jetties.

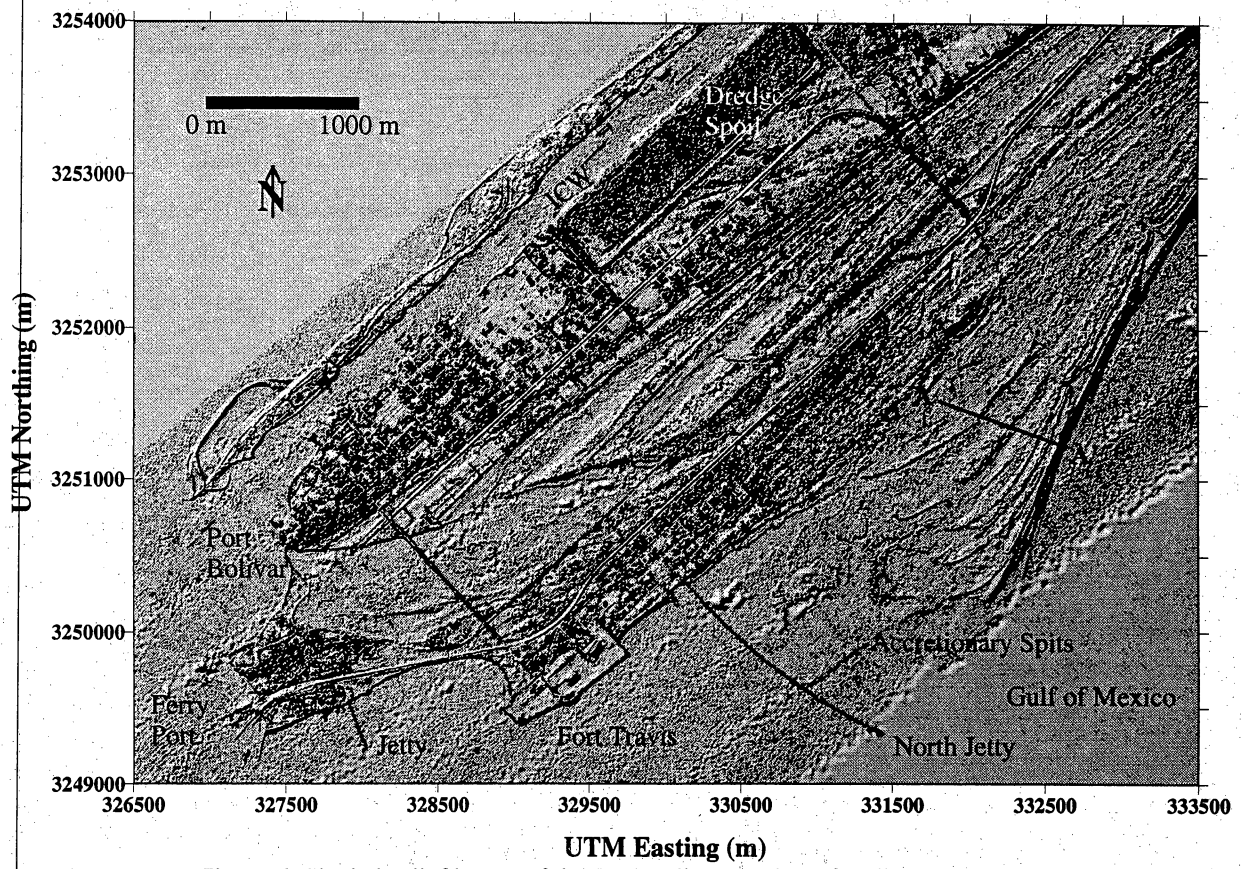

Figure 5. Shaded-relief image of the Port Bolivar portion of Bolivar Peninsula.

The shore-normal beach profile A-A' traverses an undeveloped portion of the peninsula and crosses several accretionary spits. The beach profile extends from the waterline across the beach, foredunes, and the barrier flat. The day after the ALTM mapping flight we conducted a rapid-static GPS survey to measure the topography along this beach profile. We sorted the ALTM data for laser points that fell within ± 1 m of the transect line (Figure 6). These ALTM elevation points were adjusted upward by 0.184 m, the mean δe between the GPS road survey and the ALTM in Table 1. We estimated the sand volume for beach and foredunes of the GPS ground and ALTM profiles using the U.S. Army Corps of Engineer's BMAP beach analysis software. Assuming a 1-m beach front, we computed the volume for the portion of the profiles that lie between 550 and 870 m, and above –27.5 m HAE. The ALTM profile overestimated the sand volume in the beach and dunes (240.3 m^3) by 40% in comparison to the GPS profile (171.2 m^3). This volume error is due to dense vegetation in the dune and interdune portion of the profile. Vegetation coverage on seaward side of the dunes is typically 20-50%, and the dominant plant species are relatively short: camphor daisy (*Machaeranthera phyllocephala*), Gregg amaranth (*Amaranthus greggii*), sea purslane (*Sesuvuim portacastrum*), and gulf croton (*Croton punctatus*). Vegetation coverage increases to 80-90% on the backside of the dunes and the interdune area with partridge pea (*Chamaecrista fasciclata*) and marsh-hay cordgrass (*Spartina patens*) being the dominant species. These two plants, which grow to a height of 0.2 to 1 m, were dense enough to reflect most of the laser energy before it reached the ground surface. As a result ALTM elevation errors are as large as +0.4 m on the backside of dunes and in the interdune areas.

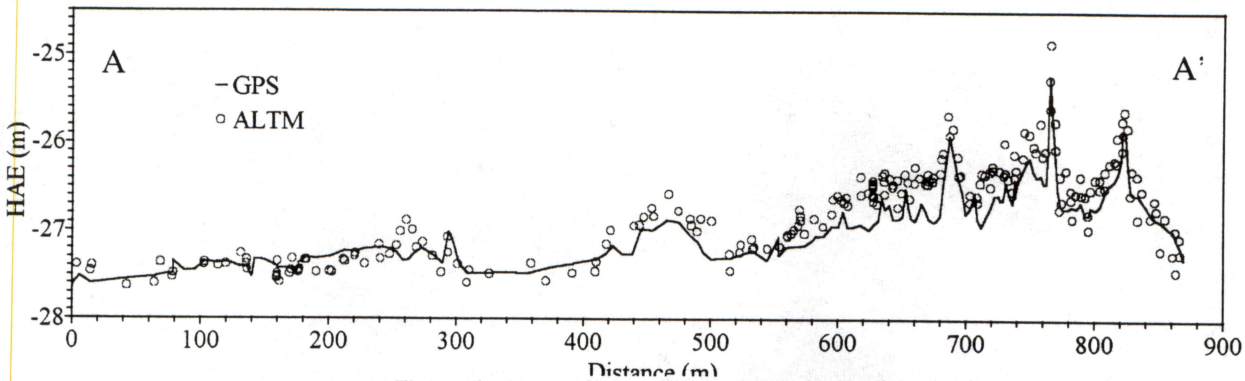

Figure 6. Shore-Normal Topographic Profile A - A'.

Because the shoreline is of critical interest, we flew two flightlines along the beach. The pilot reduced the aircraft altitude to 470 m and guided the aircraft along the dune vegetation line with the aid of a floor window and a cockpit display from a video camera bore-sighted with the laser. A single, continuous swath was mapped down the entire length of Bolivar Peninsula along the Gulf shoreline. The Gulf shoreline along the northern half of Galveston Island was mapped in a second, continuous swath. Figure 7 is a three-dimensional contoured image of a 650-m-long portion of the Galveston seawall created from the Galveston beach flightline. The swath width is approximately 340 m. The image shows shorefront buildings, several piers and a groin extending from the seawall, and a gently sloping beach in front of the seawall. The chaotic contours in front of the beach represent the surf zone. Cars parked and driving along the top of the seawall are visible as small, closed contours. Shorefront buildings appear to have wavy or scalloped sides because of the 2-m ground spacing between laser scan lines. Even operating at the reduced laser pulse rate of 2000 Hz, ALTM provides detailed information about beach morphology, engineering structures, and nearshore wave heights.

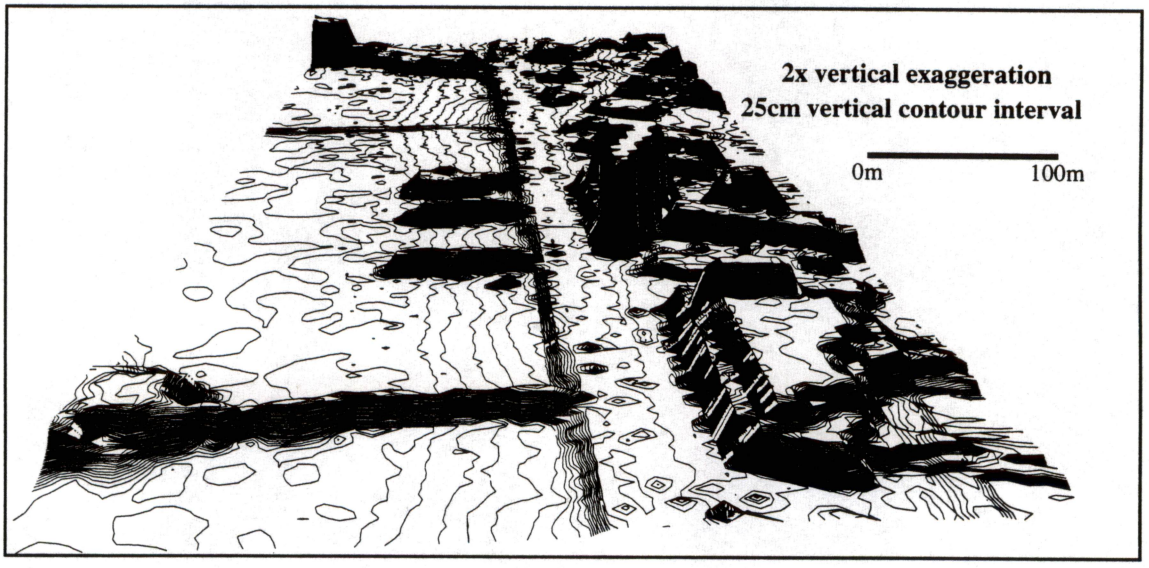

Figure 7. ALTM contoured topographic image looking southwest along the Galveston Seawall.

5.0 DISCUSSION

The accuracy of ALTM is currently limited by atmospheric effects and errors in the measurement of aircraft attitude and laser scan angle. To minimize these effects and obtain elevation measurements with 0.10-m precision requires operating at altitudes of 400-500 m and with laser scan angles restricted to ±15° from nadir. Unfortunately

this limits the mapping swath width to only about 240 m. Mapping at higher altitudes and flying long baselines while maintaining precision requires a very accurate GPS aircraft trajectory. An ionospherically corrected (L3), ambiguity-fixed, GPS phase solution is essential. In addition, the tropospheric zenith delay should be accurately estimated as part of the aircraft GPS solution. We believe that the differential tropospheric zenith delay between the aircraft and the ground GPS base station contributes 0.04 to 0.06 m to the ALTM elevation bias. If 0.10-m precision is desired over the entire swath width, then the laser geometry needs to be measured with an accuracy better than 0.025°.

Vegetation is another factor affecting the accuracy of ALTM in coastal applications. Assessing the ability of a shoreline to withstand a storm surge requires measurements of the foredune height, the continuity of the foredunes, and the sand volume in the beach and dune system. Likewise, estimating a coastal sediment budget requires monitoring changes in sediment volume stored in the beach and foredunes. The 40% overestimation of dune sand volume along our ALTM beach profile indicates that strategies need to be devised to minimize the elevation errors caused by dense dune vegetation. It may be possible to configure an ALTM system for better penetration of coastal vegetation and develop algorithms for discriminating grass and low shrub cover from the ground surface in data processing. Simply scheduling surveys during times when vegetation cover is minimal may be sufficient in some coastal areas. Despite these problems ALTM is the best instrument for the study of beach ridge systems. Repeated ALTM surveys can provide rates of beach ridge growth and reveal details of beach ridge evolution. The geometry, orientation, and elevation of beach ridges as mapped by ALTM can provide information about sea-level change, morphodynamics, and climatic conditions [Taylor and Stone, 1996].

6.0 CONCLUSIONS

The Optech ALTM-1020 system, despite technical problems during our flight, easily provided topographic information comparable to other laser swath mapping systems [Krabill and others, 1995; Armstrong and others, 1996]. Our experience convinces us that airborne laser swath mapping has the potential to revolutionize coastal geology. Until now, observations of coastal processes have been restricted to either detailed surveys at widely distributed points along a coastline or regional studies using maps, aerial photography, or remote sensing systems of relatively low resolution. Airborne laser mapping combines the resolution of ground surveys with large area coverage. The accuracy of GPS positioning and the high resolution of airborne laser mapping will allow us to compare coastal surveys conducted years apart and identify areas of change. By monitoring such changes, we will be able to delineate areas at risk from storms, land subsidence, and beach erosion with unprecedented accuracy.

7.0 REFERENCES

Armstrong, E. M., J. C. Brock, M. W. Evans, W. B. Krabill, R. Swift, and S. S. Manizade, "Beach morphology in the southeastern U.S. from airborne laser altimetry" (abs), *AGU Fall Meeting*, 1996.

Carter, W. E. and R. Shretha, "Airborne laser swath mapping: instant snapshots of our changing beaches", In *Proceedings of the Fourth International Conference: Remote Sensing for Marine and Coastal Environments*, Environmental Research Institute of Michigan (ERIM), Ann Arbor, MI, Vol. 1, pp.298-307, 1997.

Cole, M. L. and J. B. Anderson, "Detailed grain size and heavy mineralogy of sands of the northeastern Texas Gulf coast: implications with regard to coastal barrier development", *Transactions-Gulf Coast Association of Geological Societies*, Vol. 32, pp.555-563, 1982.

Fisher, W. L., J. H. McGowen, L. F. Brown, and C. G. Groat, *Environmental Geologic Atlas of the Texas Coastal Zone - Houston-Galveston Area*, Bureau of Economic Geology, Austin, TX, 91p., 1972.

Krabill, W. R., J. G. Collins, L. E. Link, R. N. Swift, and M. L. Butler, "Airborne laser topographic mapping results", *Photogrammetric Engineering And Remote Sensing*, Vol. 50, No. 6, pp.685-694, 1984.

Krabill, W. B., R. H. Thomas, C. F. Martin, R. N. Swift, and E. B. Fredrick, "Accuracy of airborne laser altimetry over the Greenland ice sheet", *International Journal Remote Sensing*, Vol. 16, No. 7, pp.1211-1222, 1995.

Morton, R. A., *Gulf Shoreline Movement Between Sabine Pass and the Brazos River: 1997 to 1996*, Bureau of Economic Geology, Austin, TX, 46p., 1997.

Siringan, F. P and J. B. Anderson, "Seismic facies, architecture, and evolution of the Bolivar Roads tidal inlet/delta complex, east Texas Gulf coast", *Journal of Sedimentary Petrology*, Vol. 63, No. 5, pp.794-808, 1993.

Taylor, M. and G. W. Stone, "Beach-ridges: a review", *Journal of Coastal Research*, Vol. 12, No. 3, pp.612-621, 1996.

ACKNOWLEDGMENTS

This project was conducted with funding from the NASA Topography and Surface Change Program (Grant No. NAG 5-2954) and the Texas Coastal Management Program (GLO Contract No. 98-022). In addition we would like to acknowledge the assistance of Ross Adkins, Berl Mumy, and Bill McLennan at the Texas State Aircraft Pooling Board and Gene Hall of Starlink, Inc. of Austin. Publication authorized by the Director, Bureau of Economic Geology, The University of Texas at Austin.

Appendix D

Abstract published in the proceedings of the 1998 Fall Meeting of the American Geophysical Union, AGU Volume 79, Number 45, p. F200

Multi-Sensor Analysis of Coastal Hazards and Environments Using Airborne Laser Terrain Mapping and Synthetic Aperture Radar

R Gutierrez[1] (512-471-0342; oskar@mail.utexas.edu)
A Neuenschwander[2] (512-471-7149; amy@csr.utexas.edu)
J C Gibeaut[1] (512-471-0344; gibeautj@begv.beg.utexas.edu)
M M Crawford[2] (512-471-7993; crawford@csr.utexas.edu)
S Kumar[2] (512-471-7993;skumar@csr.utexas.edu)
W Gutelius[3] (416-661-5904; billg@optech.on.ca)
R Sherma[3] (416-661-5904; rajive@optech.on.ca)
E MacPherson[3] (416-661-5904; elise@optech.on.ca)

[1]Bureau of Economic Geology, University Station, Box X, The University of Texas at Austin, Austin, TX, 78713-8924, USA
[2]Center for Space Research, 3925 W. Braker Lane, Suite 200, The University of Texas at Austin, Austin, TX, 78759-5321, USA
[3]Optech, Inc., North York, ONT, M3J 2Z9, CAN

University of Texas at Austin has collected multi-sensor data over barrier islands along the Texas Gulf coast. These data include imagery and digital terrain models (DTM) from the NASA/JPL airborne synthetic aperture radar operating in the polarimetric (AIRSAR) and interferometric (TOPSAR) modes. In November 1997 and August 1998 we conducted airborne laser terrain mapping (ALTM) of the north Texas Gulf coast. We have compiled these ALTM data into a high-resolution DTM for shoreline monitoring and flood-hazard analysis. In addition, we have combined radar, ALTM, and optical data for the classification of coastal habitats.

Land cover classification using remotely sensed data is important for mapping and monitoring changes in coastal wetlands. Because of the similarity in spectral signatures and backscatter responses, we often find it difficult to separate individual classes within both herbaceous vegetation classes and upland shrubs using either optical or radar data. In coastal marshes and the low relief areas associated with ridge and swale topography, the frequency of inundation, the soil salinity, and the vegetation distribution are all dependent upon elevation. An elevation change of only tens of centimeters can result in dramatic changes in vegetation. We investigated improvements in the classification of land cover on Bolivar Peninsula, Texas, using a multi-sensor approach based on polarimetric AIRSAR and topographic information from TOPSAR and ALTM. We employed a hierarchical approach based on multi-resolution neural networks both as a non-parametric classification procedure and for combining information from multiple sensors.

Appendix E

Abstract published in the 1999 AAPG Annual Convention official program: American Association of Petroleum Geologists, p. A46.

Mapping Topography and Bathymetry of Barrier Islands Using Airborne, Terrestrial, and Marine Systems

GIBEAUT, J. C., R. GUTIERREZ, R. C. SMYTH, Bureau of Economic Geology, The University of Texas at Austin, Austin, TX; M. M. CRAWFORD, K. C. SLATTON, A. L. NEUENSCHWANDER, Center for Space Research, The University of Texas at Austin, Austin, TX

The shapes and elevations of barrier islands can change dramatically during a storm. And between storms sediment is constantly shifting to and from these islands and among various depositional subenvironments. To investigate these changes coastal geologists have had to either settle for regional studies with sparse topographic data or small-area studies with more detailed data. With the advent of the Global Positioning System (GPS) and its incorporation into air, land, and sea surveying systems we are now able to map 10's of kilometers of coast in a day with unprecedented accuracy and detail.

We are applying the following four topographic/bathymetric surveying methods to monitor 150 km of the upper Texas coast: (1) airborne laser altimeter surveys of the backbarrier, foredune, and upper beach with 15 cm accuracy and 2 m data spacing, (2) vehicular kinematic GPS surveys of the upper and lower beach with horizontal and vertical accuracy of 2 cm, (3) electronic total station surveys of selected transects from landward of the foredune into the surf zone, and (4) nearshore GPS/echosounder surveys with 6-cm accuracy extending selected transects to approximately 7-m water depth. We are also experimenting with interferometric airborne synthetic aperture radar to rapidly acquire regional topographic coverage in the low-relief coastal zone. These topographic data allow us to develop a sediment budget for an entire barrier island system. We are also using the detailed topography to aid the interpretation and classification of optical and radar remote sensing imagery.